ACCELERATED DISTRIBUTION DEMONSTRATION SYSTEM

REGULATORY INFORMATION DISTRIBUTION SYSTEM (RIDS)

ACCESSION NBR:9201060130 DOC.DATE: 91/12/26 NOTARIZED: NO DOCKET #
FACIL:50-275 Diablo Canyon Nuclear Power Plant, Unit 1, Pacific Ga 05000275
50-323 Diablo Canyon Nuclear Power Plant, Unit 2, Pacific Ga 05000323
AUTH.NAME AUTHOR AFFILIATION
RUEGER,G.M. Pacific Gas & Electric Co.
RECIP.NAME RECIPIENT AFFILIATION
Document Control Branch (Document Control Desk)

SUBJECT: Forwards "Adequacy of Seismic Margins Assuming Increase in Amplitude of Diablo Canyon Long-Term Seismic Program, Horizontal & Vertical Ground Motions as Described in SSER 34."

DISTRIBUTION CODE: D031D COPIES RECEIVED:LTR 1 ENCL 2 SIZE: 1+39
TITLE: Diablo Canyon Long-Term Seismic Program

NOTES: See Reports

	RECIPIENT ID CODE/NAME	COPIES LTTR	COPIES ENCL	RECIPIENT ID CODE/NAME	COPIES LTTR	COPIES ENCL
	PD5 LA	1	0	PD5 PD	1	1
	ROOD,H	2	2			
INTERNAL:	ACRS	6	6	ADM/LFMB	1	0
	NRR ASHAR,H	1	1	NRR BAGCHI,G	1	1
	NRR JENG,D	1	1	NRR PICHUMANI,R	1	1
	NRR ROTHMAN,R	1	1	NRR/DST 8E2	1	1
	NRR/PMAS/ILRB12	1	1	OGC/HDS1	1	0
	REG FILE 01	1	1	RES/DE/SSEB/SES	1	1
EXTERNAL:	NRC PDR	1	1	NSIC	1	1

RIDS/ADDS

RIDS/ADDS

NOTE TO ALL "RIDS" RECIPIENTS:

PLEASE HELP US TO REDUCE WASTE! CONTACT THE DOCUMENT CONTROL DESK, ROOM P1-37 (EXT. 20079) TO ELIMINATE YOUR NAME FROM DISTRIBUTION LISTS FOR DOCUMENTS YOU DON'T NEED!

TOTAL NUMBER OF COPIES REQUIRED: LTTR 23 ENCL ~~20~~ 18

Pacific Gas and Electric Company

77 Beale Street
San Francisco, CA 94106
415 973-4684

Gregory M. Rueger
Senior Vice President and
General Manager
Nuclear Power Generation

December 26, 1991

PG&E Letter No. DCL-91-313

U.S. Nuclear Regulatory Commission
ATTN: Document Control Desk
Washington, D.C. 20555

Re: Docket No. 50-275, OL-DPR-80
Docket No. 50-323, OL-DPR-82
Diablo Canyon Units 1 and 2
Long Term Seismic Program - Confirmation of Plant Seismic Margins

Gentlemen:

In the Diablo Canyon Supplemental Safety Evaluation Report 34 (SSER 34), the NRC Staff required that PG&E submit additional analyses to confirm Long Term Seismic Program (LTSP) conclusions that the seismic margins for structures and equipment at Diablo Canyon are adequate to accommodate the Staff's spectral estimates of horizontal and vertical ground motions defined in SSER 34. The results of these analyses are enclosed.

The confirmatory evaluations show that the overall plant seismic margin reported in the LTSP Final Report (July 1988) is not affected by Staff estimates of ground motion. The evaluations also show that the assumed increase in SSER 34 ground motions does not alter the conclusions of the probabilistic risk assessment reached in the LTSP Final Report. Submittal of these evaluations satisfies the open item in SSER 34 regarding Element 4 of License Condition 2.C.(7) of Facility Operating License DPR-80 for Diablo Canyon Unit 1.

Sincerely,

Greg Rueger /KBR

Gregory M. Rueger

cc: Ann P. Hodgdon
John B. Martin
Philip J. Morrill
Harry Rood (3)
Howard J. Wong
CPUC
Diablo Distribution

Enclosure

5449S/0085K/DWO/1587

D031

1/2

300095

9201060130 911226
PDR ADOCK 05000275
E PDR

ADEQUACY OF SEISMIC MARGINS ASSUMING AN INCREASE IN AMPLITUDE OF THE DIABLO CANYON LONG TERM SEISMIC PROGRAM HORIZONTAL AND VERTICAL GROUND MOTIONS AS DESCRIBED IN SSER 34

December 1991

Docket # 50-275
Accession # 9201060130
Date 12/26/91 of Ltr
Regulatory Docket File

This volume responds to confirmatory analysis asked of PG&E by the U.S. Nuclear Regulatory Commission (NRC) staff in their Safety Evaluation Report, Supplement No. 34, dated June 1991, to confirm PG&E's conclusions that the plant seismic margins are adequate to accommodate the horizontal and vertical spectral exceedances that result from use of the staff's estimates of horizontal and vertical spectra.

Pacific Gas and Electric Company

Diablo Canyon Power Plant
Long Term Seismic Program

ADEQUACY OF SEISMIC MARGINS ASSUMING AN INCREASE IN AMPLITUDE OF THE DIABLO CANYON LONG TERM SEISMIC PROGRAM HORIZONTAL AND VERTICAL GROUND MOTIONS AS DESCRIBED IN SSER 34

At the request of the U. S. Nuclear Regulatory Commission (NRC) Staff, PG&E submitted discussions of the effects on the Diablo Canyon Power Plant structures and equipment of an assumed increase in amplitudes of the Diablo Canyon Long Term Seismic Program (LTSP) 84th-percentile site-specific ground motions (PG&E, 1988) in the horizontal and vertical directions at certain discrete frequency ranges (PG&E, 1991 and PG&E, 1991a). The NRC Staff reviewed these submittals and accepted PG&E's conclusions that the plant seismic margins remained adequate to accommodate the postulated ground motion exceedances. However, in the Supplemental Safety Evaluation Report (SSER) No. 34, the NRC Staff required that PG&E perform analyses to confirm that the seismic margins are adequate to accommodate the Staff's estimate of spectral acceleration levels. We have performed the analytical evaluations; a summary of the results is provided below. Note that the evaluations consider simultaneous effects of horizontal and vertical components of earthquake motions.

INCREASE IN HORIZONTAL SPECTRAL AMPLITUDE

Figure 1 shows the 5 percent damped free-field horizontal ground motions as postulated by the NRC Staff in SSER 34 and as developed in PG&E, 1988. Both the median and the 84th-percentile nonexceedance probability spectra are shown. In both the SSER 34 and the PG&E, 1988, only the 84th-percentile site-specific ground motion was considered in the evaluation of plant seismic margins.

As shown in Figure 1, the PG&E, 1988 spectrum completely envelops the SSER 34 spectrum at frequencies greater than 1 hertz. However, below 1 hertz, the SSER 34 spectrum shows an increase in spectral amplitudes of about 10 to 20 percent over the LTSP spectrum. As stated in PG&E, 1991, no essential equipment or components have fundamental frequencies lower than 1 hertz. Therefore, an increase in the ground motion spectrum in the range of 1 hertz and below would have no impact on the seismic margins of essential equipment and components.

Likewise, none of the essential building structures or structural elements are in the frequency range below 1 hertz. However, the sloshing modes of outdoor water storage tanks have low frequency responses (in the range of 0.2 to 0.4 hertz), which caused PG&E to examine what effect, if any, could be expected by the increase in spectral amplitude. The refueling water storage tank, which is a typical example of outdoor water storage tanks, was analyzed to examine the effect on seismic margin of the SSER 34 spectral amplitude increases.

Refueling Water Storage Tank

The refueling water storage tank has a relatively high median capacity of 9.92 g* (Table 6-23 of PG&E, 1988), governed by overturning moment at the concrete/bedrock interface. The base overturning moment of tank structures results from the combined effects from two modes; the impulsive mode, which includes the tank inertia and the part of the fluid that is moving in unison with the tank, and the sloshing mode. The impulsive mode typically has a much higher frequency (7.6 hertz) response and contributes significantly more to the overall demand than does the sloshing mode. A horizontal spectral amplitude increase in the range of 1 hertz and below has no effect on the dominant impulsive mode.

---

* Capacities of plant structures and equipment are expressed in terms of site-specific horizontal spectral acceleration averaged over 3 to 8.5 hertz frequency range ($\bar{S}_{a\ 3\ to\ 8.5\ hertz}$)

Revised fragility estimates for the refueling water storage tank were made by considering the increased effect due to the tank sloshing mode. These revised fragilities are compared with the original estimates (PG&E, 1988) in Table 1. There is a small reduction in the High-Confidence-of-Low-Probability-of-Failure (HCLPF) value; however, the seismic margin remains high and the overall plant margin is therefore not affected.

Table 1

COMPARISON OF FRAGILITY ESTIMATES

Refueling Water Storage Tank

	Median $\bar{S}_a$	HCLPF$_{50}$	HCLPF$_{84}$	Scale Factor[1]
LTSP 1988	9.92 g	3.40 g	4.08 g	2.10
SSER 34	9.54 g	3.27 g	3.92 g	2.02

Note:

[1]Demand $\bar{S}_{a\ 3\ \text{to}\ 8.5\ \text{hertz}}$ = 1.94 g

INCREASE IN VERTICAL SPECTRAL AMPLITUDE

Figure 2 shows the 5 percent damped free-field vertical ground motion developed by PG&E in PG&E, 1988. Both the median and the 84th-percentile nonexceedance probability spectra are shown. The NRC Staff postulated a vertical ground motion that, for the 84th-percentile spectrum, exceeds the PG&E, 1988 spectrum in the frequency range 1 to 10 hertz by 15 percent. The NRC Staff spectrum (SSER 34) is shown as a broken line in Figure 2 and extends between the frequencies of 1 and 10 hertz.

EQUIPMENT AND COMPONENTS

There are two factors that determine which essential equipment and components are affected by the vertical spectral increases. First, components having vertical natural frequencies in the 1 to 10 hertz range, and, second, components supported at locations where the structural floor slab vertical frequency falls within the 1 to 10 hertz range. Based on this component screening criteria, the following nine components were identified for assessment:

- NSSS Piping
- Main Steam PORV
- Diesel Generator Fuel Oil Day Tank
- 4.16 Kv Switchgear
- 4.16 Kv Potential Transformer
- Safeguard Relay Panel
- Impulse Lines
- Balance of Plant Piping and Supports
- Conduits, Cable Trays, and Supports

A summary discussion of analytical evaluations of the effect of the SSER 34 spectral amplitude increase on these components is given below:

NSSS Piping

The fragility evaluation of NSSS piping established that the median spectral acceleration capacity was "high", i.e., greater than 10 g (PG&E, 1988). The critical seismic stresses in NSSS piping are due to bending moment in the pipes associated with loadings from the attached equipment components (the steam generator and the reactor coolant pump) resulting from seismic effects in the horizontal direction. The vertical natural frequencies of the steam generator and the reactor coolant pump are 23 hertz and 20.6 hertz, respectively, which are well beyond the frequency range where the spectral increases are identified. Therefore, a 15 percent increase of the PG&E, 1988 vertical ground spectrum in the 1 to 10 hertz frequency range does not impact the fragility of the NSSS piping.

Main Steam Power Operated Relief Valves

Piping attached to the main steam power operated relief valves (PORVs) has vertical frequencies in the 10 to 20 hertz range. Thus, vertical seismic loads generated from attached piping and transmitted to the PORVs are unlikely to be affected by spectral acceleration increases in SSER 34 . In addition, the main steam PORVs are mounted in a vertical position and are primarily sensitive to horizontal accelerations. Therefore, an increase in the PG&E, 1988 vertical ground spectrum in the 1 to 10 hertz frequency range does not affect the fragility of the main steam PORVs.

Diesel Generator Fuel Oil Day Tank

The fragility evaluation of the diesel generator fuel oil day tank showed the median spectral acceleration capacity greater than 10 g (PG&E, 1988). The critical failure mode is associated with bending of the tank flat bottom plate. The vertical frequency of the tank is 10.4 hertz and the critical failure mode is governed entirely by the vertical excitation. In the fragility evaluation, the seismic load was conservatively based on a vertical spectral acceleration at the peak frequency, further increased by a factor of 1.5 to allow for variations in the frequency of the tank due to the depth of the fuel oil and possible higher modes. While an increase in the vertical spectrum in the 1 to 10 hertz range does increase the seismic stress, the median spectral acceleration capacity of the tank still remains higher than 10 g. Therefore, we conclude that a 15 percent increase over the PG&E, 1988 vertical ground spectrum in the 1 to 10 hertz range has an insignificant effect on the seismic capability of the diesel generator fuel oil day tank.

4.16 Kv Switchgear

The vertical frequencies of 4.16 Kv switchgear are greater than 33 hertz for the structural failure mode and between 19 and 21 hertz for the functional failure mode. The switchgears are, however, located at turbine building elevation 119 feet, where the flexible floor slab has a fundamental vertical frequency in the 7 to 8 hertz range. Thus, an increase in the vertical ground spectrum in the 1 to 10 hertz range affects the switchgear through the local floor response. The structural failure mode of the switchgear corresponds to a bending failure of the switchgear carriage rod, which is controlled only by the horizontal response and which has a negligible contribution from the vertical excitation. Therefore, the structural failure mode is not affected by any increase in spectral accelerations of the vertical ground spectrum.

On the other hand, the functional failure mode, associated with chatter of the General Electric IAC 53 protective relay, is attributable to the vertical excitation alone. The functional failure mode fragility

capacity factor was evaluated by comparing the Generic Equipment Ruggedness Spectra for the IAC 53 with the demand vertical spectral acceleration obtained at the location of the relay.

The functional failure mode fragility for the 4.16 Kv switchgear, as revised to include the effect due to the SSER 34 vertical ground spectrum, is compared below with the fragility value previously reported in PG&E, 1988.

LTSP 1988		SSER 34	
Median $\bar{S}_a$	= 3.53 g	Median $\bar{S}_a$	= 3.06 g
β_R	= 0.35	β_R	= 0.35
β_U	= 0.25	β_U	= 0.25
$HCLPF_{50}$	= 1.31 g	$HCLPF_{50}$	= 1.14 g
$HCLPF_{84}$	= .1.57 g	$HCLPF_{84}$	= 1.37 g

We note that the functional failure mode capacity is reduced as a result of an increase of 15 percent in spectral accelerations of the PG&E, 1988 vertical ground response spectrum. However, since the functional failure of the 4.16 Kv switchgear is recoverable by operator action, the plant seismic margin remains unchanged. In the discussion of the turbine building floor system at elevation 119 feet later in this document, the effect of deflection of the floor on the functionality of the switchgear is described.

4.16 Kv Potential Transformers

Similar to the 4.16 Kv switchgear, the fundamental vertical frequencies of the 4.16 Kv potential transformers are also very high. This equipment is also supported on the turbine building floor slab at elevation 119 feet, which has a vertical frequency in the range of 7 to 8 hertz. As a result, the increase in the SSER 34 vertical ground spectrum over the PG&E, 1988 spectrum at the frequency of the floor slab would increase the floor slab response, which in turn would affect the equipment fragility. In the fragility evaluation, two configurations were included: Bus F, which has three cabinets on a single stand and Buses G and H, which have two cabinets on a single stand. The vertical frequency of the three-cabinet stand is 33.7 hertz, while the vertical frequency of the two-cabinet stand is greater than 50 hertz. For both configurations, the critical failure mode corresponded to failure of the fillet weld anchoring each support leg to the floor embedment plate, for which the contribution of the vertical earthquake component is relatively small. The revised fragility evaluation showed that the fragility capacity remained very high, i.e., above 10 g. Therefore, the increased vertical ground spectral accelerations do not affect the fragility value of the 4.16 Kv potential transformers reported in PG&E, 1988.

Safeguard Relay Panel

The safeguard relay panel is also supported on the turbine building elevation 119 feet floor slab, similar to the 4.16 Kv switchgear and the potential transformers. Thus, the increased vertical ground spectral accelerations affect the panel through the local structure response. In the fragility evaluation reported in PG&E, 1988, the critical failure mode is associated with failure of the anchor welds.

By incorporating the 15 percent increase in the vertical spectral acceleration, the seismic demand load is increased. However, since the vertical response of this component makes a small contribution to the critical stress, the net effect on the median spectral acceleration and HCLPF capacities is very small. A comparison of the fragility reported in PG&E, 1988 with the values obtained using the 15 percent increase in the vertical ground spectral accelerations is shown below:

LTSP 1988	SSER 34
Median $\bar{S}_a$ = 10.76 g	Median $\bar{S}_a$ = 10.70 g
β_R = 0.34	β_R = 0.34
β_U = 0.36	β_U = 0.36
$HCLPF_{50}$ = 3.39 g	$HCLPF_{50}$ = 3.37 g
$HCLPF_{84}$ = 4.07 g	$HCLPF_{84}$ = 4.04 g

Impulse Lines

The potential failure of impulse lines is related to their excessive deflections as a result of interactions with equipment and components to which the lines are connected. Since the lines typically have small diameters, failure is not associated with inertial loads on the lines. The components in the vicinity of the impulse lines, which were included in the fragility evaluation, have median spectral acceleration capacities in the range of 7 g to 9 g. In addition, these components have vertical frequencies that are greater than 10 hertz and failure modes that have negligible contributions for the vertical excitation. Therefore, we conclude that since the failure of impulse lines is not controlled by their inertial loads and the nearby components are not sensitive to the vertical excitation, the fragility of impulse lines is not affected by vertical spectral accelerations exceeding the LTSP 84th percentile spectrum in the 1 to 10 hertz range.

Balance of Plant Piping and Supports

As discussed in PG&E, 1988, a generic fragility was developed for the balance of plant piping based on pipe support design specifications for allowable stresses corresponding to various loading conditions and failure modes. The critical failure mode is associated with failure of fillet welds in pipe supports. As discussed in PG&E, 1988, a frequency range of 6 to 20 hertz was judged to envelope the probable piping frequencies. In addition, in the fragility evaluation, it was found that the piping systems with a frequency of 8 hertz show the least relative factor of safety. Therefore, the fragility for the balance of plant piping is affected by the increase in the vertical ground spectral accelerations in the 1 to 10 hertz range.

By incorporating the increased vertical spectral accelerations, the median spectral acceleration capacity and the HCLPF value are reduced approximately 5 to 6 percent. The results reported in PG&E, 1988 are compared with evaluations for SSER 34 below.

LTSP 1988	SSER 34
Median $\bar{S}_a$ = 11.03 g	Median $\bar{S}_a$ = 10.34 g
β_R = 0.40	β_R = 0.40
β_U = 0.39	β_U = 0.38
$HCLPF_{50}$ = 3.00 g	$HCLPF_{50}$ = 2.85 g
$HCLPF_{84}$ = 3.60 g	$HCLPF_{84}$ = 3.42 g

Cable Trays, Conduit, and Supports

As discussed in PG&E, 1988, flexible cable tray systems will not fail. For cable trays, conduit, and supports, a generic fragility was developed based on the seismic qualification analyses for typical cable tray supports located at various elevations in the auxiliary building and the containment building.

As shown in Table D-1 of Kipp, 1989, the contribution of the vertical excitation to the critical stress

ranged up to 95 percent and the vertical frequencies ranged from 6 to 35 hertz. However, for each of the typical supports, the vertical frequency ranged from 18.9 hertz to greater than 33 hertz. The low frequencies reported in PG&E, 1988 correspond to vertical modes of the cable trays themselves rather than the supports; the important frequencies for the cable tray supports fall outside of the 1 to 10 hertz range. While some vertical frequencies of the cable trays may fall into the 1 to 10 hertz range, the trays themselves are expected to perform well as demonstrated by previous tests on cable tray systems, which stayed intact and remained functional well above the design amplitude of motion (Linderman, 1981). Therefore, vertical ground spectral accelerations exceeding the LTSP 1988 spectrum in the 1 to 10 hertz range will have minor effect on the fragility values in PG&E, 1988 and Kipp, 1989, where it was reported that cable trays and supports have high capacity, i.e., greater than 10 g.

STRUCTURES AND STRUCTURAL ELEMENTS

The plant seismic margin assessment based on probabilistic methods described in PG&E, 1988, and later bench-marked by deterministic assessments in PG&E, 1990, established that shear walls are the governing elements that control seismic capacities of major civil structures. These walls are primarily horizontal earthquake resisting elements; also, the shear walls are rigid in the vertical direction having frequencies much greater than 10 hertz. We, therefore, conclude that there would be no effect of an increase in the LTSP 1988 vertical ground spectrum in the 1 to 10 hertz frequency range on the seismic capacity of major structures.

Vertical earthquake motions, however, may have some effect on parts of structures, such as flexible floors and floor beams. These vertical load carrying elements are usually controlled by ductile bending behavior, which is accompanied by a large inelastic energy absorption capability. Thus, these types of structural elements are highly unlikely to fail; however, it is necessary to examine supported equipment important to plant safety to see the effects of the attendant motions. Based upon these considerations, we have identified two vertically flexible slab systems for analysis to examine the effect of the SSER 34 spectrum. These are the control room roof slab located in the auxiliary building and the 4.16 Kv switchgear area floor slab located at elevation 119 feet in the turbine building.

Auxiliary Building Control Room Roof Slab

The auxiliary building has 11 vertically flexible slabs; however, the control room roof slab located at elevation 163 feet is the only slab that has a fundamental frequency in the vertical direction in the range of 1 to 10 hertz. Figures 3 and 4 show respectively the plan and section of the control room roof slab. As shown in Figure 3, the 3 feet-4 inch thick reinforced concrete slab is supported by embedded structural steel beams with a span of 57 feet and with end moment restraints provided by reinforced concrete shear walls. Attachments to the slab consist of light-weight lighting fixtures and ceiling tiles. These components are suspended from the underside of the slab via a grid of unistrut steel channels welded to insert plates embedded in the slab. The insert plates are anchored to the slab by steel flat bars that are welded to the bottom flange of the embedded steel beams. A few HVAC ducts are also attached to the slab by concrete expansion anchors.

The seismic margin evaluation of the slab was performed by using the conservative deterministic failure margin (CDFM) approach discussed in attachment DE-Q6A of PG&E, 1990. As described in PG&E, 1990, the seismic margin factor, which represents the amount by which the deterministic spectrum (in this case SSER 34) can be scaled to produce a demand equal to the HCLPF capacity of a structure or component, is given by the elastic scale factor times a factor F_μ. The elastic scale factor is the factor by which the deterministic spectrum can be scaled to produce a demand equal to the yield capacity of the structure or component, and F_μ is the CDFM inelastic energy absorption factor.

Progressive softening of the slab due to concrete cracking and development of plastic hinges at the end restraints of the slab together with formation of a plastic hinge near the midspan results in a fundamental frequency of the slab of about 5 hertz. The elastic scale factor was computed from the slab response just before a mechanism is formed. Capacities were based upon composite construction provisions of the Load and Resistance Factor Design Specification of the AISC.

The inelastic energy absorption factor was determined as a function of target displacement beyond yield displacement (i.e., ductility, μ) by using the Riddell-Newmark approach. For the control room roof slab, the ductility of the system is directly related to the ultimate displacement of the slab near midspan. The HCLPF value of the ultimate displacement of the slab is based upon structural capability considerations. The inelastic rotation capacity limit specified in the ACI 349 code is considered to be a HCLPF value.

For floors subjected to a significant gravity load, however, it is necessary to account for ratcheting behavior of the slab or beam when estimating the system ductility. Ratcheting refers to the progressive downward displacement that occurs following multiple seismic load reversals in the inelastic range and has the effect of reducing the available ductility of the system. To account for this behavior, a reduced effective ductility value was used in the inelastic energy absorption calculation. The process is described in Appendix A.

A sensitivity study was performed to investigate the variation of the seismic margin with displacement. The results are shown in Figure 5. We note that, at a seismic margin factor of 1.64 that corresponds to the auxiliary building seismic margin reported in PG&E, 1988, the displacement of the slab is only about 4 inches near the center of the 57-feet span. This displacement is less than about 0.6 percent of the slab span (i.e., span over 120) and corresponds to a member ductility of about 3. This can be compared to a ductility limit of about 9 determined from the rotation capacity specified in the ACI 349 code. At such small displacements, no significant degradation of the capability of anchored components is expected. We, therefore, conclude that the control room roof slab has an acceptable seismic margin over the SSER 34 vertical ground motion spectrum.

Turbine Building Floor System at Elevation 119 feet

The turbine building houses portions of three major safety-related systems: the emergency diesel generators, 4.16 kV switchgear, and the component cooling water heat exchangers. The emergency diesel generators and the component cooling heat exchangers are supported on the basemat. The diesel generator silencers at elevation 107 feet and the 4.16 kV switchgear at elevation 119 feet are located on floor systems that consist of reinforced concrete slabs supported by structural steel beams. Both floors have similar frequency responses in the vertical direction, with the fundamental mode in the 1 to 10 Hz range, and have seismic demands that are dominated by vertical ground motion. Of these two slabs, the 4.16 kV switchgear floor is located at a higher elevation, and hence has higher amplification of response. The switchgear floor also supports equipment that are more displacement sensitive, more massive, and is, therefore, subjected to greater seismic demands. Thus, the switchgear floor at elevation 119 feet was selected for evaluation.

The switchgear floor consists of a 10-inch thick reinforced concrete slab supported by compact wide flange structural steel beams and columns (Figures 6 and 7). Welded studs are used to anchor the slab to the steel beams. Thus, the concrete slab provides continuous lateral support to the compression flanges of the supporting beams. The switchgear panels are arranged in three rows that are separated by masonry walls. In addition to the building columns shown in Figure 7, the columns supporting masonry walls along column lines 3 and 4, from E.2 to G, and connected to the slabs at Elevations 119 feet and 140 feet by through bolts, also provide mechanisms for load transfer between the two floors. Note that the

connections of columns along column lines 3 and 4 to the slabs at the top and the bottom, were made during the Hosgri reevaluation in order to connect the two floors, and thus, to reduce the response of the slab at elevation 119 feet.

The seismic margin evaluation was performed by using the (CDFM) approach. It was determined that the beams along column lines 2 and 3, from E.2 to G, that support masonry partition walls on each side of Bus "G" panels, were the controlling structural elements, whose failure was governed by bending (ductile behavior). Since the steel columns supporting the masonry wall along column line 2 are not connected rigidly to the floors above and below, the beam along column line 2 does not receive any support from the beam above. However, the floor beam along column line 3 acts in unison with the floor beam at elevation 140 feet; thus, the elastic scale factor for this combined system was calculated by considering the total seismic demand and their combined capacities.

The evaluation of the structural steel beams, and consequently the switchgear floor system, consisted of performing a sensitivity study wherein seismic margins (i.e., the scale factors by which the input vertical ground motion would have to be raised) corresponding to specific target displacements (or, pre-assigned ductilities) were calculated. The calculations accounted for the ratcheting effect due to dead load in accordance with the procedure described in Appendix A.

Figure 8 shows the results of the sensitivity study where the seismic margin factor is plotted against the ultimate target displacement of the floor. We observe that, for a seismic margin factor of 1.45, which is approximately the seismic margin of the turbine building reported in PG&E, 1990, the maximum displacement of the switchgear floor is about 1.7 inches. This displacement is equivalent to a member ductility of about 2 which can be compared to a value of 10, corresponding to a structural capability limit given by the AISC commentary to the Load and Resistance Factor Design specification. We have evaluated the switchgear cabinets for such a postulated displacement of the supporting floor of 1.7 inches. The evaluation is described below.

IMPACT OF TURBINE BUILDING FLOOR DEFLECTION ON 4.16 KV SWITCHGEAR

The 4.16 kV switchgear is an assembly of 4.16 kV magneblast circuit breakers, buses, insulators, wiring, control, and protecting and monitoring devices that are contained in a metal-clad enclosure. Power is made available to all load circuits through three electrically contiguous and high conductivity buses running through the entire length of the switchgear. At each cubicle a vertical tap is made for connection to the circuit breaker. The breaker is held in place by a cradle that prevents it from falling under severe conditions of vertical and horizontal seismic conditions.

The maximum displacement of 1.7 inches is reduced by the dead load displacement of 0.3 inch to obtain the differential displacement of 1.4 inches affecting the supported equipment. The 1.4 inches maximum sag of the switchgear floor, applicable to bus G, is equivalent to 0.2 inch dip of one edge of the 26-inch wide switchgear cubicle. A review and walkdown of the control and protective devices located in the switchgear cubicle, including relays, switches, fuses, terminal blocks and wiring, indicates that this deflection has no significant functional impact on these devices. Certain switchgear mounted relays could potentially trip the breaker due to chattering. Following the trip the breaker will stay open. Control room annunciation and indication of the breaker status will remain operational. After the event, realignment of the breakers can be made through operator control. Also, the copper buses have adequate flexibility so that small deflections will not affect the integrity of the bus and conductivity will be maintained.

The structural integrity of the 4.16 kV switchgear was evaluated for the combined horizontal and vertical seismic loads as well as the effect due to turbine building floor displacement. The results of the evaluation indicate that the switchgear will maintain its structural integrity with acceptable margin for loadings due to SSER 34 seismic spectra.

Note that each row of switchgear cabinets (see Figures 6 and 7) consist of several individual cabinets connected to one another in series by a line of bolts along their heights. These cabinets are thus structurally affected by the deflection of the supporting floor. In contrast, the other two equipment items, considered essential in LTSP risk assessment and margin studies, namely, the 4.16 kV potential transformer and the safeguard relay panel are individual units, and consequently, the effect of floor displacement on these equipment items is insignificant.

Fuel Handling Building Crane

In PG&E 1990, we reported results of the deterministic evaluation of the fuel handling building crane. As noted in that submittal, the crane was chosen for evaluation because its response is primarily governed by the vertical component of ground motion. The failure modes identified in PG&E 1990 lie within the frequency range from 1 to 10 hertz, and therefore, these failure modes are affected by the SSER 34 vertical spectrum.

We have reevaluated the fuel handling building crane for the SSER 34 spectra. The results are reported in Table 3, which shows that the fuel handling building crane continues to have an acceptable seismic margin over the SSER 34 vertical ground motion spectrum. Please note that, as stated in PG&E, 1990, the margins reported for the lifted case are very conservative because of the analysis methodology assumptions and low probability of a 125-ton lift concurrent with a significant seismic event.

Structural Steel Frames and Truss Systems - Pipeway Structure

The last class of structures that may potentially be affected by the vertical ground motion in the frequency range of 1 to 10 Hz are structural steel frame and truss systems. Effects of vertical seismic excitation on these types of structures are generally small compared to horizontal ground motion effects. Furthermore, steel framing systems are generally highly redundant and consist of elements that are usually controlled by ductile bending behavior, which is accompanied by large inelastic energy absorption capability.

We have selected the pipeway structure among the class of structures composed of structural steel framing and truss system for evaluation of increased vertical ground motion. In contrast to the structural steel roof truss system over the turbine building, certain safety-related systems are directly attached to the pipeway structure. For example, the pipeway structure provides support to the auxiliary feedwater pipe line as well as smaller piping and safety-related instrumentation tubing and conduits. The pipeway structure also supports the main steam and feedwater pipe lines between the containment and the auxiliary building. In addition, the pipeway holds pipe whip restraints designed to restrain pipes from whipping after a postulated pipe break.

The pipeway structure is a three-dimensional structural steel frame attached to the outside of the containment shell, the auxiliary building and the turbine building. Figure 9 shows locations of the Unit 1 and Unit 2 pipeway structures, which are basically similar to one another. The structure has five levels of plane frames with the main platform at elevation 109 feet (shown in Figure 10), and includes ten radial bents that cantilever out from the containment wall by horizontal beams and/or inclined beam columns. Connections between the pipeway structure and the auxiliary and the turbine buildings are provided with

slotted holes oriented such that horizontal forces cannot be transmitted between the pipeway structure and these adjacent buildings.

In a manner similar to that applied to the control room roof slab and the 4.16 kV switchgear floor, the pipeway structure seismic margin was evaluated by using the CDFM approach. Critical structural elements were identified for margin assessment on the basis of seismic capacity-to-demand ratios determined during the Hosgri reevaluation, as well as the importance of the members to the overall structural system. Capacities were determined by using the Load and Resistance Factor Design (LRFD) specification of the AISC. In some cases, CDFM capacities were taken to correspond to 1.7 times the AISC allowable stress, which is approximately at the first yield of a ductile member.

As noted previously, for ductile structural systems beyond the elastic yield limit, the seismic margin factor can be assessed by limiting the ultimate target displacement from consideration of functionality of supported systems and components. For the pipeway structure, however, we calculated the displacement corresponding to a preassigned seismic margin factor. Thus, to reach a seismic margin factor of 1.76, which is the seismic margin for balance of plant piping, beams along Bents 2B and 6.6B (see Figure 10) that become inelastic, displace vertically by up to about one inch. Long-span, flexible piping systems that are typically attached to the pipeway structure are expected to accommodate displacements of such small magnitude.

CONCLUSIONS

Based upon the confirmatory analysis described above, we conclude that the essential structures, equipment and components important to plant safety have adequate seismic margins to accommodate the NRC Staff's estimate of the horizontal and vertical ground motions shown in the SSER 34. We have also shown that the SSER 34 spectra have minor effects on the seismic fragility estimates of the structures and components. We can thus conclude that the assumed increase in amplitude of the Diablo Canyon LTSP 84th-percentile site-specific ground motions in the horizontal and vertical directions, shown in SSER 34, will not alter the conclusions of the probabilistic risk assessment (PG&E, 1988).

REFERENCES

U. S. Nuclear Regulatory Commission, June 1991, Safety Evaluation Report, related to the operation of Diablo Canyon Nuclear Power Plant, Units 1 and 2, Docket Nos. 50-275 and 50-323, NUREG-0675, Supplement No. 34.

Pacific Gas and Electric Company, 1991, Adequacy of seismic margins assuming an increase in amplitude of the Diablo Canyon Long Term Seismic Program horizontal ground motion in the frequency range below 2.5 hertz: PG&E Letter No. DCL-91-108.

Pacific Gas and Electric Company, 1991a, Adequacy of seismic margins assuming an increase in amplitude of the Diablo Canyon Long Term Seismic Program vertical ground motion in the frequency range from 2 to 10 hertz: PG&E Letter No. DCL-91-131.

Pacific Gas and Electric Company, 1988, Final Report of the Diablo Canyon Long Term Seismic Program: Docket Nos. 50-275 and 50-323.

Kipp, T. R., Wesley, D. A., and Nakaki, D. K., 1989, Seismic fragilities of civil structures and equipment components at the Diablo Canyon Power Plant, NTS Engineering Report No. 1643.02, Revision 0, Prepared for PG&E.

Pacific Gas and Electric Company, 1990, Additional deterministic evaluations performed to assess seismic margins of the Diablo Canyon Power Plant, Units 1 and 2: PG&E Letter No. DCL-90-226.

Linderman, R.B. and Hadjian, A.H., 1981, Development of Bechtel's electrical raceway system test program, Proceedings of the American Power Conference, Vol. 43.

Table 2

EFFECT OF INCREASE OF SPECTRAL ACCELERATIONS SHOWN IN SSER 34 FRAGILITIES OF AFFECTED EQUIPMENT AND COMPONENTS

(Based on Hazard Defined Over 3 to 8.5 Hertz Range)

EQUIPMENT/ COMPONENT	VERTICAL FREQUENCY (Hz)	SPECTRAL ACCELERATION CAPACITY							
		LTSP 1988				SSER 34			
		$\breve{S}_a$ (g)	β_R	β_U	HCLPF (g)	$\breve{S}_a$ (g)	β_R	β_U	HCLPF (g)
NSSS Piping	7-9	> 10.00				> 10.00			
Main Steam PORV	Piping 10-20	11.50	0.34	0.38	3.51	Unchanged			
Diesel Generator Fuel Oil Day Tank	10.4	> 10.00				> 10.00			
4.16 kV Switchgear*	> 33	3.53	0.35	0.25	1.31	3.06	0.35	0.25	1.14
4.16 kV Potential Transformer*	> 33	10.83	0.31	0.38	3.47	> 10.00			
Safeguard Relay Panel*	> 33	10.76	0.34	0.36	3.39	10.70	0.34	0.36	3.37
Impulse Lines	5-20	7.09	0.28	0.32	2.63	Unchanged			
Balance of Plant Piping and Supports	6-20	11.03	0.40	0.39	3.00	10.34	0.40	0.38	2.85
Conduits, Cable Trays, and Supports	6-35	> 10.00				> 10.00			

* Equipment supported on vertically flexible floor slab having vertical frequency less than 10 hertz.

Table 3

Fuel Handling Building Crane Seismic Margin Factors

Crane Element or Failure Mode	Lifted Load (tons)	Seismic Margin Factors	
		LTSP 1988	SSER 34
Cable	125	2.90	2.52
Bridge Girder	125	1.55	1.35
Bridge Resistance to Global Uplift	0	3.2	2.7
Trolley Resistance to Uplift	0	2.4	2.0

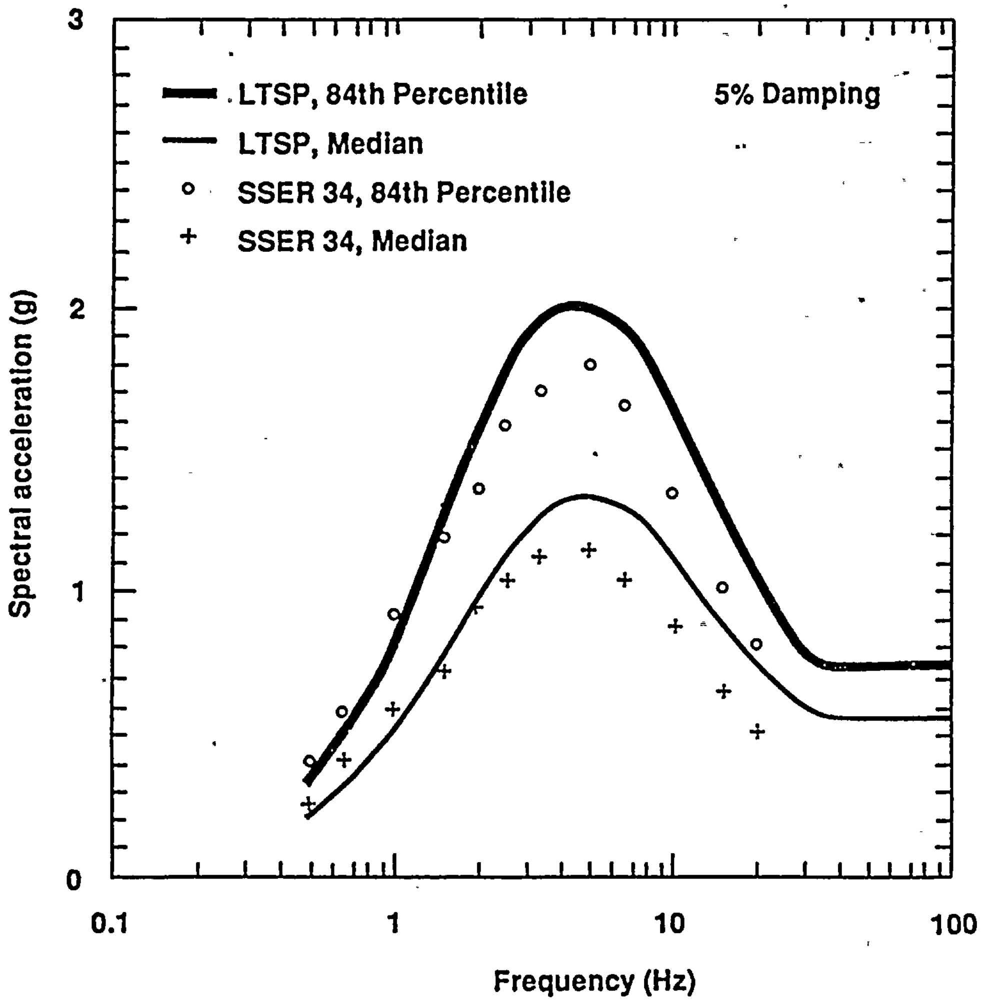

Figure 1

Site-speciifc horizontal ground motion response spectra.

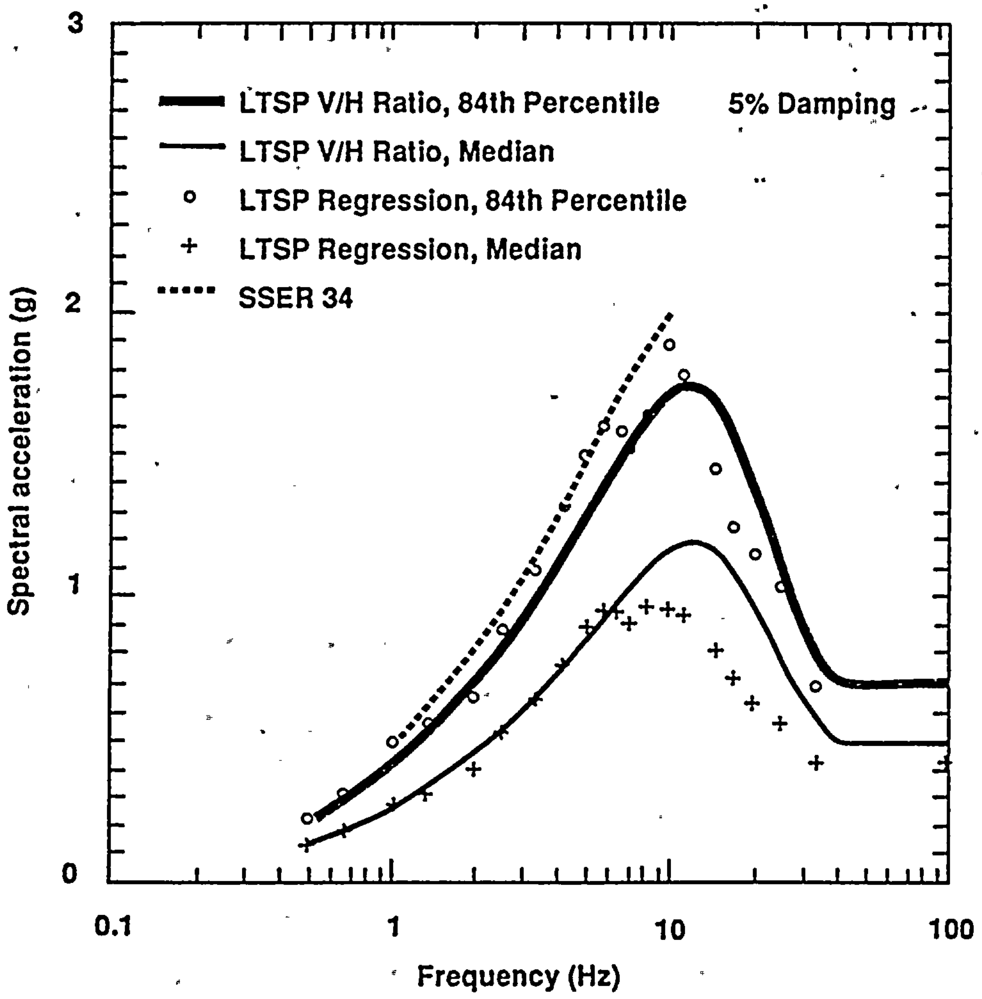

Figure 2

Site-specific vertical ground motion response spectra.

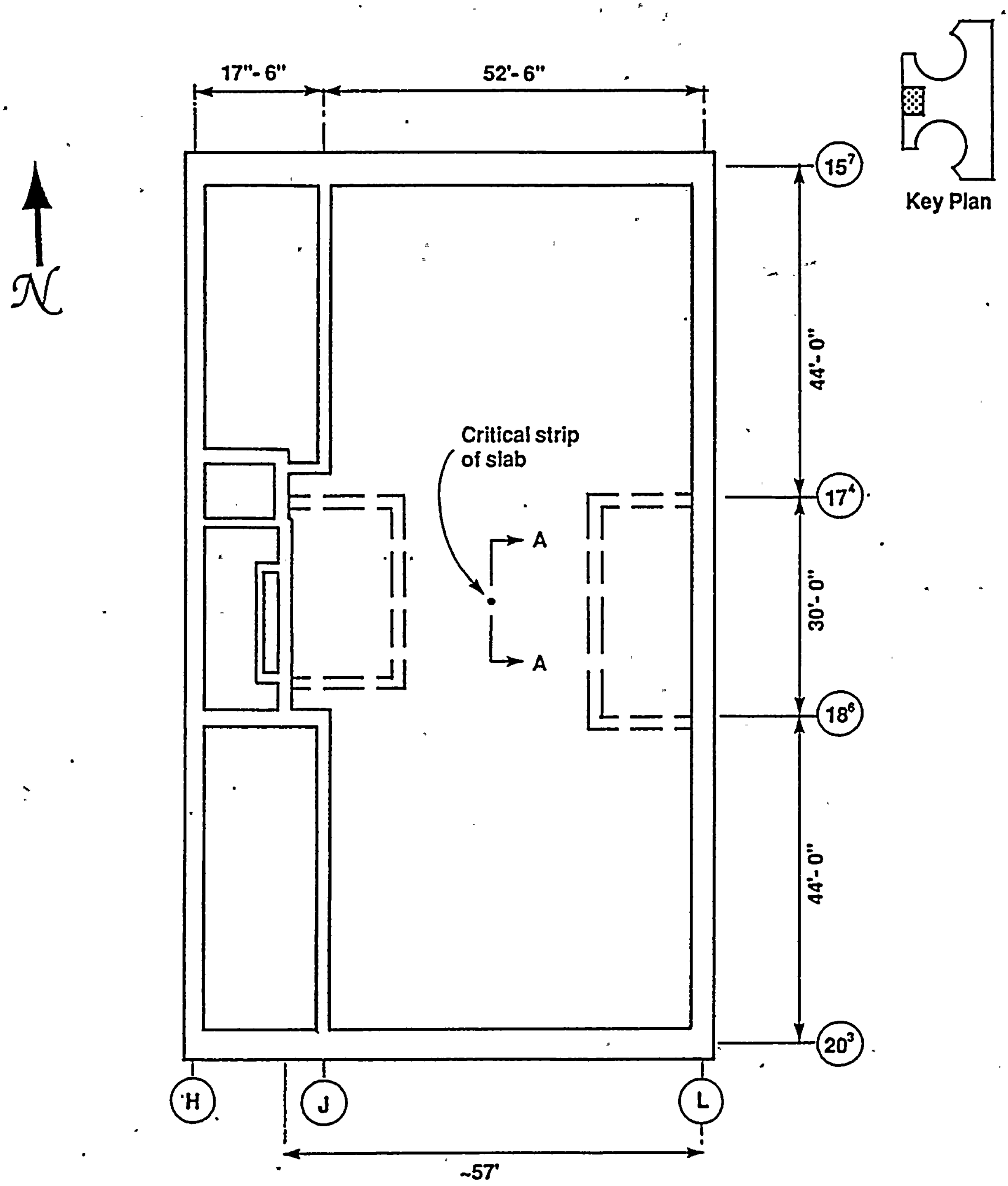

Figure 3

Auxiliary building control room roof slab.

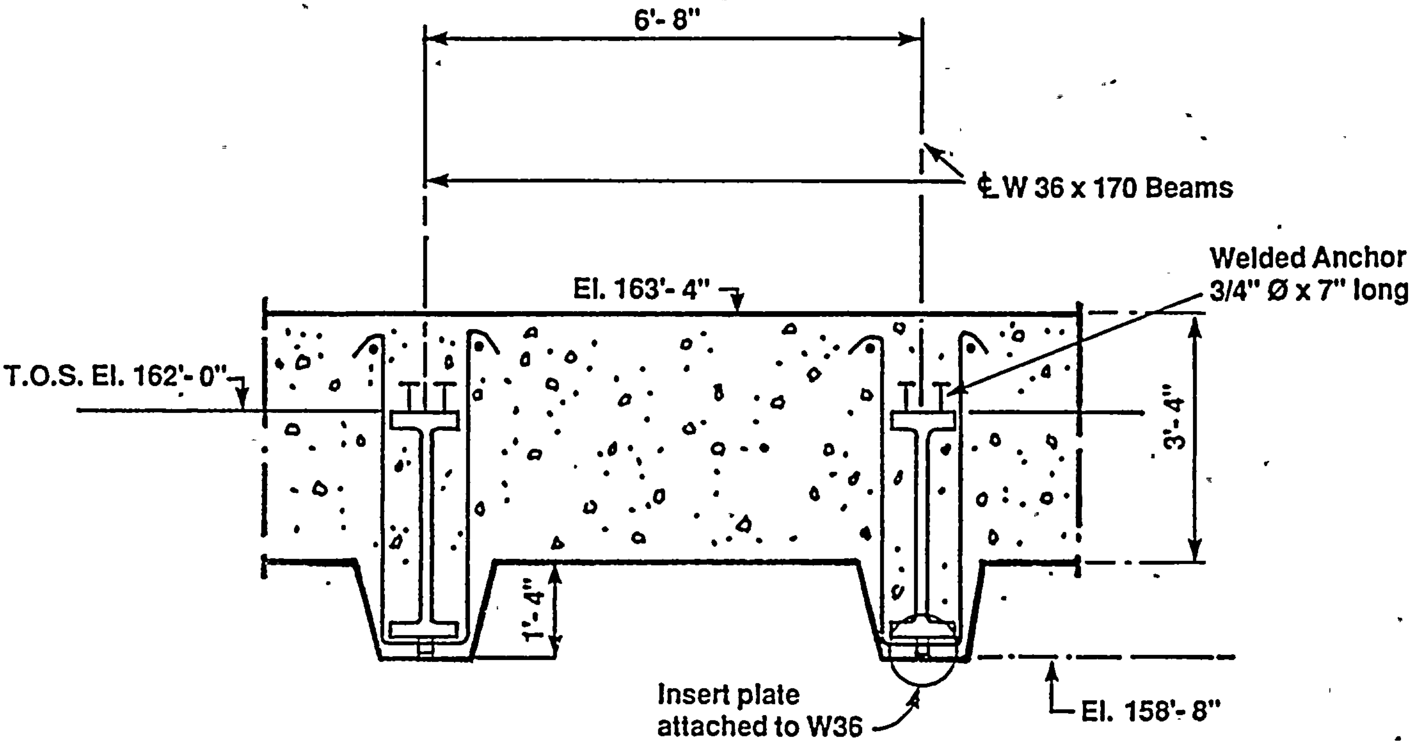

Section A - A

Figure 4

Auxiliary building control room roof slab. Section A - A

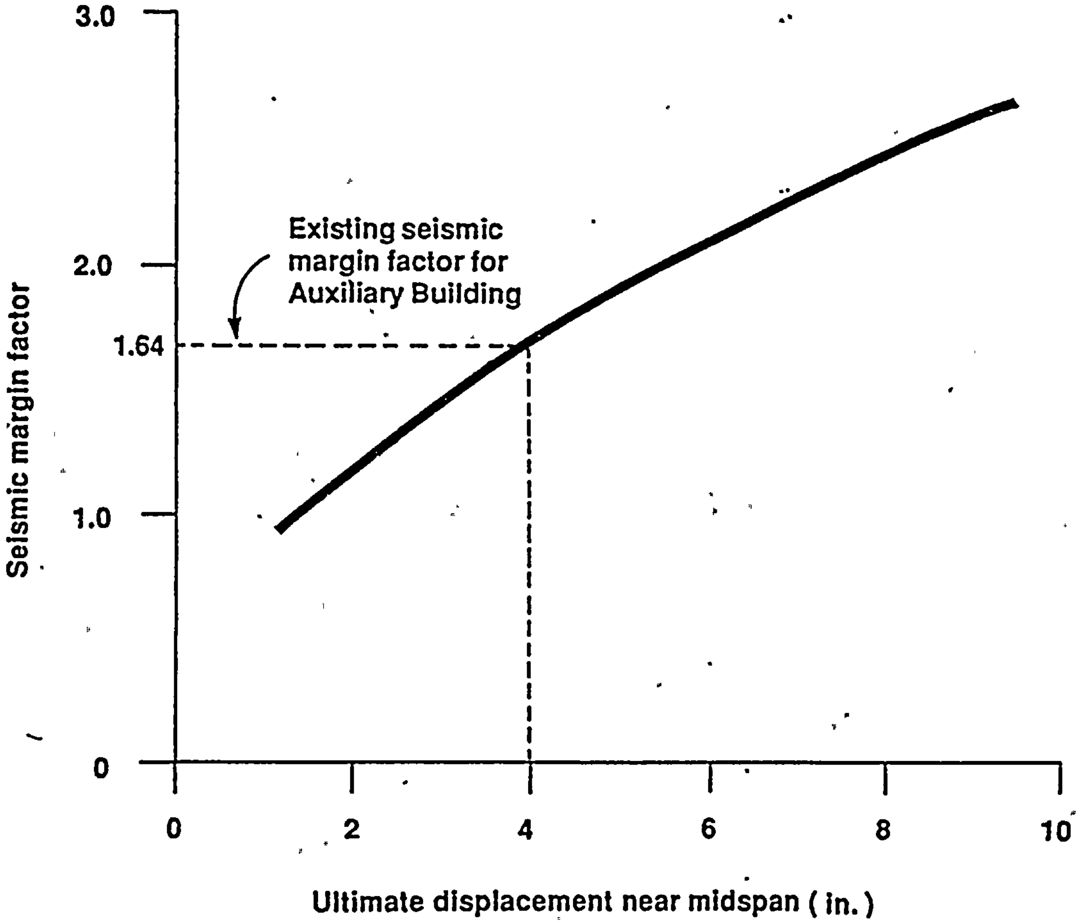

Figure 5

Ultimate displacement near midspan of control room roof slab vs. seismic margin factor.

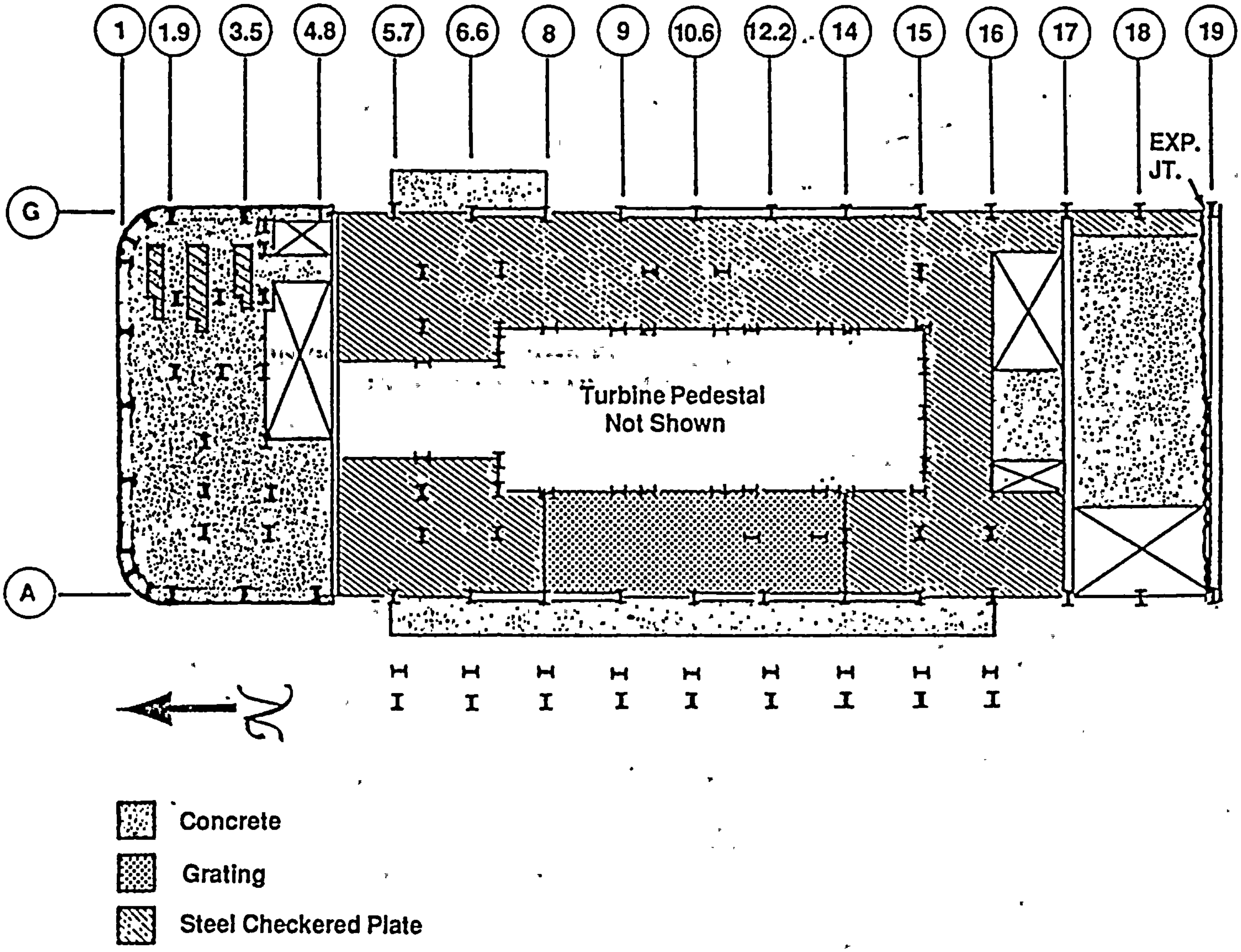

Figure 6

Unit 1 turbine biuilding plan at elevation 119 feet.

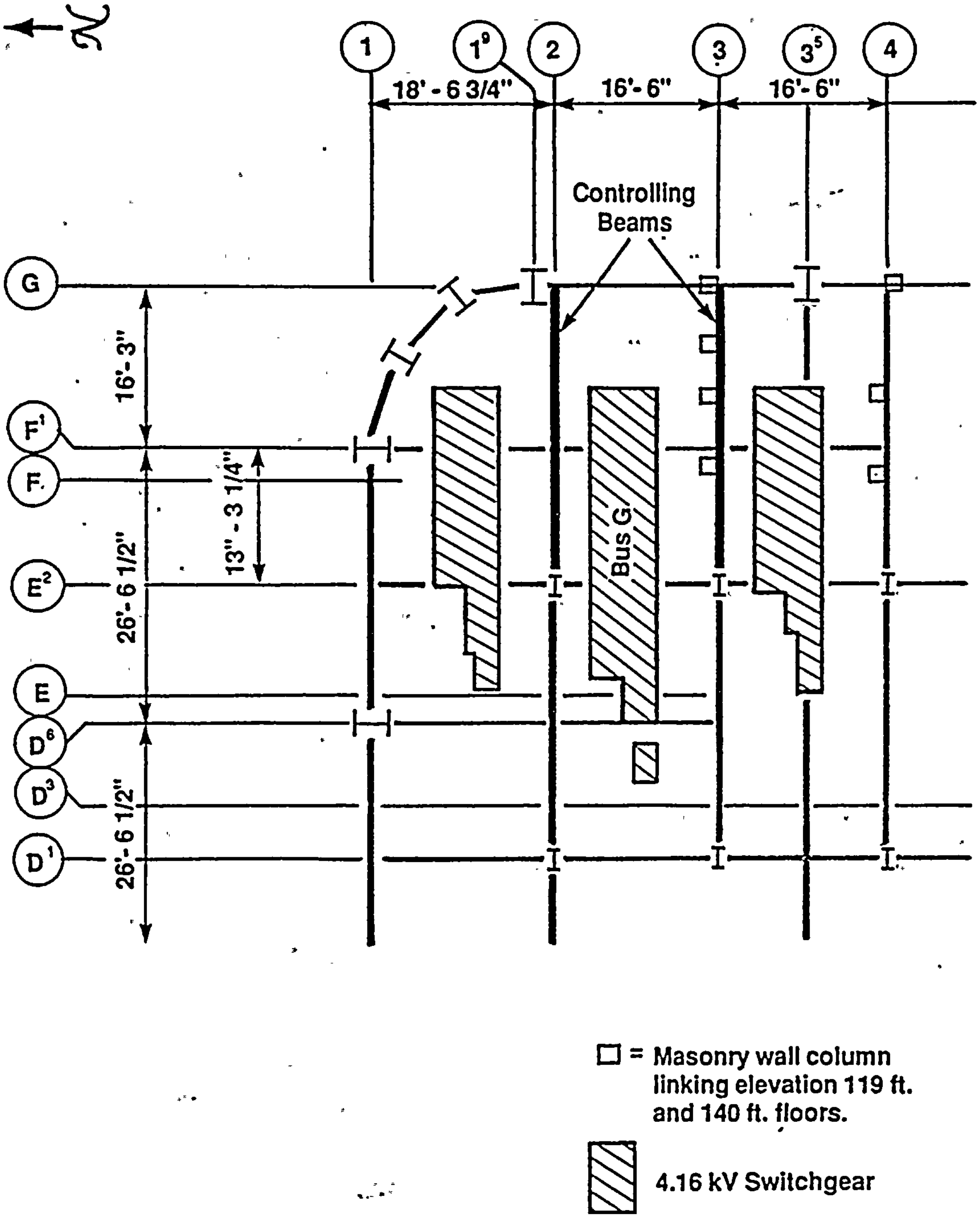

Figure 7

Turbine building 4kV switchgear floor partial plan.

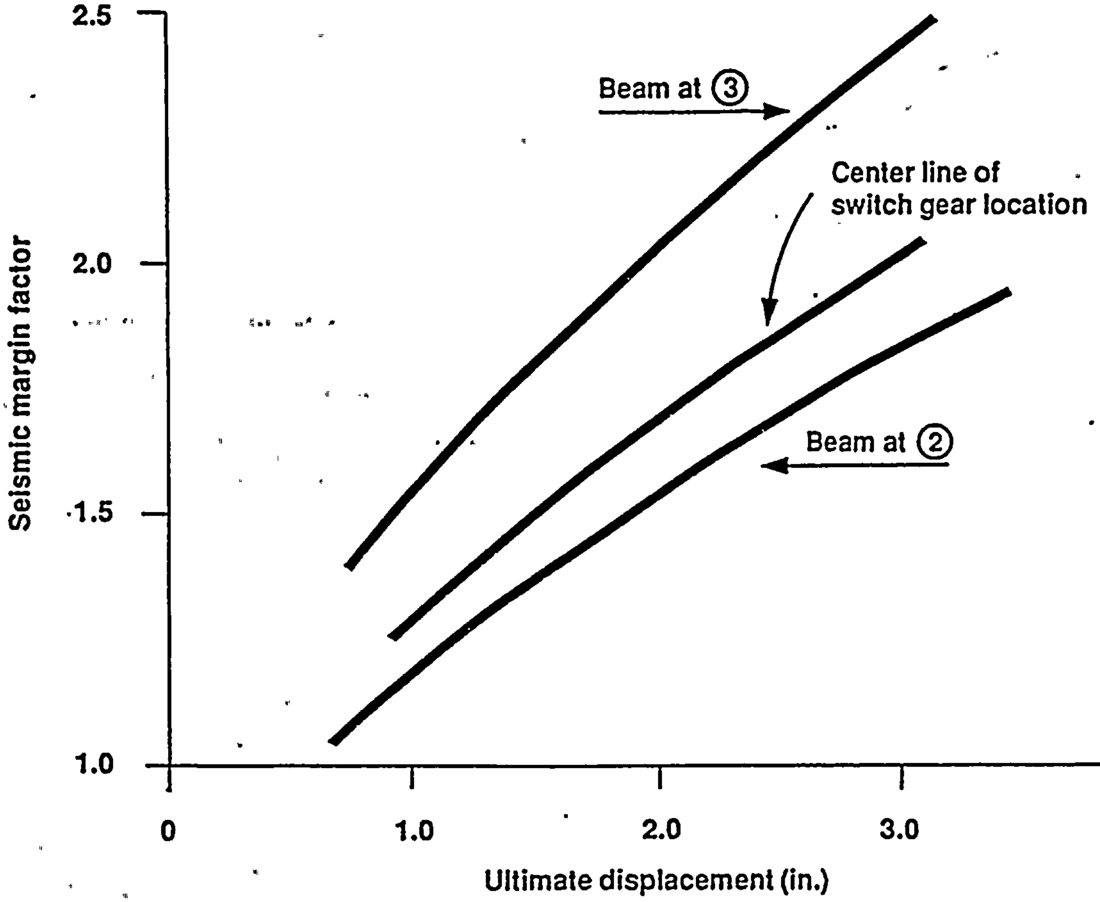

Figure 8

Ultimate displacement of floor beams vs. seismic margin factor.

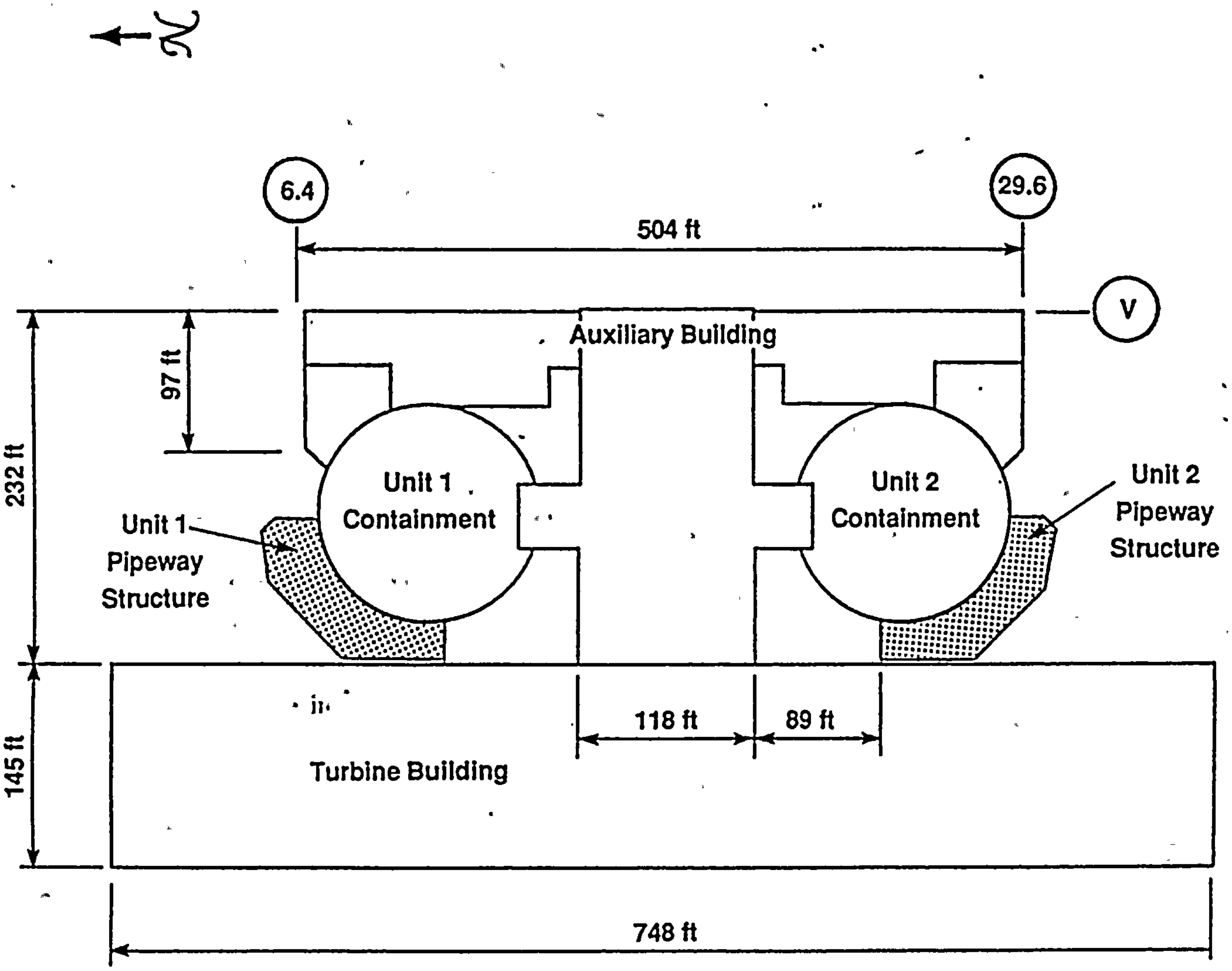

Figure 9

Power block structures with pipeway structures of units 1 and 2 highlighted.

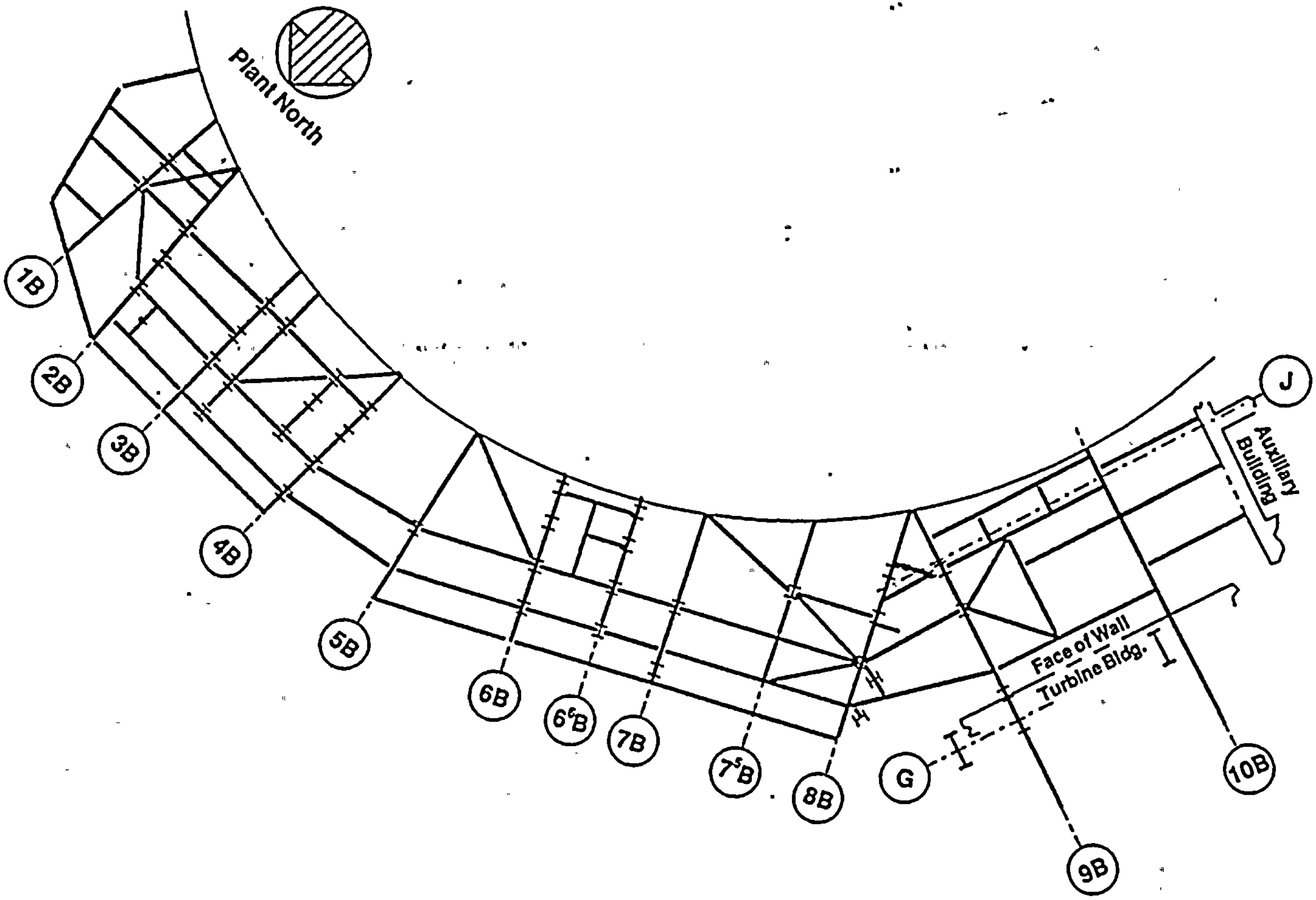

Figure 10

Unit 1 pipeway structure, platform at elevation 109 feet.

APPENDIX A

INVESTIGATION OF THE EFFECTS OF DEAD LOAD ON DUCTILITY OF FLOOR SYSTEM

December 1991

APPENDIX A

INVESTIGATION OF THE EFFECTS OF DEAD LOAD ON DUCTILITY OF FLOOR SYSTEM

Introduction

This report presents results of a study to investigate the effects of dead load on the inelastic energy absorption factor of floor systems. Previous testing and studies by others have demonstrated that both reinforced concrete and steel structures have significant capability to absorb earthquake energy inelastically at ground motion levels above the static strength. This increased capacity can be quantified by the ductility scale factor, F_μ, which scales the earthquake time history from the point at which static strength is reached to the *target level of ductility*.

The ductility scale factor was studied in Kennedy, 1984 for *vertically mounted* shear walls subjected to horizontal motions. Nonlinear analyses were performed and simplified procedures were developed and investigated in that report. Other simplified procedures for obtaining F_μ for *vertically-mounted* elements can be found in Riddell, 1979 and Reed, 1991.

Because of the constant downward pull on a horizontally-oriented structural element due to gravity, the nonlinear vertical displacement of a floor structure, when subjected to vertical motion, is biased downward. This ratcheting phenomenon reduces the ductility scale factor for a horizontal element compared to the case where the same element is mounted vertically and is subjected to horizontal motion.

The objective of this study was to develop a simple modification to the procedure for calculating the ductility scale factor for *vertically-mounted* components to calculate the F_μ factor for *horizontal elements*. This was achieved by first performing nonlinear time history analyses for *horizontally-* and *vertically-mounted* elements and then using the results to obtain a simplified procedure for including the effects of dead load.

Model and Procedure

The response of a concrete floor structure can be idealized as a one-degree-of-freedom (1-DOF) system since its response to seismic motion is predominantly due to the response of its fundamental mode. Figure A-1 shows the 1-DOF model mounted both vertically and horizontally. Also shown in Figure A-1 is the force-deformation relationship assumed for the model. This relationship is used for both orientations of the model.

The capacity of typical floor slabs in nuclear power plants, composed of both reinforced concrete and structural steel members, is due primarily to ductile flexural behavior. Since the slabs are under-reinforced, the capacity is controlled by the strength of reinforcing steel, not due to crushing of concrete. This leads to full hysteretic loops where there is very little, if any, cyclic strength or stiffness degradation. Thus, the force-deformation curve is assumed to be bilinear with a small amount of strain-hardening to reflect the characteristics of both structural steel members and reinforcing steel, as shown in Figure A-1.

The time history used in the analysis is the modified Pacoima Dam vertical record used in the Diablo

Canyon Long Term Seismic Program (PG&E, 1988). Figures A-2 and A-3 show plots of the time history and the 5-percent damped response spectrum for this time history, respectively. The absolute level of the input time history is not significant since F_μ is equal to the earthquake scale factor required to reach the capacity corresponding to the desired ductility level divided by the scale factor to reach yield. Thus, the absolute level of the input time history cancels out.

Two fundamental frequencies for the models, one at 4 hertz and the other at 7 hertz, were analyzed to reach three levels of ductility, μ. The values assigned to μ were 2, 5 and 10, μ being the ratio of the displacement at the desired ductility level to the displacement at yield (see Figure A-1). The damping was assumed to be 7 percent of critical, although additional sensitivity studies were performed to show that the ductility scale factor was only weakly influenced by the elastic damping value. Tangent stiffness-proportional damping was assumed, which implied that, beyond yield, the damping was almost equal to zero (i.e., 0.03 x 7 percent equals 0.2 percent). Finally, for all cases where the model was mounted horizontally the dead load stress was fixed at 30 percent of the yield level. This level is representative of the dead load stress level for typical floor slabs at the Diablo Canyon Plant.

Procedure and Results of Nonlinear Analysis

Nonlinear analyses were performed using the computer program DRAIN2D (Kannan, 1973, revised 1985). The bilinear truss model was used to simulate the inelastic behavior of the model, and a time step of 0.001 second was used for all computer runs.

A target displacement corresponding to an assigned value of ductility μ, was chosen and an iterative procedure was followed to determine the level of earthquake time history required to create the target displacement. Certain features in DRAIN2D ensured convergence of the iterative process in about 5 to 10 iterations.

Table A-1 shows results of the nonlinear analyses. Scale factors are shown for 4 hertz and 7 hertz models, and for both the cases of no dead load and dead load equal to 30 percent of yield. The "Yield FS" column is the factor used to scale the earthquake time history to reach yield level (i.e., the point defined by P_y and Δ_y in Figure A-1c). Similarly, the "Ultimate FS" column is the factor required to scale the time history to reach the target displacement level (i.e., the displacement equal to $\mu\Delta_y$ in Figure A-1c). Finally, the ductility scale factor, F_μ, is the ratio of the corresponding values in these two columns.

Note that the yield scale factor for the "dead load equal to 30 percent P_y" cases do not exactly equal to 70 percent of the yield scale factors for the corresponding "no load" cases. This is because peak response for the dead load is sensitive to the sign of the input motion (i.e., plus or minus). For the "no load" case, the peak of the two direction responses is always used, while for the "dead load equal to 30 percent P_y case the downward component was used. It turned out that the signs were opposite for the cases considered. The effect of reversing the input direction on the ductility scale factor is discussed below.

Table A-1 shows that the ductility scale factor is reduced for the case where dead load is present. Figures A-4 and A-5 show example response time histories for the "no dead load" case and the "dead load equal to 30 percent P_y" case, respectively. The effect of the dead load can be clearly seen by comparing these two figures.

The effect of reversing the earthquake time history sign was also studied. Table A-2 gives results of changing the earthquake direction and compares the results to the original case (i.e., from Table A-1). Although the scale factors to reach yield and ultimate are both less for the reversed sign case, which

produced the greatest response elastically, the ductility scale factors are very close. This implies that the earthquake sign does not have a significant effect on F_μ.

Development of Simplified Procedure

A simplified procedure was developed for estimating F_μ by first computing an "effective" system ductility (μ_e), which takes into account the effects of ratcheting. The Riddell-Newmark method (Riddell, 1979) was then directly applied to compute F_μ.

The effective ductility μ_e was determined by adjusting the system ductility as follows:

$$\mu_e = 1 + \frac{\mu - 1}{n}$$

Where:

μ_e = Effective system ductility by considering effect of ratcheting

μ = System ductility without ratcheting effects

n = Adjustment factor to account for ratcheting (n=3 was used in this evaluation)

The value of "n" may be interpreted as the number of strong motion ratcheting cycles to which the structure is subjected, and may depend upon, among other variables, duration of ground motion, difference in the available resistances in the upward vs. downward directions before yield, and input time history of ground motion. Such an interpretation of "n" is illustrated in Figure A-6.

In the Riddell-Newmark method, the ductility scale factor is predicted from equations that are defined for the amplified acceleration, velocity and displacement regions of the input response spectrum. For a damping ratio of 7 percent of critical, the following equations predict F_μ for systems in different frequency ranges. For systems considered in this study, only the acceleration and velocity regions are of interest.

Amplified Acceleration Region: $F_\mu = (2.673\mu - 1.673)^{0.411}$ (1)

Amplified Velocity Region: $F_\mu = (2.24\mu - 1.24)^{0.611}$ (2)

Rigid Range Limit: $F_\mu = \mu^{0.11}(S_a/ZPA)$ (3)

Where:

S_a = 7 percent damped spectral acceleration

ZPA = Zero period acceleration

For the amplified acceleration region, F_μ is defined as the lesser of either equation (1) or equation (3).

Also, since both the 4 hertz and 7 hertz oscillators have frequencies that lie below the peak of the input spectrum, the rigid range limit was not applied.

Note that, for this study, the simplified procedure was established by modifying the above Riddell-Newmark equations by substituting effective ductility, μ_e, for the value of system ductility, μ.

Comparisons of Results of Simplified Procedure with Nonlinear Analyses

The simplified procedure was used to calculate values of ductility scale factor, F_μ, assuming an earthquake having 3 strong motion ratcheting cycles. These were compared with the corresponding quantities from nonlinear time history analyses and the results are shown in Table A-3.

As shown in the table, F_μ for the 4 Hz system agree well with the prediction by the Riddell-Newmark method using the velocity region equations. Since the 4 Hz frequency lies far below the peak of the input spectrum, use of velocity region equation is appropriate. For a ductility of 10, however, the Riddell-Newmark method under predicts the F_μ value. For the 7 Hz system, the results agree well when, for the Riddell-Newmark method, the geometric mean of the acceleration and the velocity region equations are used.

Conclusions

The study was performed to examine the effect of the constant downward pull on a horizontally-oriented structural element due to gravity on the nonlinear vertical displacement of a floor being subjected to vertical motion. We observe from the results of nonlinear time-history analyses that the ratcheting phenomenon created by the dead load reduces the ductility scale factor for a horizontal element compared to the case where the same element is mounted vertically and is subjected to horizontal motion i.e., with no dead load.

A simplified procedure is developed by modifying the Riddell-Newmark method. The procedure incorporates the effect of ratcheting by dead load and is achieved by using an "effective ductility", μ_e, that is a function of the system ductility, μ, and the number of strong motion cycles, n. For LTSP application using the LTSP vertical ground motion spectral shape, the simplified procedure is considered to be valid when a value of $n = 3$ is used, and for structures subjected to gravity loads in the range of about 30 percent of the yield strength of the system.

References

Kennedy, R. P., et al. Engineering characterization of ground motion - Task 1, Effects of characteristics of free-field motion on structural response, NUREG/CR-3805, 1984, prepared for the U. S. Nuclear Regulatory Commission.

Riddell, R., and Newmark, N. M., 1979, Statistical analysis of the response of nonlinear systems subjected to earthquake, SRS 468, Department of Civil Engineering, University of Illinois.

Reed, J. W., Kennedy, R. P., and Lashkari, B., 1991 Analysis of high-frequency seismic effects, Jack R. Benjamin and Associates Report, prepared for Electric Power Research Institute.

Pacific Gas and Electric Company, 1988, Final Report of the Diablo Canyon Long Term Seismic Program: Docket Nos. 50-275 and 50-323.

Kannan, A. E. and Powell, G. H., DRAIN-2D: A general computer program for dynamic analysis of inelastic plane structures, 1973 (Revised 1985), distributed by NISEE/Computer Applications, EERC, University of California, Berkeley, Reports No. EERC 73-6 and EERC 73-22.

Table A-1

Scale Factor for No Dead Load and Dead Load Cases

Ductility, μ	4 Hz Model			7 Hz Model		
	Yield FS	Ultimate FS	F_μ	Yield FS	Ultimate FS	F_μ
No Dead Load						
2	4.83	8.52	1.76	-	-	-
5	4.83	17.77	3.68	3.78	8.57	2.27
10	-	-	-	-	-	-
Dead Load Equal to 30 Percent P_y						
2	3.71	5.29	1.43	3.03	4.09	1.35
5	3.71	8.27	2.23	3.03	5.55	1.83
10	3.71	18.22	4.91	3.03	9.16	3.02

Table A-2

Comparison of Scale Factor Based on Earthquake Sign

	4 Hz Model			7 Hz Model		
	Yield FS	Ultimate* FS	F_μ	Yield FS	Ultimate* FS	F_μ
Original Sign (+)	3.71	8.27	2.23	3.03	5.55	1.83
Reversed Sign (-)	3.38	7.75	2.29	2.65	5.08	1.92

* Ductility, μ, equal to 5

Table A-3

Comparison of Nonlinear Analysis Results with Modified Riddell-Newmark Method

Frequency (Hz)	Target Ductility μ	Ductility Scale Factor, F_μ			
		Nonlinear Analysis* (see Table A-1)	Modified Riddell-Newmark Method		
			Velocity Region	Acceleration Region	Geometric Mean
4	2	1.43	1.41	1.30	1.35
	5	2.23	2.33	1.87	2.09
	5**	2.29	2.33	1.87	2.09
	10	4.91	3.49	2.47	2.94
7	2	1.35	1.41	1.30	1.35
	5	1.83	2.33	1.87	2.09
	5**	1.92	2.33	1.87	2.09
	10	3.02	3.49	2.47	2.94

* Dead load equal to 30 percent P_y

** Denotes case where the input time history is applied with a reverse sign.

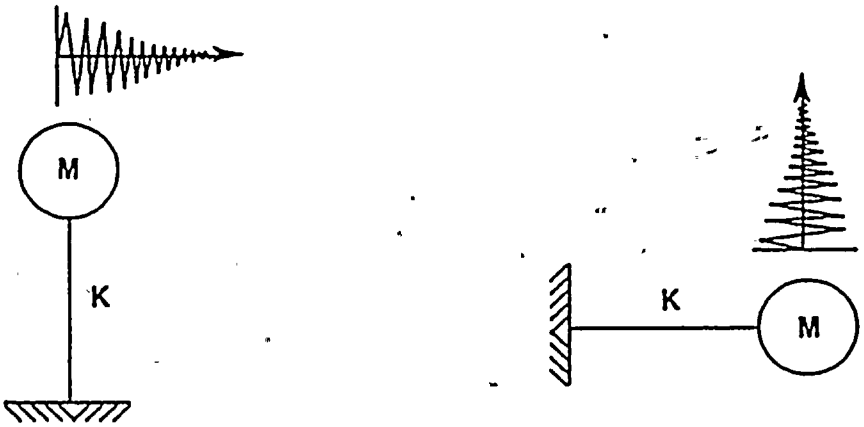

1a) Vertical model

1b) Horizontal model

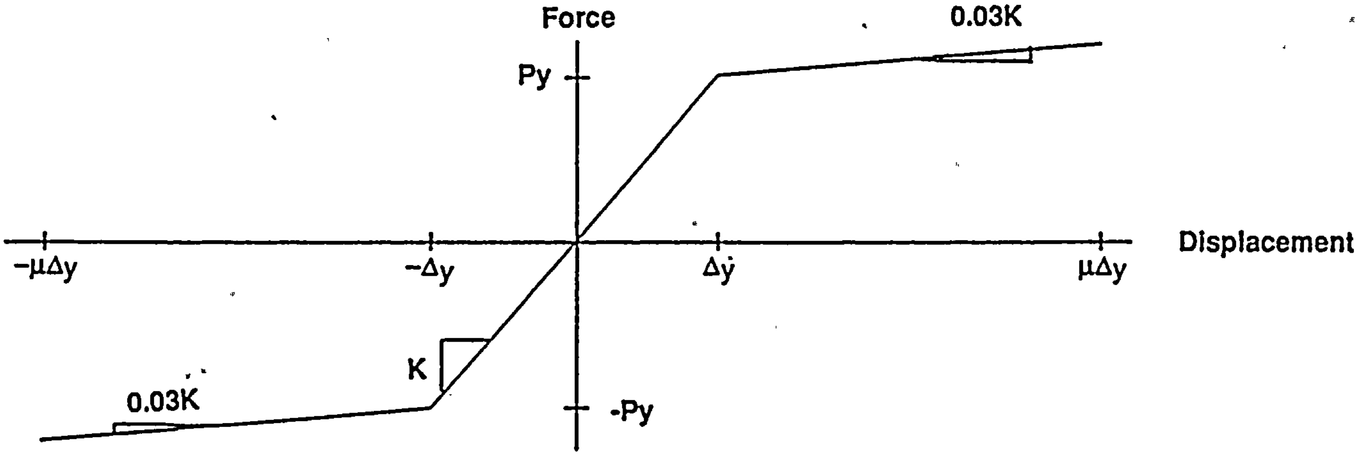

1c) Force-deformation relationship

Figure A-1

Models used in the nonlinear analysis.

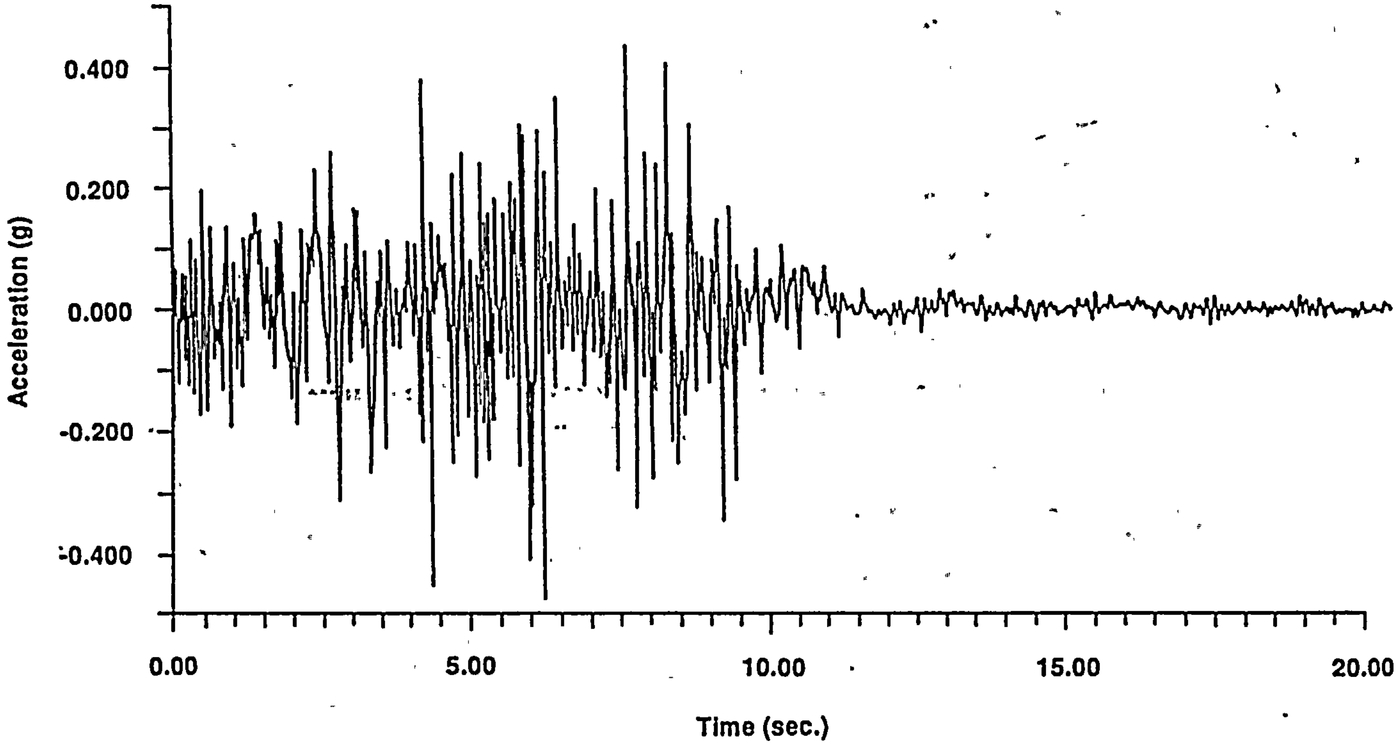

Figure A-2

Input time history used in the nonlinear analysis.

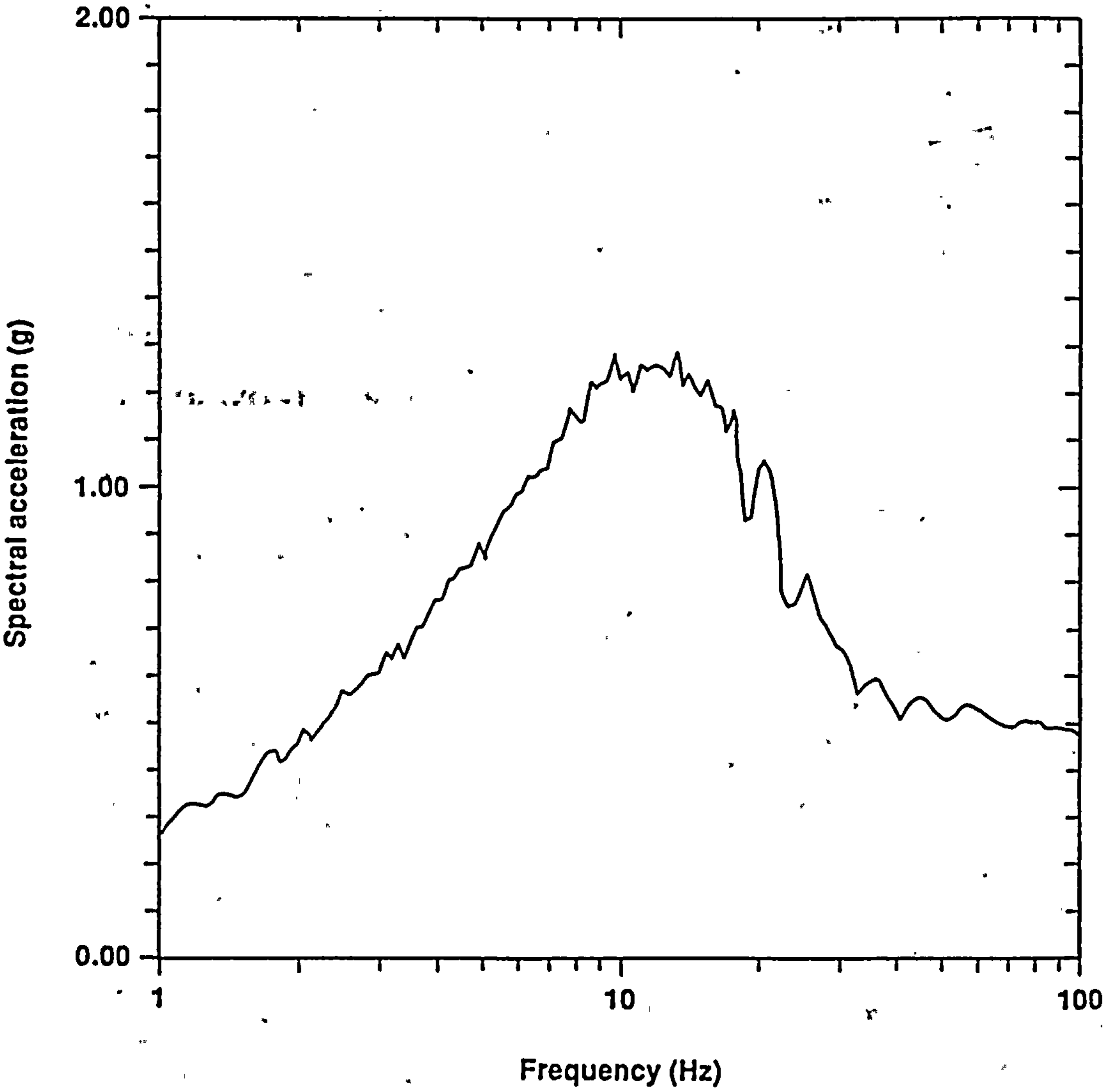

Figure A-3

Response spectrum of the input time history.

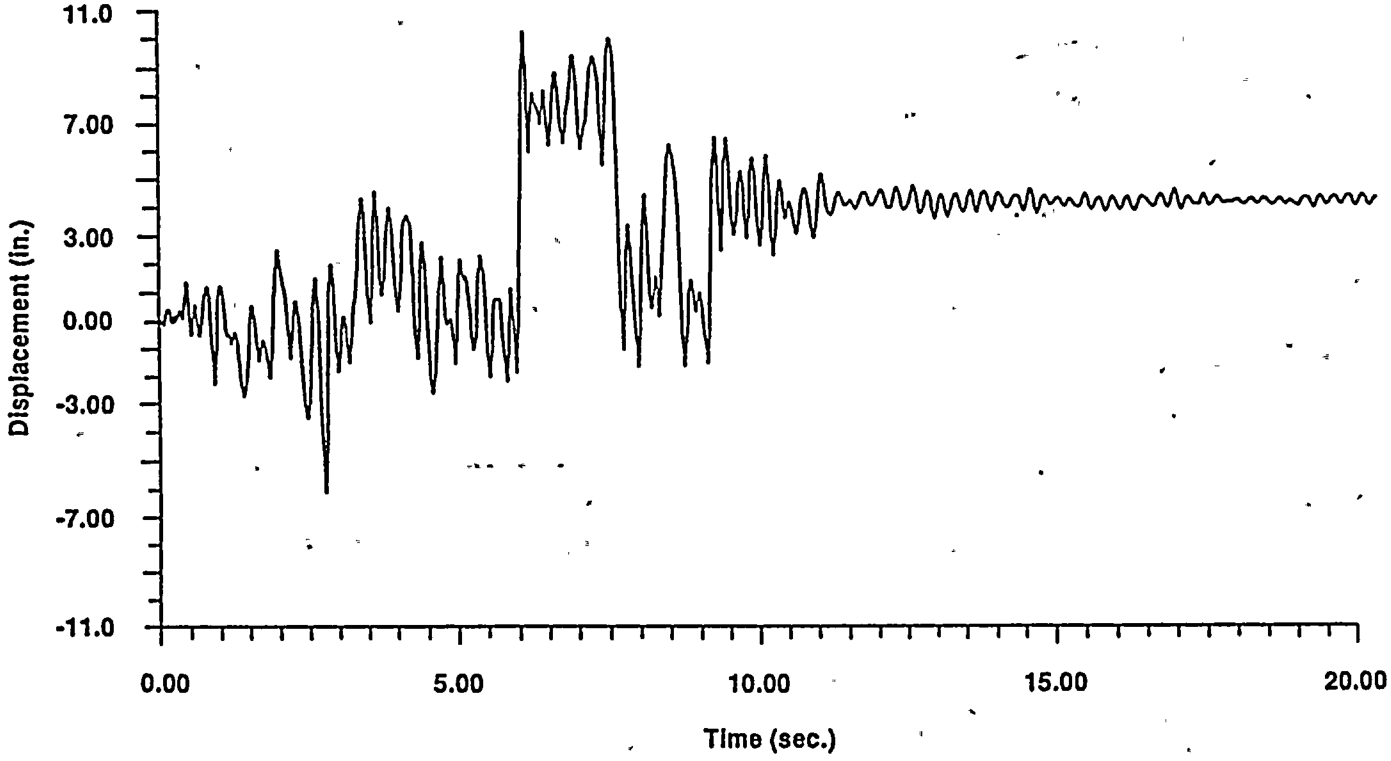

Figure A-4

Response time history for the case without dead load.

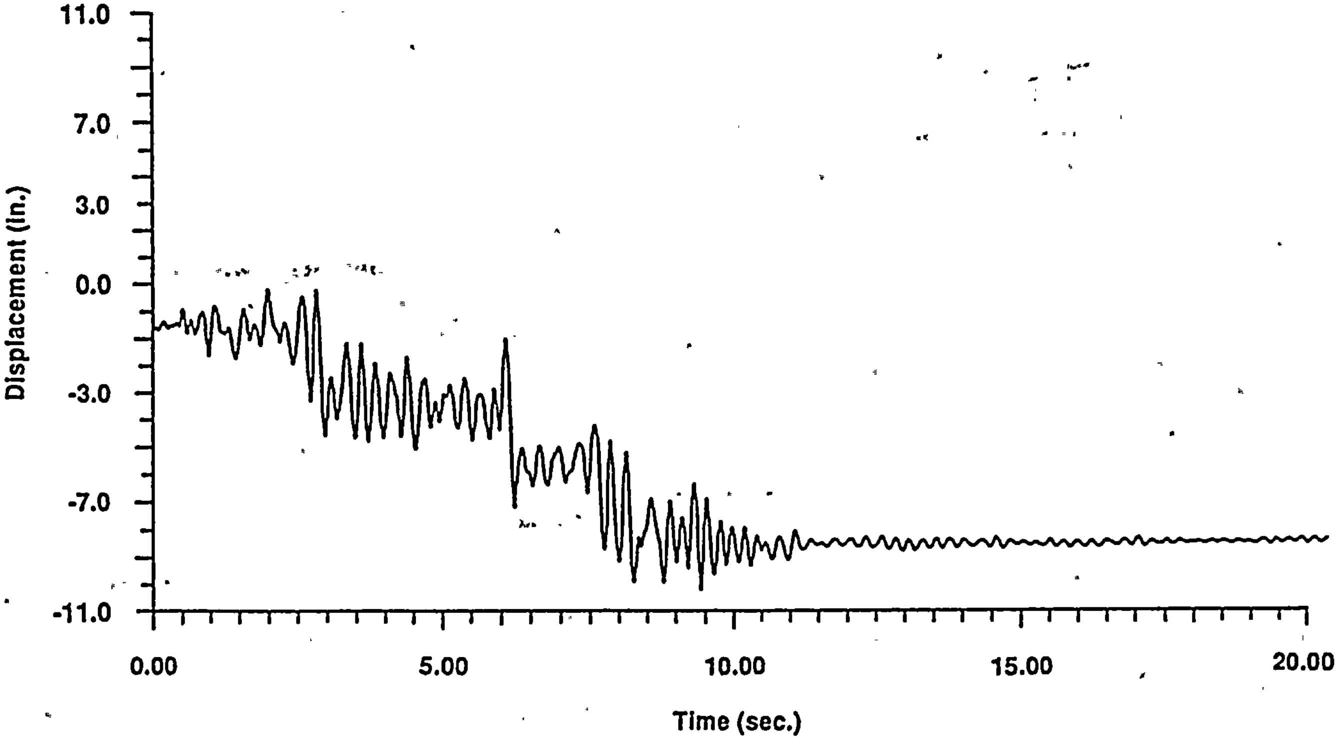

Figure A-5

Response time history for the case with dead load equal to 30 percent yield.

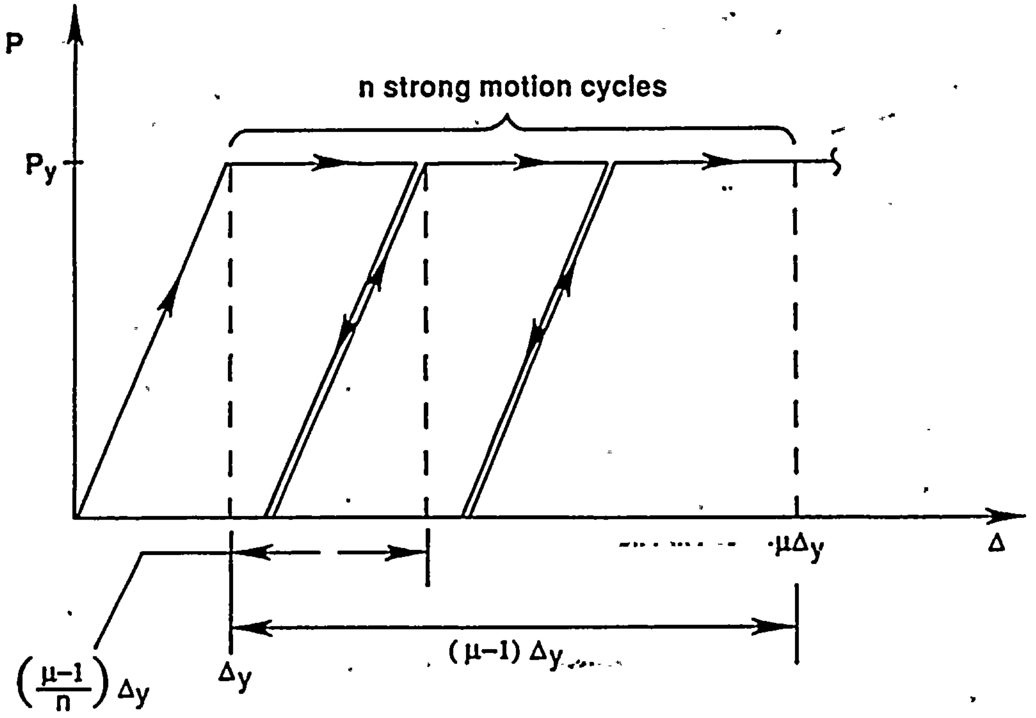

$$\text{Ductility per cycle} = \frac{\left(\frac{\mu-1}{n}\right)\Delta y + \Delta y}{\Delta y}$$

$$\text{Effective ductility,}\quad \mu_e = \frac{1}{n}(\mu-1)+1$$

Figure A-6

Effective ductility considering multiple strong motion cycles.

WCAP-13039

TECHNICAL JUSTIFICATION FOR ELIMINATING LARGE PRIMARY LOOP PIPE RUPTURE AS THE STRUCTURAL DESIGN BASIS FOR THE DIABLO CANYON UNITS 1 AND 2 NUCLEAR POWER PLANTS

NOVEMBER 1991

J. C. Schmertz
F. J. Witt
S. A. Swamy
Y. S. Lee

VERIFIED: D. Bhowmick
D. C. Bhowmick

APPROVED: DC Adamonis
D. C. Adamonis, Acting Manager
Structural Mechanics Technology

Work Performed Under Shop Order LQXP 950

This document contains information proprietary to Westinghouse Electric Corporation; it is submitted in confidence and is to be used solely for the purpose for which it is furnished and returned upon request. This document and such information is not to be reproduced, transmitted, disclosed or used otherwise in whole or in part without prior written authorization of Westinghouse Electric Corporation, Nuclear and Advanced Technology Division.

WESTINGHOUSE ELECTRIC CORPORATION
Nuclear and Advanced Technology Division
P. O. Box 2728
Pittsburgh, Pennsylvania 15230-2728

FOREWORD

This document contains Westinghouse Electric Corporation proprietary information and data which has been identified by brackets. Coding associated with the brackets sets forth the basis on which the information is considered proprietary. These codes are listed with their meanings in WCAP-7211.

The proprietary information and data contained in this report were obtained at considerable Westinghouse expense and its release could seriously affect our competitive position. This information is to be withheld from public disclosure in accordance with the Rules of Practice 10 CFR 2.790 and the information presented herein be safeguarded in accordance with 10 CFR 2.903. Withholding of this information does not adversely affect the public interest.

This information has been provided for your internal use only and should not be released to persons or organizations outside the Directorate of Regulation and the ACRS without the express written approval of Westinghouse Electric Corporation. Should it become necessary to release this information to such persons as part of the review procedure, please contact Westinghouse Electric Corporation, which will make the necessary arrangements required to protect the Corporation's proprietary interests.

The proprietary information is deleted in the unclassified version of this report (WCAP-13038).

TABLE OF CONTENTS

TABLE OF CONTENTS

TABLE OF CONTENTS

LIST OF TABLES

LIST OF TABLES (Cont'd)

LIST OF FIGURES

LIST OF FIGURES (Cont'd)

EXECUTIVE SUMMARY

The existing structural design basis for the reactor coolant systems of the Diablo Canyon Units 1 and 2 nuclear reactor power plants requires that the dynamic effects of pipe breaks be evaluated and that protective measures for such breaks be incorporated into the design. However, within the last decade, such breaks have been shown to be highly unlikely and should not be included, in general, in the structural design basis of Westinghouse type pressurized water reactors, for example. To eliminate primary loop pipe breaks from the design basis, it must be demonstrated to the satisfaction of the U.S. Nuclear Regulatory Commission that a leak-before-break situation exists. This report provides such a demonstration for the Diablo Canyon Units 1 and 2 nuclear power plants.

In this report it is shown that the primary loops are highly resistant to stress corrosion cracking and high and low cycle fatigue. Water hammer is mitigated by system design and operating procedures.

The primary loops were extensively examined. The as-built geometries for the pipe and elbows and loadings were obtained. The materials were evaluated using the Certified Materials Test Reports. Mechanical properties were determined at operating temperatures. Since the piping systems are fabricated from cast stainless steel, fracture toughnesses considering thermal aging were determined for each heat of material.

Based on loading, pipe geometry and fracture toughness considerations, enveloping critical locations were determined at which leak-before-break crack stability evaluations were made. Through-wall flaw sizes were found which would leak at a rate of ten times the leakage detection system capabilities of the plants. Large margins in such flaw sizes were shown against flaw instability. Finally, fatigue crack growth was shown not to be an issue for the primary loops.

It is concluded that dynamic effects of reactor coolant system primary loop pipe breaks need not be considered in the structural design basis of the Diablo Canyon Units 1 and 2 nuclear power plants.

SECTION 1.0
INTRODUCTION

1.1 Purpose

This report applies to the Diablo Canyon Nuclear Power Plant Units 1 and 2 (Diablo Canyon) Reactor Coolant System (RCS) primary loop piping. It is intended to demonstrate that for the specific parameters of the Diablo Canyon plants, RCS primary loop pipe breaks need not be considered in the structural design basis. The approach taken has been accepted by the Nuclear Regulatory Commission (NRC) (reference 1-1).

1.2 Scope

The existing structural design basis for the RCS primary loop requires that dynamic effects of pipe breaks be evaluated. Specifically, as part of the LOCA design basis for the Diablo Canyon plants the following breaks are postulated in the RCS primary loop piping: the six terminal ends in the cold, hot, and crossover legs; a split in the steam generator inlet elbow, and the loop closure weld in the crossover leg. However, Westinghouse has demonstrated on a generic basis that RCS primary loop pipe breaks are highly unlikely and should not be included in the structural design basis of Westinghouse plants (see reference 1-2). In order to demonstrate this applicability of the generic evaluations to the Diablo Canyon plants, Westinghouse has performed a fracture mechanics evaluation, a determination of leak rates from a through-wall crack, a fatigue crack growth evaluation, and an assessment of margins against crack instability consistent with the leak-before-break (LBB) methodology. Through this successful application of the LBB methodology, the above eight break locations in the RCS primary loop piping are eliminated from Diablo Canyons plants' structural design basis.

1.3 Objectives

In order to validate the elimination of RCS primary loop pipe breaks for the Diablo Canyon plants, the following objectives must be achieved:

a. Demonstrate that margin exists between the critical crack size and a postulated crack which yields a detectable leak rate.

b. Demonstrate that there is sufficient margin between the leakage through a postulated crack and the leak detection capability of the Diablo Canyon plants.

c. Demonstrate margin on applied load.

d. Demonstrate that fatigue crack growth is negligible.

1.4 Background Information

Westinghouse has performed considerable testing and analysis to demonstrate that RCS primary loop pipe breaks can be eliminated from the structural design basis of all Westinghouse plants. The concept of eliminating pipe breaks in the RCS primary loop was first presented to the NRC in 1978 in WCAP-9283 (reference 1-3). That topical report employed a deterministic fracture mechanics evaluation and a probabilistic analysis to support the elimination of RCS primary loop pipe breaks. That approach was then used as a means of addressing Generic Issue A-2 and Asymmetric LOCA Loads.

Westinghouse performed additional testing and analysis to justify the elimination of RCS primary loop pipe breaks. This material was provided to the NRC along with Letter Report NS-EPR-2519 (reference 1-4).

The NRC funded research through Lawrence Livermore National Laboratory (LLNL) to address this same issue using a probabilistic approach. As part of the LLNL research effort, Westinghouse performed extensive evaluations of specific plant loads, material properties, transients, and system geometries to demonstrate that the analysis and testing previously performed by Westinghouse and the research performed by LLNL applied to all Westinghouse plants (references 1-5 and 1-6). The results from the LLNL study were released at a March 28, 1983 ACRS Subcommittee meeting. These studies which are applicable to all Westinghouse plants east of the Rocky Mountains determined the mean probability of a direct LOCA (RCS primary loop pipe break) to be 4.4×10^{-12} per reactor year and the mean probability of an indirect LOCA to be 10^{-7} per reactor year. Thus, the results previously obtained by Westinghouse (reference 1-3) were confirmed by an independent NRC research study.

Based on the studies by Westinghouse, LLNL, the ACRS, and the AIF, the NRC completed a safety review of the Westinghouse reports submitted to address asymmetric blowdown loads that result from a number of discrete break locations on the PWR primary systems. The NRC Staff evaluation (reference 1-1) concludes that an acceptable technical basis has been provided so that asymmetric blowdown loads need not be considered for those plants that can demonstrate the applicability of the modeling and conclusions contained in the Westinghouse response or can provide an equivalent fracture mechanics demonstration of the primary coolant loop integrity. In a more formal recognition of LBB methodology applicability for PWRs, the NRC appropriately modified 10 CFR 50, General Design Criterion 4, "Requirements for Protection Against Dynamic Effects for Postulated Pipe Rupture" (reference 1-7).

This report provides a fracture mechanics demonstration of primary loop integrity for the Diablo Canyon plants consistent with the NRC position for exemption from consideration of dynamic effects.

Several computer codes are used in the evaluations. The main-frame computer programs are under Configuration Control which has requirements conforming to Standard Review Plan 3.9.1. The fracture mechanics calculations are independently verified (benchmarked).

1.5 References

1-1 USNRC Generic letter 84-04, Subject: "Safety Evaluation of Westinghouse Topical Reports Dealing with Elimination of Postulated Pipe Breaks in PWR Primary Main Loops," February 1, 1984.

1-2 Letter from Westinghouse (E. P. Rahe) to NRC (R. H. Vollmer), NS-EPR-2768, dated May 11, 1983.

1-3 WCAP-9283, "The Integrity of Primary Piping Systems of Westinghouse Nuclear Power Plants During Postulated Seismic Events," March, 1978.

1-4 Letter Report NS-EPR-2519, Westinghouse (E. P. Rahe) to NRC (D. G. Eisenhut), Westinghouse Proprietary Class 2, November 10, 1981.

1-5 Letter from Westinghouse (E. P. Rahe) to NRC (W. V. Johnston) dated April 25, 1983.

1-6 Letter from Westinghouse (E. P. Rahe) to NRC (W. V. Johnston) dated July 25, 1983.

1-7 Nuclear Regulatory Commission, 10 CFR 50, Modification of General Design Criteria 4 Requirements for Protection Against Dynamic Effects of Postulated Pipe Ruptures, Final Rule, Federal Register/Vol. 52, No. 207/Tuesday, October 27, 1987/Rules and Regulations, pp. 41288-41295.

SECTION 2.0
OPERATION AND STABILITY OF THE REACTOR COOLANT SYSTEM

2.1 Stress Corrosion Cracking

The Westinghouse reactor coolant system primary loops have an operating history that demonstrates the inherent operating stability characteristics of the design. This includes a low susceptibility to cracking failure from the effects of corrosion (e.g., intergranular stress corrosion cracking). This operating history totals over 450 reactor-years, including five plants each having over 17 years of operation and 15 other plants each with over 12 years of operation.

In 1978, the United States Nuclear Regulatory Commission (USNRC) formed the second Pipe Crack Study Group. (The first Pipe Crack Study Group established in 1975 addressed cracking in boiling water reactors only.) One of the objectives of the second Pipe Crack Study Group (PCSG) was to include a review of the potential for stress corrosion cracking in Pressurized Water Reactors (PWR's). The results of the study performed by the PCSG were presented in NUREG-0531 (reference 2-1) entitled "Investigation and Evaluation of Stress Corrosion Cracking in Piping of Light Water Reactor Plants." In that report the PCSG stated:

> "The PCSG has determined that the potential for stress-corrosion cracking in PWR primary system piping is extremely low because the ingredients that produce IGSCC are not all present. The use of hydrazine additives and a hydrogen overpressure limit the oxygen in the coolant to very low levels. Other impurities that might cause stress-corrosion cracking, such as halides or caustic, are also rigidly controlled. Only for brief periods during reactor shutdown when the coolant is exposed to the air and during the subsequent startup are conditions even marginally capable of producing stress-corrosion cracking in the primary systems of PWRs. Operating experience in

> PWRs supports this determination. To date, no stress-corrosion cracking has been reported in the primary piping or safe ends of any PWR."

During 1979, several instances of cracking in PWR feedwater piping led to the establishment of the third PCSG. The investigations of the PCSG reported in NUREG-0691 (reference 2-2) further confirmed that no occurrences of IGSCC have been reported for PWR primary coolant systems.

As stated above, for the Westinghouse plants there is no history of cracking failure in the reactor coolant system loop. The discussion below further qualifies the PCSG's findings.

For stress corrosion cracking (SCC) to occur in piping, the following three conditions must exist simultaneously: high tensile stresses, susceptible material, and a corrosive environment. Since some residual stresses and some degree of material susceptibility exist in any stainless steel piping, the potential for stress corrosion is minimized by properly selecting a material immune to SCC as well as preventing the occurrence of a corrosive environment. The material specifications consider compatibility with the system's operating environment (both internal and external) as well as other material in the system, applicable ASME Code rules, fracture toughness, welding, fabrication, and processing.

The elements of a water environment known to increase the susceptibility of austenitic stainless steel to stress corrosion are: oxygen, fluorides, chlorides, hydroxides, hydrogen peroxide, and reduced forms of sulfur (e.g., sulfides, sulfites, and thionates). Strict pipe cleaning standards prior to operation and careful control of water chemistry during plant operation are used to prevent the occurrence of a corrosive environment. Prior to being put into service, the piping is cleaned internally and externally. During flushes and preoperational testing, water chemistry is controlled in accordance with written specifications. Requirements on chlorides, fluorides, conductivity, and Ph are included in the acceptance criteria for the piping.

During plant operation, the reactor coolant water chemistry is monitored and maintained within very specific limits. Contaminant concentrations are kept below the thresholds known to be conducive to stress corrosion cracking with the major water chemistry control standards being included in the plant operating procedures as a condition for plant operation. For example, during normal power operation, oxygen concentration in the RCS is expected to be in the ppb range by controlling charging flow chemistry and maintaining hydrogen in the reactor coolant at specified concentrations. Halogen concentrations are also stringently controlled by maintaining concentrations of chlorides and fluorides within the specified limits. Thus during plant operation, the likelihood of stress corrosion cracking is minimized.

2.2 Water Hammer

Overall, there is a low potential for water hammer in the RCS since it is designed and operated to preclude the voiding condition in normally filled lines. The reactor coolant system, including piping and primary components, is designed for normal, upset, emergency, and faulted condition transients. The design requirements are conservative relative to both the number of transients and their severity. Relief valve actuation and the associated hydraulic transients following valve opening are considered in the system design. Other valve and pump actuations are relatively slow transients with no significant effect on the system dynamic loads. To ensure dynamic system stability, reactor coolant parameters are stringently controlled. Temperature during normal operation is maintained within a narrow range by control rod position; pressure is controlled by pressurizer heaters and pressurizer spray also within a narrow range for steady-state conditions. The flow characteristics of the system remain constant during a fuel cycle because the only governing parameters, namely system resistance and the reactor coolant pump characteristics, are controlled in the design process. Additionally, Westinghouse has instrumented typical reactor coolant systems to verify the flow and vibration characteristics of the system. Preoperational testing and operating experience have verified the Westinghouse approach. The operating transients of the RCS primary piping are such that no significant water hammer can occur.

2.3 Low Cycle and High Cycle Fatigue

Low cycle fatigue considerations are generally accounted for in the design of the piping system. A further evaluation of the low cycle fatigue loadings was carried out as part of this study in the form of a fatigue crack growth analysis, as discussed in section 8.0. High cycle fatigue loads in the system would result primarily from pump vibrations. These are minimized by restrictions placed on shaft vibrations during hot functional testing and operation. During operation, an alarm signals the exceedence of the vibration limits. Field measurements have been made on a number of plants during hot functional testing, including plants similar to the Diablo Canyon Units 1 and 2. Stresses in the elbow below the reactor coolant pump resulting from system vibration have been found to be very small, between 2 and 3 ksi at the highest. These stresses are well below the fatigue endurance limit for the material and would also result in an applied stress intensity factor below the threshold for fatigue crack growth.

2.4 References

2-1 Investigation and Evaluation of Stress-Corrosion Cracking in Piping of Light Water Reactor Plants, NUREG-0531, U.S. Nuclear Regulatory Commission, February 1979.

2-2 Investigation and Evaluation of Cracking Incidents in Piping in Pressurized Water Reactors, NUREG-0691, U.S. Nuclear Regulatory Commission, September 1980.

SECTION 3.0

PIPE GEOMETRY AND LOADING

3.1 Introduction to Methodology

The general approach is discussed first. As an example a segment of the primary coolant hot leg pipe is shown in figure 3-1. The as-built outside diameter and minimum wall thickness of the pipe are 33.99 in. and 2.395 in., respectively, as seen in the figure. Normal stresses at the weld locations result from the load combination procedure discussed in section 3.3 while faulted loads are developed as outlined in section 3.4. The components for normal loads are pressure, dead weight and thermal expansion. An additional component, Safe Shutdown Earthquake (SSE), is considered for faulted loads. As seen later the highest stressed location in the entire loop is at the reactor vessel outlet nozzle to pipe weld. This location is called the load critical location and is one of the locations at which, as an enveloping location, leak-before-break is to be established. Essentially a circumferential flaw is postulated to exist at this location thus the normal loads and faulted loads must be available to assess leakage and stability, respectively. The loads (developed below) at this location are also given in Figure 3-1.

Since the elbows are cast stainless steel, thermal aging must be considered (see section 4.0). Thermal aging results in lower fracture toughness criteria; thus, other locations than the highest stressed location must be examined taking into consideration both fracture toughness and stress. The enveloping locations so determined are called toughness critical locations. The single most critical location is apparent only after the full analysis is completed. Once loads (this section) and fracture toughnesses (section 4.0) are available, the load critical and toughness critical locations are determined (see section 5.0). At these locations, leak rate evaluations (see section 6.0) and fracture mechanics evaluations (see section 7.0) are performed per the guidance of Reference 3-1. Fatigue crack growth (see section 8.0) and stability margins are also evaluated (see section 9.0).

The locations for evaluation are those shown in figure 3-2.

3.2 Calculation of Loads and Stresses

The stresses due to axial loads and bending moments are calculated by the following equation:

$$\sigma = \frac{F}{A} + \frac{M}{Z} \tag{3-1}$$

where,

σ = stress
F = axial load
M = bending moment
A = pipe cross-sectional area
Z = section modulus

The bending moments for the desired loading combinations are calculated by the following equation:

$$M = \sqrt{M_Y^2 + M_Z^2} \tag{3-2}$$

where,

M = bending moment for required loading
M_Y = Y component of bending moment
M_Z = Z component of bending moment

The axial load and bending moments for leak rate predictions and crack stability analysis are computed by the methods to be explained in sections 3.3 and 3.4.

3.3 Loads for Leak Rate Evaluation

The normal operating loads for leak rate predictions are calculated by the following equations:

$$F = F_{DW} + F_{TH} + F_{P} \qquad (3-3)$$

$$M_Y = (M_Y)_{DW} + (M_Y)_{TH} + (M_Y)_{P} \qquad (3-4)$$

$$M_Z = (M_Z)_{DW} + (M_Z)_{TH} + (M_Z)_{P} \qquad (3-5)$$

The subscripts of the above equations represent the following loading cases:

DW = deadweight
TH = normal thermal expansion
P = load due to internal pressure

This method of combining loads is often referred as the algebraic sum method.

The loads based on this method of combination are provided in table 3-1 at all the locations identified in Figure 3-2. The as-built dimensions are also given.

3.4 Load Combination for Crack Stability Analysis

In accordance with Standard Review Plan 3.6.3 the absolute sum of loading components can be applied which results in higher magnitude of combined loads. If crack stability is demonstrated using these loads, the LBB margin on loads can be reduced from √2 to 1.0. The absolute summation of loads results in the following equations:

$$F = |F_{DW}| + |F_{TH}| + |F_{P}| + |F_{SSEINERTIA}| + |F_{SSEAM}| \qquad (3-6)$$

$$M_Y = |(M_Y)_{DW}| + |(M_Y)_{TH}| + |(M_Y)_{P}| + |(M_Y)_{SSEINERTIA}| + |(M_Y)_{SSEAM}| \qquad (3-7)$$

$$M_Z = |(M_Z)_{DW}| + |(M_Z)_{TH}| + |(M_Z)_P| + |(M_Z)_{SSEINERTIA}| + |(M_Z)_{SSEAM}| \qquad (3\text{-}8)$$

where subscripts SSE, INERTIA and AM mean safe shutdown earthquake, inertia and anchor motion, respectively.

The loads so determined are used in the fracture mechanics evaluations (section 7.0) to demonstrate the LBB margins at the locations established to be the governing locations. The loads at all the locations of interest (see Figure 3-2) are summarized in Tables 3-1 and 3-2.

3.5 References

3-1 USNRC Standard Review Plan 3.6.3, Leak-Before-Break Evaluation Procedures, NUREG-0800.

TABLE 3-1

DIMENSIONS, NORMAL LOADS AND NORMAL STRESSES FOR DIABLO CANYON

Location[a]	Outside Diameter (in.)	Thickness (in.)	Axial Load[b] (kips)	Bending Moment (in-kips)	Stress (ksi)
1	33.99	2.395	1495	25057	20.57
2	33.99	2.395	1478	1202	6.98
3	34.81	2.80	1582	7865	9.41
4	37.19	2.99	1491	19818	12.44
5	37.19	2.99	1601	4689	6.84
6	37.19	2.99	1596	4349	6.69
7	37.19	2.99	1591	4318	6.64
8	37.19	2.99	1692	5848	7.51
9	37.19	2.99	1692	8471	5.86
10	37.19	2.99	1833	5982	8.07
11	32.26	2.275	1348	3456	8.59
12	32.26	2.275	1348	3422	8.57
13	33.06	2.675	1347	3491	7.23
14	33.06	2.675	1348	2728	6.80

---

[a] See figure 3-2

[b] Includes pressure

TABLE 3-2

FAULTED LOADS AND STRESSES FOR DIABLO CANYON

Location[a,b]	Axial Load[c] (kips)	Bending Moment (in-kips)	Stress (ksi)
1	2161	46674	36.39
2	1933	6583	11.88
3	1943	12833	13.05
4	2360	41261	23.56
5	2006	28517	17.44
6	1955	23992	15.52
7	1919	16968	12.67
8	1845	12891	10.8
9	1839	12853	10.77
10	2053	42718	23.17
11	1826	31245	29.32
12	1668	12728	16.25
13	1667	13018	13.78
14	1701	14482	14.72

---

[a] See Figure 3-2
[b] See table 3-1 for dimensions
[c] Includes pressure

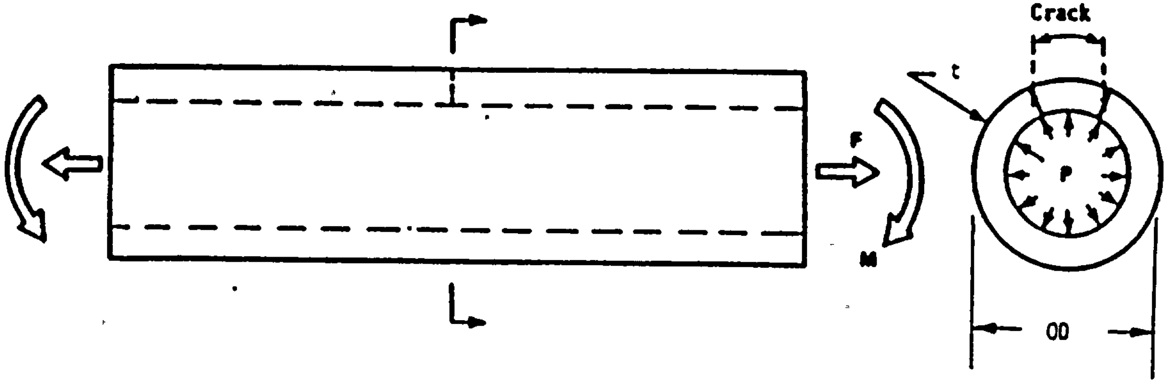

OD = 33.99 in
t = 2.395 in

Normal Loads		Faulted Loads	
force[a]:	1495 kips	force[a]:	2161 kips
bending moment:	25057 in-kips	bending moment:	46674 in-kips

---

[a] Includes the force due to a pressure of 2250 psi

Figure 3-1

Hot Leg Coolant Pipe

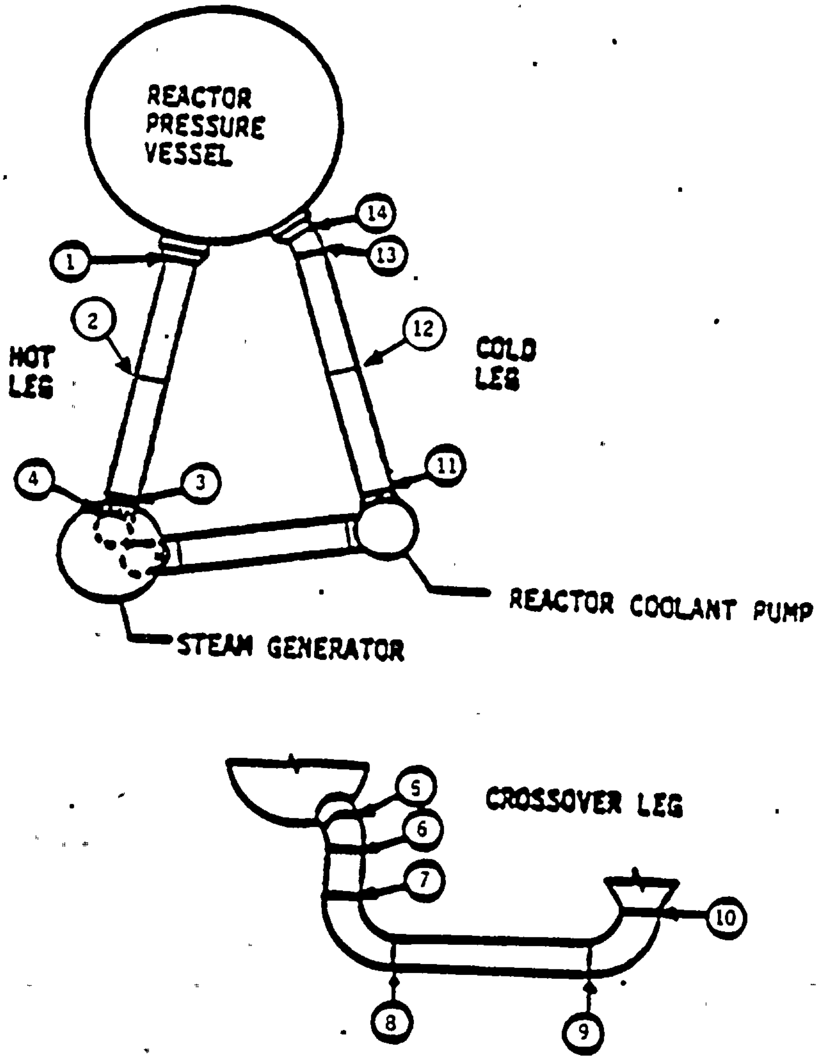

HOT LEG

Temperature 618°F, Pressure: 2250 psi

CROSSOVER LEG

Temperature 544°F, Pressure: 2250 psi

COLD LEG

Temperature 544°F, Pressure: 2250 psi

Figure 3-2

Schematic Diagram of Diablo Canyon Primary Loop Showing Weld Locations

SECTION 4.0
MATERIAL CHARACTERIZATION

4.1 Primary Loop Pipe and Fittings Materials

The primary loop pipe materials are SA376 TP316 for both Diablo Canyon units, and the elbow fittings are SA351 CF8M for both units.

4.2 Tensile Properties

The Certified Materials Test Reports (CMTRs) for Diablo Canyon Units 1 and 2 were used to establish the tensile properties for the leak-before-break analyses. The CMTRs include tensile properties at room temperature for each of the heats of material. These properties are given for Diablo Canyon Units 1 and 2 in Tables 4-1 and 4-2 respectively. The average properties are given and the lower bound properties are identified. The 1989 Code minimum properties are also given in these tables.

The properties at 544°F and 618°F were established from the tensile properties at room temperature given in Tables 4-1 and 4-2 by utilization of Tables 4-3, 4-4, and 4-5. These last three tables provide typical tensile properties at room temperature and at 650°F for both of the materials of concern. The tensile properties for typical materials at 544°F and 618°F were obtained by interpolating between the room temperature and the 650°F tensile properties given in Tables 4-3, 4-4, and 4-5. Ratios of the strengths at 544°F and 618°F to the strengths at room temperature for the typical materials were then applied to the room temperature values given in Tables 4-1 and 4-2 to obtain the Diablo Canyon properties at 544°F and 618°F.

In Table 4-3, the SA376 TP316 material properties of 'plant A' were closer to the Diablo Canyon material properties than Plant C, and therefore the 'plant A' values were used. In Tables 4-4 and 4-5 the tensile properties for all the listed components were averaged, to obtain the typical tensile properties for SA351 CF8M.

The average and lower bound yield strengths and ultimate strengths, to encompass both Diablo Canyon Units 1 and 2, are given in Table 4-6. The ASME Code Modulus of Elasticity is also given, and Poisson's ratio was taken as 0.3.

For leak-before-break fracture evaluations of the toughness critical locations the true stress-true strain curve must be available. This curve was obtained using the Nuclear Systems Materials Handbook (reference 4-1). The lower bound true stress-true strain curve is given in Figure 4-1.

4.3 Fracture Toughness Properties

The pre-service fracture toughnesses of cast materials in terms of J have been found to be very high at 600°F. Typical results for a cast material are given in figure 4-2 taken from reference 4-2. J_{Ic} is observed to be over 5000 in-lbs/in^2. However, cast stainless steels are subject to thermal aging during service. This thermal aging causes an elevation in the yield strength of the material and a degradation of the fracture toughness, the degree of degradation being somewhat proportional to the level of ferrite in the material.

To determine the effects of thermal aging on piping integrity, a detailed study was carried out in reference 4-3. In that report, fracture toughness results were presented for a material [representative of worst case aging conditions (a heat of SA351 CF8M designated Heat L). Toughness results were provided for the material in the full service life condition and these properties are also presented in figure 4-3 of this report for information. The J_{Ic} value for this material at operating temperature was 750 in-lbs/in^2, and the maximum value of J obtained in the tests was in excess of 2200 in-lb/in^2. The tests of this material were conducted on small specimens and therefore rather short crack extensions occurred, (maximum extension 4.3 mm) so it is expected that higher J values would be sustained for larger specimens. Specifically, a value of 3,000 in-lb/in^2 is acceptable (reference 4-5). T_{mat} was 60 for Heat L at operating temperature.]^{a,c,e} The effects of the aging process on the end-of-service life fracture toughness are further discussed in Appendix B.

End-of-service life toughnesses for the heats are established using the alternate toughness criteria methodology of reference 4-6 (appendix B). By that methodology a heat of material is said to be as good as [Heat L]^{a,c,e} if it can be demonstrated that its end-of-service fracture toughnesses equal or exceed those of [Heat L at the 95% confidence level. In particular the alternative toughness criteria methodology also provides a procedure for determining fracture toughness for materials not as good as Heat L]^{a,c,e}. The worst case fracture toughness values for all the loops of each plant at each location (see figure 3-2), as taken from Appendix B, are given in table 4-7.

Available data on aged stainless steel welds (references 4-3 and 4-4) indicate that J_{Ic} values for the worst case welds are of the same order as the aged material. However, the slope of the J-R curve is steeper, and higher J-values have been obtained from fracture tests (in excess of 3000 in-lb/in^2). The applied value of the J-integral for a flaw in the weld regions will be lower than that in the base metal because the yield stress for the weld materials is much higher at temperature[a]. Therefore, weld regions are less limiting than the cast material.

---

[a] In the report all $J_{applied}$ values were conservatively determined by using base metal strength properties.

It is thus conservative to choose the end-of-service life toughness properties of [Heat L]^{a,c,e} as representative of those of the welds. Also, such pipes and fittings having an end-of-service life calculated room temperature charpy U-notch energy, (KCU), greater than that of [Heat L]^{a,c,e} are also conservatively assumed to have the properties of [Heat L]^{a,c,e}.

In the fracture mechanics analyses that follow, the fracture toughness properties given in table 4-7 will be used as the criteria against which the applied fracture toughness values will be compared.

4.4 References

4-1 Nuclear Systems Materials Handbook, Part I - Structural Materials, Group 1 - High Alloy Steels, Section 2, ERDA Report TID 26666, November, 1975.

4-2 WCAP-9558 Rev. 2, "Mechanistic Fracture Evaluation of Reactor Coolant Pipe Containing a Postulated Circumferential Through-Wall Crack," Westinghouse Proprietary Class 2, June 1981.

4-3 WCAP-10456, "The Effects of Thermal Aging on the Structural Integrity of Cast Stainless Steel Piping for W NSSS," W Proprietary Class 2, November 1983.

4-4 Slama, G., Petrequin, P., Masson, S.H., and Mager, T.R., "Effect of Aging on Mechanical Properties of Austenitic Stainless Steel Casting and Welds", presented at SMiRT 7 Post Conference Seminar 6 - Assuring Structural Integrity of Steel Reactor Pressure Boundary Components, August 29/30, 1983, Monterey, CA.

4-5 Appendix II of Letter from Dominic C. DiIanni, NRC to D. M. Musolf, Northern States Power Company, Docket Nos. 50-282 and 50-306, December 22, 1986.

4-6 Witt, F.J., Kim, C.C., "Toughness Criteria for Thermally Aged Cast Stainless Steel," WCAP-10931, Revision 1, Westinghouse Electric Corporation, July 1986, (Westinghouse Proprietary Class 2).

TABLE 4-1
MEASURED ROOM TEMPERATURE TENSILE PROPERTIES FOR DIABLO CANYON UNIT 1 PRIMARY LOOP PIPING AND FITTINGS

Component	Loop No.	Heat No.	Material	Yield Strength (ksi)	Ultimate Strength (ksi)
			PIPE		
Cold Leg	1	V0630/3259	SA376 TP316	43.9 42.4	87.6 84.1
Cold Leg	2	V0629/3334	SA376 TP316	42.4 41.9	84.1 81.2
Cold Leg	3	K2011/3862	SA376 TP316	34.7 36.0	77.0 78.4
Cold Leg	4	V0630/3261	SA376 TP316	38.5 42.9	78.5 86.3
Cold Leg	1	1478/3258	SA376 TP315	37.0 33.0	77.9 81.7
Cold Leg	2	K2010/3684	SA376 TP316	38.6 35.2	81.8 77.2
Cold Leg	3	E1478/3256	SA376 TP316	45.5 43.4	84.1 87.9
Cold Leg	4	K2011/3680	SA376 TP316	34.1 43.4	75.3 82.9
Hot Leg	1	E1490/3358	SA376 TP316	43.5 44.9	85.4 84.9
Hot Leg	2	E1485/33524	SA376 TP316	42.3 45.4	85.4 87.4
Hot Leg	3	V0688/3539	SA376 TP316	39.9 40.2	81.7 81.7
Hot Leg	4	E1484/3349X	SA376 TP316	39.0 42.9	79.1 85.9

TABLE 4-1 (continued)
MEASURED ROOM TEMPERATURE TENSILE PROPERTIES FOR DIABLO CANYON UNIT 1 PRIMARY LOOP PIPING AND FITTINGS

Component	Loop No.	Heat No.	Material	Yield Strength (ksi)	Ultimate Strength (ksi)
Hot Leg	1	E1484/33494	SA376 TP316	--	--
Hot Leg	2	E1483/3350X	SA376 TP316	44.1 47.3	86.2 83.4
Hot Leg	3	E1483/3350Y	SA376 TP316	44.1 47.3	86.2 83.4
Hot Leg	4	V0684/3537X	SA376 TP316	38.9 40.6	79.8 80.7
Crossover Leg	1	F-0222/2902X	SA376 TP316	43.5 44.3	85.1 85.6
Crossover Leg	2	F0222/29024	SA376 TP316	43.5 44.3	85.1 85.6
Crossover Leg	3	F0216/2863X	SA376 TP316	43.7 39.5	86.7 82.1
Crossover Leg	4	E1485/3361X	SA376 TP316	38.3 45.9	83.9 91.4
Crossover Leg	1	E1493/3381X	SA376 TP316	41.0 43.5	84.9 86.9
Crossover Leg	2	E1493/33814	SA376 TP316	41.0 43.5	84.9 86.9
Crossover Leg	3	K2029/44384	SA376 TP316	32.5 40.0	70.9 82.4
Crossover Leg	4	E1468/3365	SA376 TP316	42.0 44.0	84.4 87.4
			Average	41.39	83.2

TABLE 4-1 (continued)
MEASURED ROOM TEMPERATURE TENSILE PROPERTIES FOR DIABLO CANYON UNIT 1 PRIMARY LOOP PIPING AND FITTINGS

Component	Loop No.	Heat No.	Material	Yield Strength (ksi)	Ultimate Strength (ksi)
FITTINGS (i.e. ELBOWS)					
Cold Leg	1	30845-1	SA351 CF8M	36.5	76.9
Cold Leg	2	33047-4	SA351 CF8M	42.3	85.3
Cold Leg	3	3242514	SA351 CF8M	42.5	85.8
Cold Leg	4	32469-2	SA351 CF8M	47.25	89.75
Hot Leg	1	10966-1	SA351 CF8M	45.0	87.5
Hot Leg	2	11937-2	SA351 CF8M	43.5	88.0
Hot Leg	3	12198-2	SA351 CF8M	42.0	85.0
Hot Leg	4	10563-2	SA351 CF8M	45.0	88.5
Crossover Leg	1	13174-2	SA351 CF8M	48.0	85.0
Crossover Leg	2	13704-1	SA351 CF8M	48.0	86.5
Crossover Leg	3	16654-2	SA351 CF8M	36.0	74.0
Crossover Leg	4	16690-2	SA351 CF8M	39.0	75.0
Crossover Leg	1	13421-1	SA351 CF8M	46.5	85.0
		14576-1	SA351 CF8M	40.5	78.75
Crossover Leg	2	14804-1	SA351 CF8M	51.0	93.0
		15560-1	SA351 CF8M	43.5	86.0
Crossover Leg	3	15987-2	SA351 CF8M	45.0	87.0
		15823-1	SA351 CF8M	42.0	83.25
Crossover Leg	4	14535-2	SA351 CF8M	41.5	80.50
		16037-3	SA351 CF8M	37.5	75.25

TABLE 4-1 (continued)
MEASURED ROOM TEMPERATURE TENSILE PROPERTIES FOR DIABLO CANYON UNIT 1 PRIMARY LOOP PIPING AND FITTINGS

Component	Loop No.	Heat No.	Material	Yield Strength (ksi)	Ultimate Strength (ksi)
Crossover Leg	1	16690-3	SA351 CF8M	40.5	81.75
		17388-2	SA351 CF8M	37.5	75.0
Crossover Leg	2	13930-5	SA351 CF8M	48.0	89.0
		14251-1	SA351 CF8M	39.0	82.5
Crossover Leg	3	11743-1	SA351 CF8M	45.0	86.0
		11556-1	SA351 CF8M	43.5	83.5
Crossover Leg	4	12281-1	SA351 CF8M	42.0	84.75
		11974-1	SA351 CF8M	43.0	83.0
			Average	42.89	83.68

a - indicates not available
b - underline indicates the lower bound values

1989 Code Minimum Properties:

SA376 TP316	30	75
SA351 CF8M	30	70

TABLE 4-2
MEASURED ROOM TEMPERATURE TENSILE PROPERTIES FOR DIABLO CANYON UNIT 2 PRIMARY LOOP PIPING AND FITTINGS

Component	Loop No.	Heat No.	Material	Yield Strength (ksi)	Ultimate Strength (ksi)
			PIPE		
Cold Leg	1	F0654/4153	SA376 TP316	38.9 42.4	81.6 86.1
Cold Leg	2	5167b/4555	SA376 TP316	38.2 41.2	81.6 83.6
Cold Leg	3	F0654/4152	SA376 TP316	38.7 43.3	83.1 86.0
Cold Leg	4	K2029/4557	SA376 TP316	38.7 36.4	80.6 88.1
Cold Leg	1	F0653/4151X	SA376 TP316	40.7 41.2	83.1 83.6
Cold Leg	2	51676/4556X	SA376 TP316	37.5 41.9	82.7 84.1
Cold Leg	3	J1677/4554X	SA376 TP316	33.7 40.4	81.6 82.6
Cold Leg	4	J1681/4677	SA376 TP316	43.7 41.2	87.4 83.6
Hot Leg	1	F0655/4132	SA376 TP316	42.4 48.3	86.9 91.6
Hot Leg	2	F0656/4131	SA376 TP316	38.7 39.1	83.0 81.5
Hot Leg	3	F0654/4136	SA376 TP316	38.9 47.4	82.1 86.6
Hot Leg	4	J1682/4627	SA376 TP316	44.9 51.0	87.6 93.1

TABLE 4-2 (continued)
MEASURED ROOM TEMPERATURE TENSILE PROPERTIES FOR DIABLO CANYON UNIT 2 PRIMARY LOOP PIPING AND FITTINGS

Component	Loop No.	Heat No.	Material	Yield Strength (ksi)	Ultimate Strength (ksi)
Hot Leg	1	K2027/4480Y	SA376 TP316	37.4	79.9
				36.4	80.9
Hot Leg	2	F0656/4131X	SA376 TP316	49.9	88.6
				50.9	92.1
Hot Leg	3	K2027/4499	SA376 TP316	37.2	80.6
				44.2	87.1
Hot Leg	4	J1676/4631X	SA376 TP316	38.2	81.9
				47.8	87.3
Crossover Leg	1	J-1681/4560X	SA376 TP316	45.0	84.9
				40.7	81.1
Crossover Leg	2	J-1681/4561X	SA376 TP316	37.7	81.9
				41.2	84.8
Crossover Leg	3	J-1682/4669X	SA376 TP316	43.7	85.9
				45.5	87.5
Crossover Leg	4	J1681/4562Y	SA376 TP316	43.0	83.9
				40.9	83.6
Crossover Leg	1	J-1681/4562X	SA376 TP316	43.3	83.9
				40.9	83.6
Crossover Leg	2	J-1682/4563Y	SA376 TP316	46.7	84.3
Crossover Leg	3	J-1681/4561Y	SA376 TP316	37.7	81.9
				41.2	84.9
Crossover Leg	4	J-1682/4563X	SA376 TP316	39.4	82.0
				46.7	84.3
			Average	41.8	84.44

TABLE 4-2 (continued)
MEASURED ROOM TEMPERATURE TENSILE PROPERTIES FOR DIABLO CANYON UNIT 2 PRIMARY LOOP PIPING AND FITTINGS

Component	Loop No.	Heat No.	Material	Yield Strength (ksi)	Ultimate Strength (ksi)
		FITTINGS (i.e. ELBOWS)			
Cold Leg	1	40874-4	SA351 CF8M	43.8	86.1
Cold Leg	2	40874-3	SA351 CF8M	43.8	86.1
Cold Leg	3	39716-4	SA351 CF8M	43.8	87.1
Cold Leg	4	39716-1	SA351 CF8M	43.8	87.1
Hot Leg	1	33756-2	SA351 CF8M	44.25	84.0
Hot Leg	2	41192-2	SA351 CF8M	34.3	73.3
Hot Leg	3	37168-1	SA351 CF8M	38.65	76.3
Hot Leg	4	39792-3	SA351 CF8M	42.3	84.3
Crossover Leg	1	38408-3	SA351 CF8M	43.6	83.1
Crossover Leg	2	39231-3	SA351 CF8M	46.8	89.6
Crossover Leg	3	39445-2	SA351 CF8M	42.3	83.5
Crossover Leg	4	34900-2	SA351 CF8M	33.75	70.5
Crossover Leg	1	55485-1	SA351 CF8M	43.3	86.35
		55485-2	SA351 CF8M	----	-----
Crossover Leg	2	519223-3	SA351 CF8M	42.45	86.9
		52665-1	SA351 CF8M	43.05	86.3
Crossover Leg	3	55282-2	SA351 CF8M	41.7	85.65
		52369-2	SA351 CF8M	41.85	85.75
Crossover Leg	4	51712-2	SA351 CF8M	39.4	80.35
		52665-2	SA351 CF8M	42.45	88.7

TABLE 4-2 (continued)
MEASURED ROOM TEMPERATURE TENSILE PROPERTIES FOR DIABLO CANYON UNIT 2 PRIMARY LOOP PIPING AND FITTINGS

Component	Loop No.	Heat No.	Material	Yield Strength (ksi)	Ultimate Strength (ksi)
Crossover Leg	1	49686-1	SA351 CF8M	46.95	89.95
		50362-2	SA351 CF8M	41.7	86.15
Crossover Leg	2	41423-1	SA351 CF8M	40.0	79.25
		52449-1	SA351 CF8M	42.75	87.5
Crossover Leg	3	51712-1	SA351 CF8M	38.25	79.50
		52369-1	SA351 CF8M	42.60	88.00
Crossover Leg	4	34900-1	SA351 CF8M	32.25	70.0
		50115-1	SA351 CF8M	42.45	81.9
			Average	41.57	83.38

a - indicates not available
b - underline indicates the lower bound values

1989 Code Minimum Properties:

SA376 TP316	30	75
SA351 CF8M	30	70

TABLE 4-3

TYPICAL TENSILE PROPERTIES OF SA376 TP316, SA351 CF8A AND WELDS OF SUCH MATERIAL FOR THE PRIMARY LOOP

a,c,e

Plant	Material	Test Temperature (°F)	Average Tensile Properties Yield (psi)	Average Tensile Properties Ultimate (psi)
A	SA376 TP316	70	40,900 (48)[a]	83,200 (48)
		650	23,500 (19)	67,900 (19)
	E 308 Weld	70	63,900 (3)	87,600 (3)
B	SA376 TP316	70	47,100 (40)	88,300 (40)
		650	26,900 (22)	69,100 (25)
	E 308 Weld	70	59,600 (8)	87,200 (8)
		650	31,500 (1)	68,800 (1)
C	SA376 TP316	70	46,600 (36)	87,300 (36)
		650	24,200 (18)	66,800 (19)
	E 308 Weld	70	61,900 (4)	85,400 (4)
D	SA351 CF8A	70	47,300 (14)	84,500 (14)
		650	26,000 (4)	60,500 (4)
	Weld	70	61,200 (31)	84,500 (32)

---

a. (______) indicates the number of test results averaged

TABLE 4-4

MECHANICAL PROPERTIES OF SA351 CF8M MATERIAL AT ROOM TEMPERATURE (FROM A TYPICAL PWR PLANT)

a,c,e

PRODUCT FORM	HEAT NR	TEST PIECE NR	MATERIAL	0.2% OFFSET YIELD STRESS (PSI)	ULTIMATE STRENGTH (PSI)	% ELONGATION	% REDUCTION IN AREA
90 DEG HALF ELBOW	4969	3/6	A351 CF8M	33843.6	71811.0	53.3	70.5
		3/6A	A351 CF8M	34270.2	70673.4	43.9	67.8
90 DEG HALF ELBOW	4663	3/1	A351 CF8M	35123.4	71953.2	41.1	63.2
		3/1A	A351 CF8M	34839.0	73659.6	45.1	68.5
90 DEG HALF ELBOW	4747	3/2	A351 CF8M	33701.4	71811.0	47.8	69.5
		3/3	A351 CF8M	34839.0	71100.0	37.8	63.2
90 DEG HALF ELBOW	4898	3/4	A351 CF8M	35123.4	75792.6	36.0	52.2
		3/5	A351 CF8M	36118.8	77072.4	51.8	67.0
90 DEG HALF ELBOW	5089	4/1	A351 CF8M	32137.2	71384.4	44.5	60.2
		4/2	A351 CF8M	31284.0	70673.4	48.1	N/A
90 DEG HALF ELBOW	5839	4/5	A351 CF8M	33132.6	71100.0	47.9	66.5
		4/6	A351 CF8M	32279.4	71526.6	40.5	68.4
90 DEG HALF ELBOW	5247	4/3	A351 CF8M	32420.0	70385.7	41.5	72.0
		4/4	A351 CF8M	32846.6	71096.6	48.6	71.2
40 DEG ELBOW	4541	2/1	A351 CF8M	34981.2	72095.4	37.7	65.0
		2/1A	A351 CF8M	34981.2	71242.2	41.9	66.0
30 DEG ELBOW	4543	5/2	A351 CF8M	33132.6	72522.0	50.7	71.2
		5/3	A351 CF8M	33417.0	72237.6	50.3	67.8
40 DEG ELBOW	5655	2/2	A351 CF8M	35123.4	72237.6	50.7	70.5
		2/2A	A351 CF8M	34128.0	71100.0	47.3	76.2
40 DEG ELBOW	5854	2/3	A351 CF8M	30999.6	72237.6	53.0	71.2
		2/3A	A351 CF8M	31852.8	71100.0	50.4	76.2
50 DEG ELBOW	4594	1/2	A351 CF8M	34128.0	72522.0	49.6	71.2
		1/2A	A351 CF8M	33843.6	72948.6	46.0	77.7
50 DEG ELBOW	4665	1/3	A351 CF8M	33701.4	70246.8	50.6	67.8
		1/3A	A351 CF8M	32279.4	70389.0	51.6	71.2

TABLE 4-4 (continued)

MECHANICAL PROPERTIES OF SA351 CF8M MATERIAL AT ROOM TEMPERATURE (FROM A TYPICAL PWR PLANT)

a,c,e

PRODUCT FORM	HEAT NR	TEST PIECE NR	MATERIAL	0.2% OFFSET YIELD STRESS (PSI)	ULTIMATE STRENGTH (PSI)	% ELONGATION	% REDUCTION IN AREA
50 DEG ELBOW	4205	1/1	A351 CF8M	31568.4	76788.0	37.5	61.2
		1/1A	A351 CF8M	38962.8	75508.2	47.0	66.0
30 DEG ELBOW	64422	5/1	A351 CF8M	40669.2	81907.2	43.3	64.0
		5/1A	A351 CF8M	36403.2	71242.2	42.5	71.2

TABLE 4-5

MECHANICAL PROPERTIES OF SA351 CF8M MATERIAL AT 650°F (FROM A TYPICAL PWR PLANT)

a,c,e

PRODUCT FORM	HEAT NR	TEST PIECE NR	MATERIAL	0.2% OFFSET YIELD STRESS (PSI)	ULTIMATE STRENGTH (PSI)	% ELONGATION	% REDUCTION IN AREA
90 DEG HALF ELBOW	4969	3/6	A351 CF8M	22225.9	53040.6	35.7	67.9
		3/6A	A351 CF8M	23008.0	53182.8	39.7	63.2
90 DEG HALF ELBOW	4663	3/1	A351 CF8M	23178.6	57733.2	33.3	73.8
		3/1A	A351 CF8M	23463.0	57448.8	34.6	61.3
90 DEG HALF ELBOW	4747	3/2	A351 CF8M	23747.4	57448.8	34.2	58.3
		3/3	A351 CF8M	23178.6	57022.2	28.9	47.5
90 DEG HALF ELBOW	4898	3/4	A351 CF8M	24174.0	59439.6	39.3	57.3
		3/5	A351 CF8M	24245.1	59724.0	34.4	59.3
90 DEG HALF ELBOW	5089	4/1	A351 CF8M	20988.7	55372.7	39.5	64.2
		4/2	A351 CF8M	21017.2	56254.3	35.8	58.3
90 DEG HALF ELBOW	5839	4/5	A351 CF8M	21244.7	53026.4	31.1	62.3
		4/6	A351 CF8M	21031.4	54107.1	40.0	59.3
90 DEG HALF ELBOW	5247	4/3	A351 CF8M	21400.1	55045.6	33.2	48.7
		4/4	A351 CF8M	21371.6	54931.9	33.9	65.1
40 DEG ELBOW	4541	2/1	A351 CF8M	23463.0	57022.2	22.2	60.3
		2/1A	A351 CF8M	23889.6	57448.8	26.6	57.3
30 DEG ELBOW	4543	5/2	A351 CF8M	22041.0	57448.8	30.0	65.1
		5/3	A351 CF8M	22609.8	57022.2	31.1	55.2
40 DEG ELBOW	5655	2/2	A351 CF8M	21244.7	52756.2	37.8	62.3
		2/2A	A351 CF8M	21258.9	52528.7	37.3	48.7
40 DEG ELBOW	5854	2/3	A351 CF8M	20960.3	54562.1	39.5	67.9
		2/3A	A351 CF8M	21287.3	54107.1	38.6	67.9
50 DEG ELBOW	4594	1/2	A351 CF8M	22894.2	57591.0	34.9	56.2
		1/3A	A351 CF8M	22680.9	57164.4	38.4	64.2
50 DEG ELBOW	4665	1/3	A351 CF8M	22894.2	56453.4	40.9	64.2
		1/3A	A351 CF8M	22680.9	56880.0	43.9	69.6

TABLE 4-5 (continued)

MECHANICAL PROPERTIES OF SA351 CF8M MATERIAL AT 650°F (FROM A TYPICAL PWR PLANT)

a,c,e

PRODUCT FORM	HEAT NR	TEST PIECE NR	MATERIAL	0.2% OFFSET YIELD STRESS (PSI)	ULTIMATE STRENGTH (PSI)	% ELONGATION	% REDUCTION IN AREA
50 DEG ELBOW	4205	1/1	A351 CF8M	24245.1	57448.8	24.4	56.3
		1/1A	A351 CF8M	24031.8	57591.0	30.3	55.2
30 DEG ELBOW	64422	5/1	A351 CF8M	25169.4	57875.4	25.0	38.0
		5/1A	A351 CF8M	25027.2	58728.6	24.4	60.3
			Total	680.6526	1686.4067	N=30	
			Avg.	22.6884	56.2136		
			Min.	20.4603	52.5287		

TABLE 4-6
MECHANICAL PROPERTIES FOR DIABLO CANYON UNITS 1 AND 2 MATERIALS AT 544°F AND 618°F

a,c,e

Material	Temperature (°F)	Average Yield Stress (psi)	Average Ultimate Strength (psi)	Lower Bound Yield Stress (psi)	Lower Bound Ultimate Strength (psi)
SA376 TP316	544	27130	71230	21040	60240
	618	24870	69260	19440	58580
SA351 CF8M	544	26630	64770	20330	54300
	618	24190	61850	18470	51850

Modulus of Elasticity for Both Materials:

SA376 TP316 $E = 25.21 \times 10^6$ psi at 618°F
SA351 CF8M $E = 25.58 \times 10^6$ psi at 544°F

Poisson's Ratio: 0.3

TABLE 4-7

ENVELOPED FRACTURE TOUGHNESS PROPERTIES FOR DIABLO CANYON UNITS 1 AND 2 PRIMARY LOOPS FOR LEAK-BEFORE-BREAK EVALUATION

Diablo Canyon Unit 1

a,c,e

Location[a,b]	HT. NO.	KCU (daJ/cm^2)	J_{IC} (in-lb/in^2)	T_{mat} (non-dim)	J_{max} (in-lb/in^2)
3	10966-1	3.98	693	52.8	1970
4	10966-1	3.98	693	52.8	1970
5	13704-1	3.25	567	36.6	1451
6	13704-1	3.25	567	36.6	1451
7	14804-1	1.56	272	6.9	438
8	14804-1	1.56	272	6.9	438
9	13930-5	3.81	664	45.1	1755
10	13930-5	3.81	664	45.1	1755
13	33047-4	3.76	656	48	1816
14	33047-4	3.76	656	48	1816

Diablo Canyon Unit 2

All locations		≥4.3	750	60	2200[c]

---

[a] The locations are shown in figure 3-2.

[b] The lower of the values for all the loops are given here.

[c] A value of 3000 in-lb/in^2 is acceptable per reference 4-5.

a.c.e

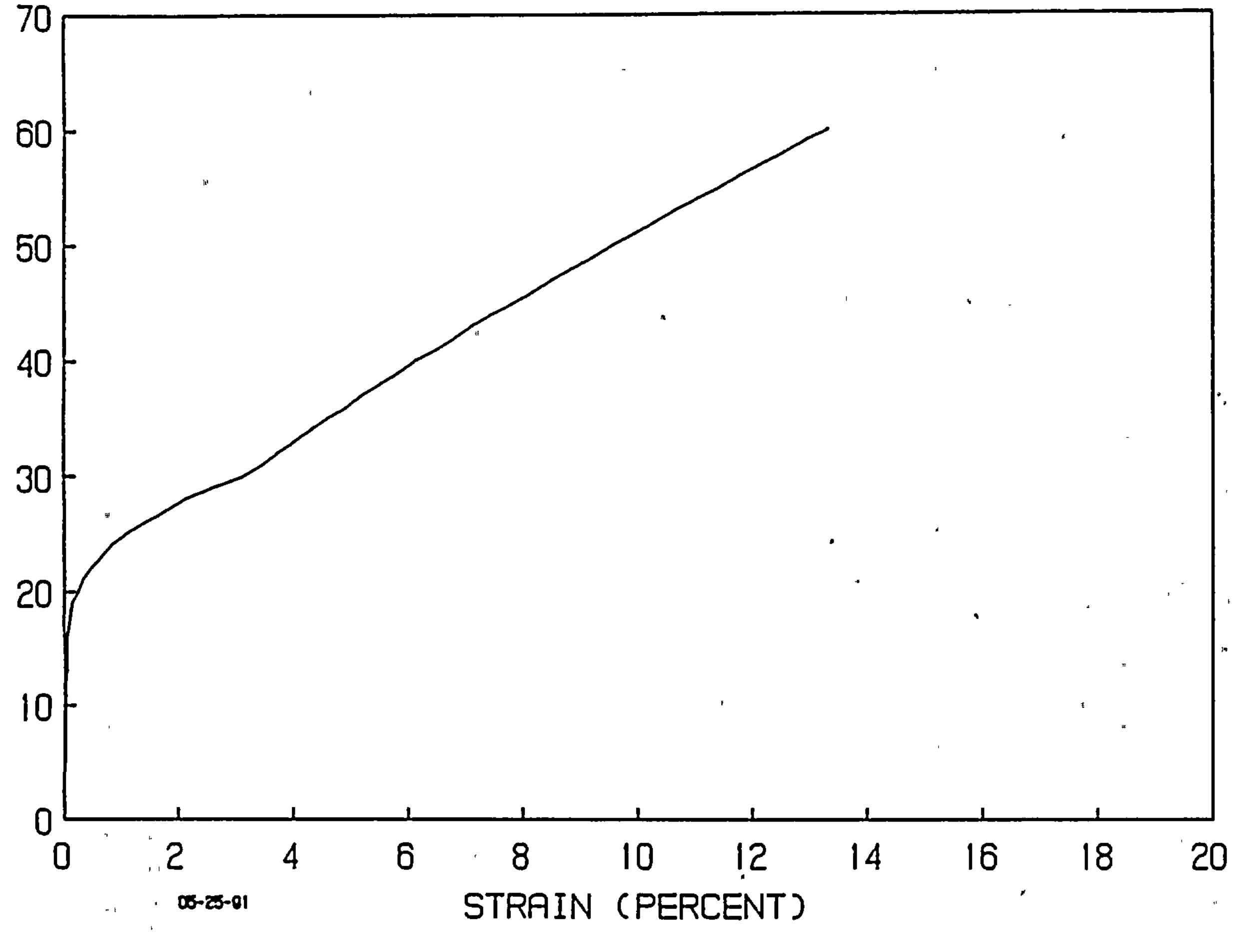

Figure 4-1

Representative Lower Bound True Stress - True Strain Curve for the SA351 CF8M at 544°F

a,c,e

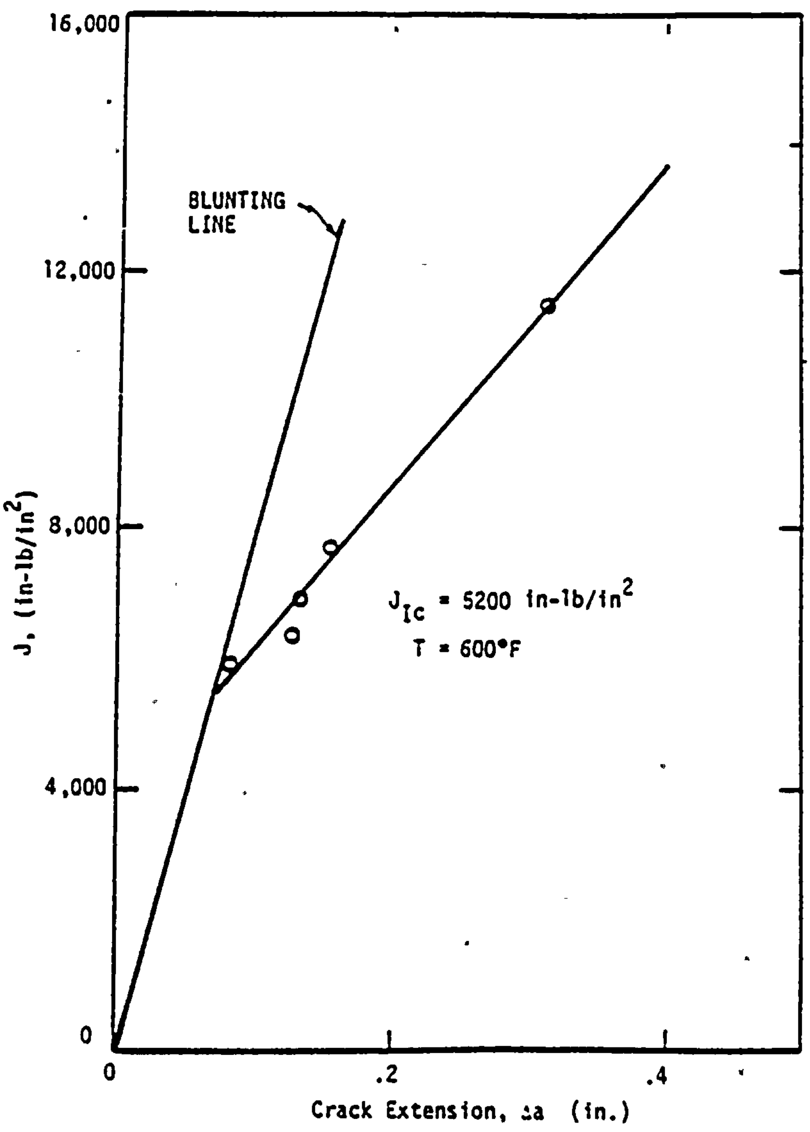

Figure 4-2

J vs. Δa for SA351 CF8M Cast Stainless Steel at 600°F

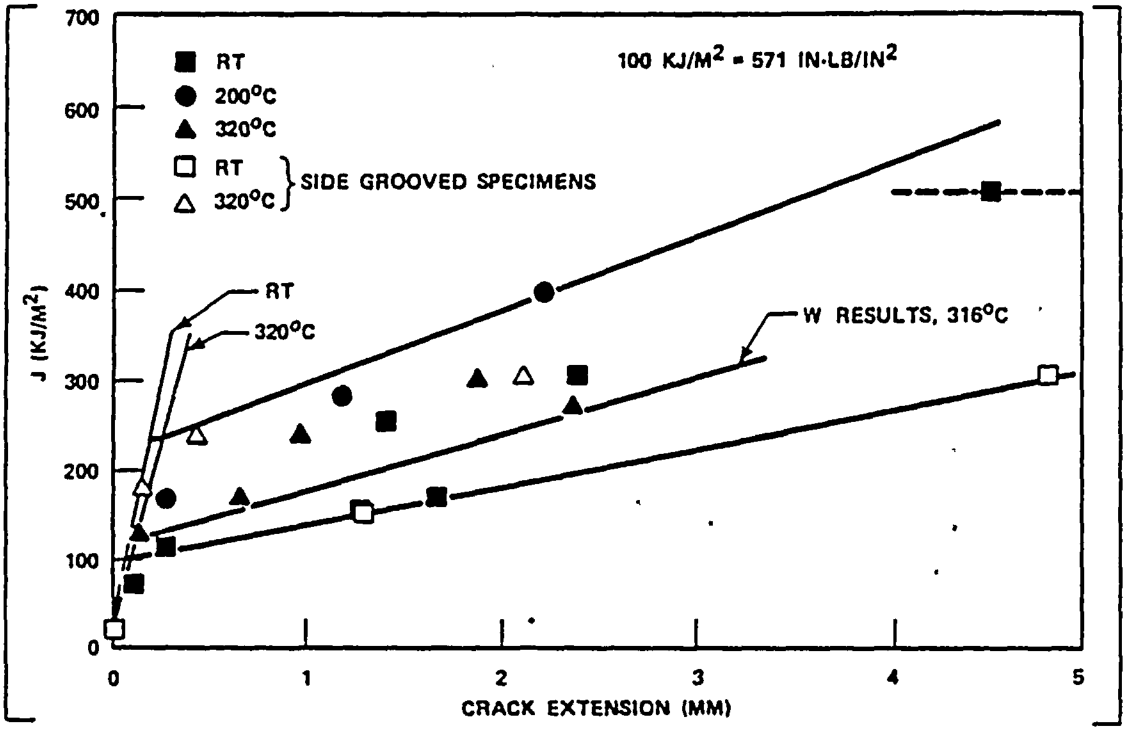

Figure 4-3

J Vs. Δa at Different Temperatures for Aged Material [Heat L]^{a,c,e} (7500 Hours at 400°C)

SECTION 5.0
CRITICAL LOCATIONS AND EVALUATION CRITERIA

5.1 Critical Locations

The leak-before-break (LBB) evaluation margins are to be demonstrated for the limiting location (governing location). Candidate locations are designated load critical locations or toughness critical locations as discussed in Section 3.0. Such locations are established considering the loads (section 3.0) and the material properties established in section 4.0. These locations are defined below for Diablo Canyon Units 1 and 2. Table 3-2 as well as Table 4-7 are used for this evaluation, along with Figure 3-2.

Diablo Canyon Unit 1

Location 1 is the highest stressed location and is the load critical location by definition. Furthermore, since it is on a straight pipe, it is a high toughness location. Low toughness locations are at the ends of every elbow. On an elbow-by-elbow basis, these are location pairs 3 and 4, 5 and 6, 7 and 8, 9 and 10, and lastly 13 and 14. The higher stressed of each location pair are weld locations 4, 6, 7, 10, and 13. Weld Location 10 has a faulted stress comparable to weld location 4, but it is less tough. Because of the lower toughness, weld location 10 is more limiting. Weld location 10 has a toughness comparable to weld location 13, but it has a much higher faulted stress. Because of the higher stress, location 10 is more limiting. It is thus concluded that the enveloping locations in Diablo Canyon Unit 1 for which LBB methodology is to be applied are locations 1, 6, 7 and 10.

Diablo Canyon Unit 2

Location 1 is the highest stressed location and is thus the load critical location. Since this location is at the higher temperature (i.e. has the worst tensile properties) and none of the other Unit 2 locations has toughnesses as low as the low toughness locations of Unit 1, the Unit 1 toughness critical locations envelope the Unit 2 toughness critical locations.

5.2 Fracture Criteria

As discussed later, fracture mechanics analyses are made based on loads and postulated flaw sizes related to leakage. The stability criteria against which the calculated J (i.e. J_{app}) and tearing modulus (T_{app}) are compared are:

(1) If $J_{app} < J_{Ic}$, then the crack is stable;

(2) If $J_{app} \geq J_{Ic}$, then, if $T_{app} < T_{mat}$

and $J_{app} < J_{max}$, the crack is stable.

The toughness criteria at each location have previously been determined and are given in table 4-7.

SECTION 6.0
LEAK RATE PREDICTIONS

6.1 Introduction

The purpose of this section is to discuss the method which is used to predict the flow through postulated through-wall cracks and present the leak rate calculation results for through-wall circumferential cracks.

6.2 General Considerations

The flow of hot pressurized water through an opening to a lower back pressure causes flashing which can result in choking. For long channels where the ratio of the channel length, L, to hydraulic diameter, D_H, (L/D_H) is greater than [40]^{a,c,e}, both [choking and frictional effects must be considered. In this situation the flow can be described as being single-phase through the channel until the local pressure equals the saturation pressure of the fluid. At this point, the flow begins to flash and choking occurs. Pressure losses due to momentum changes will dominate for $L/D_H<40$. However, for large L/D_H values, friction pressure drop will become important and must be considered along with the momentum losses due to flashing]^{a,c,e}.

6.3 Calculation Method

The basic method used in the leak rate calculations is the method developed by [Fauske (Reference 6-1) for the two-phase choked flow, and then adding to it the additional frictional pressure loss upstream of the choked exit plane.]

The flow rate through a crack was calculated in the following manner. Figure 6-1 from Reference 6-1 was used to estimate the critical pressure, Pc, for the primary loop enthalpy condition and an assumed flow. Once Pc was found for a given mass flow, the [stagnation pressure upstream of the choked plane]^{a,c,e} was found from Figure 6-2 taken from Reference 6-1. For all cases considered, since [$L/D_H<40$, $Pc/Po = 0.55$.]^{a,c,e} Therefore, this method will yield the two-phase pressure drop due to momentum effects as illustrated in Figure 6-3. Now using the assumed flow rate, G, the frictional pressure drop can be calculated using

$$\Delta\ P_f = [f\frac{(L/D_H - 40)\,G^2}{\rho\ 2g_c(144)}]^{a,c,e} \tag{6-1}$$

where the friction factor f is determined using the [Moody diagram.]^{a,c,e} The crack relative roughness, ε, was obtained from fatigue crack data on stainless steel samples. The relative roughness value used in these calculations was [300 micro-inches RMS.]^{a,c,e}

The frictional pressure drop using equation 6-1 is then calculated for the assumed flow and added to the [momentum pressure drop calculated using the Fauske model]^{a,c,e} to obtain the total pressure drop from the primary system to the atmosphere. That is, for the primary loop

$$\text{Absolute Pressure} - 14.7 = [\Delta P_T = (\Delta P_f + \Delta P_{2\phi}\ \text{choked flow})]^{a,c,e} \tag{6-2}$$

for a given assumed flow G. If the right-hand side of equation 6-2 does not agree with the pressure difference between the primary loop and the atmosphere, then the procedure is repeated until equation 6-2 is satisfied to within an acceptable tolerance and this results in the flow value through the crack.

6.4 Leak Rate Calculations

Leak rate calculations were made as a function of crack length at the four locations previously identified in section 5.1. The normal operating loads of Table 3-1 were applied, in these calculations. The crack opening areas were estimated using the method of Reference 6-2 and the leak rates were calculated using the two-phase flow formulation described above. The average material properties of section 4.0 were used for these calculations.

The flaw sizes to yield a leak rate of 10 gpm were calculated at the four locations and are given in Table 6-1. The flaw sizes so determined are called leakage flaws.

The Diablo Canyon plant RCS pressure boundary leak detection system meets the intent of Regulatory Guide 1.45. Thus, to satisfy the margin of 10 on the leak rate, the flaw sizes (leakage flaws) are determined which yield a leak rate of 10 gpm.

6.5 References

6-1 [Fauske, H. K., "Critical Two-Phase, Steam Water Flows," Proceedings of the Heat Transfer and Fluid Mechanics Institute, Stanford, California, Stanford University Press, 1961]^{a,c,e}.

6-2 Tada, H., "The Effects of Shell Corrections on Stress Intensity Factors and the Crack Opening Area of Circumferential and a Longitudinal Through-Crack in a Pipe," Section II-1, NUREG/CR-3464, September 1983.

TABLE 6-1
FLAW SIZES YIELDING A LEAK RATE OF 10 GPM AT THE FOUR LOCATIONS

a,c,e

Location	Flaw Size (in)
1	2.9
6	8.4
7	8.4
10	5.6

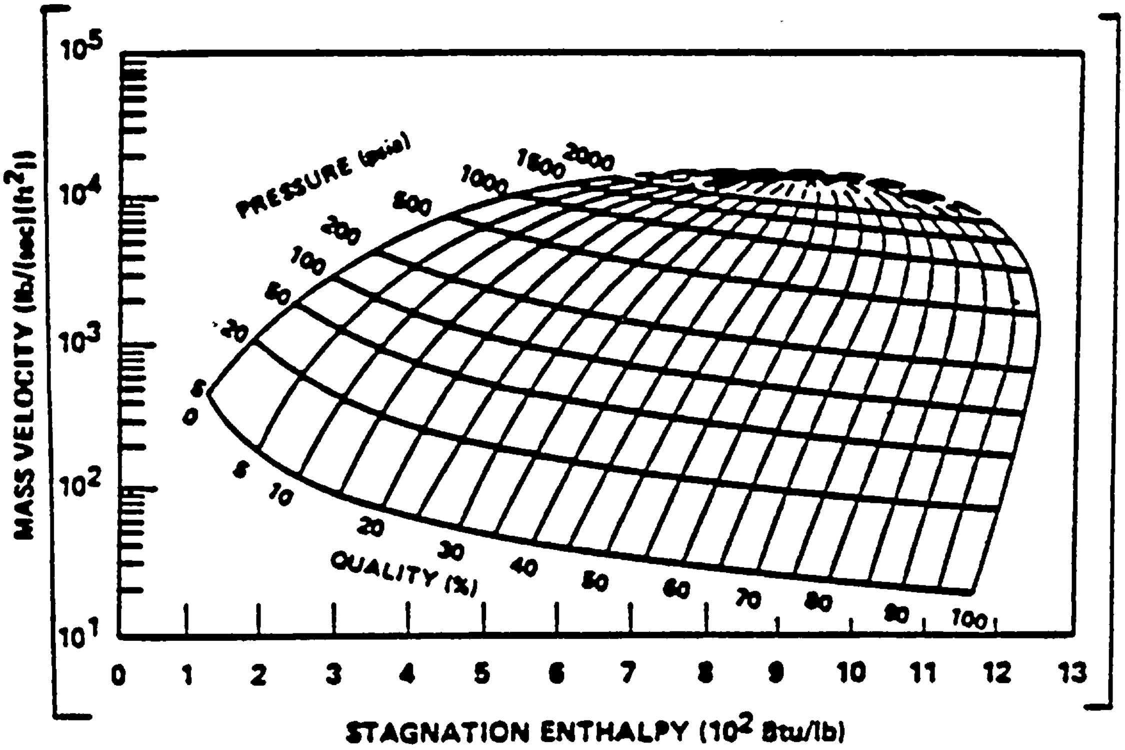

a,c,e

Figure 6-1. Analytical Predictions of Critical Flow Rates of Steam-Water Mixtures

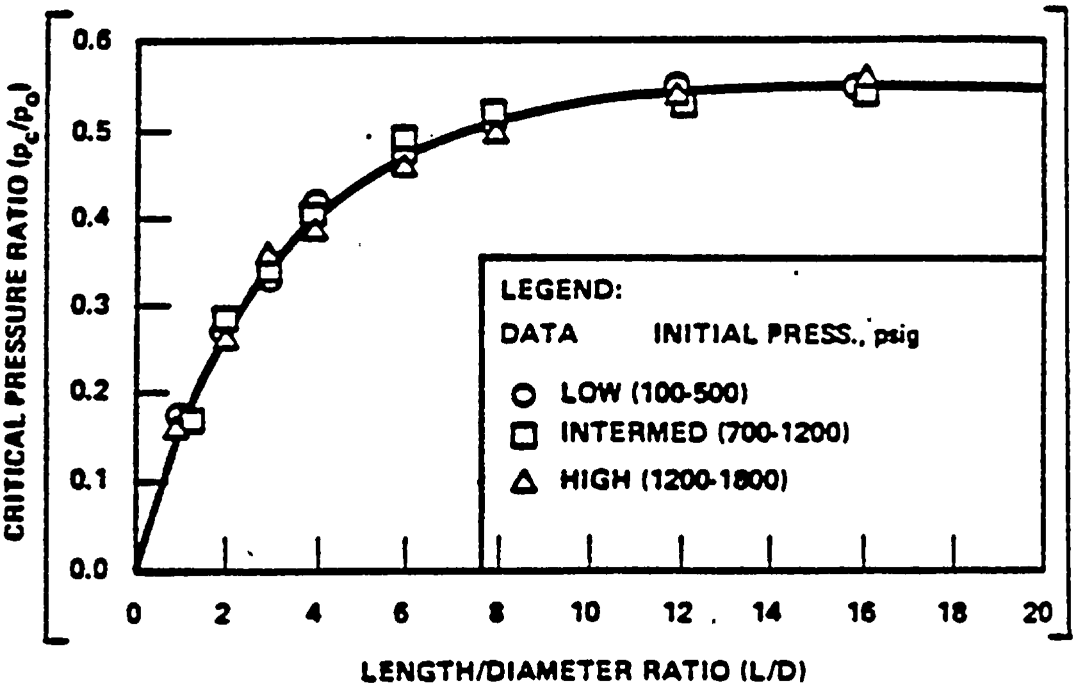

a,c,e

Figure 6-2 [Critical or Choked]^{a,c,e} Pressure Ratio as a Function of L/D

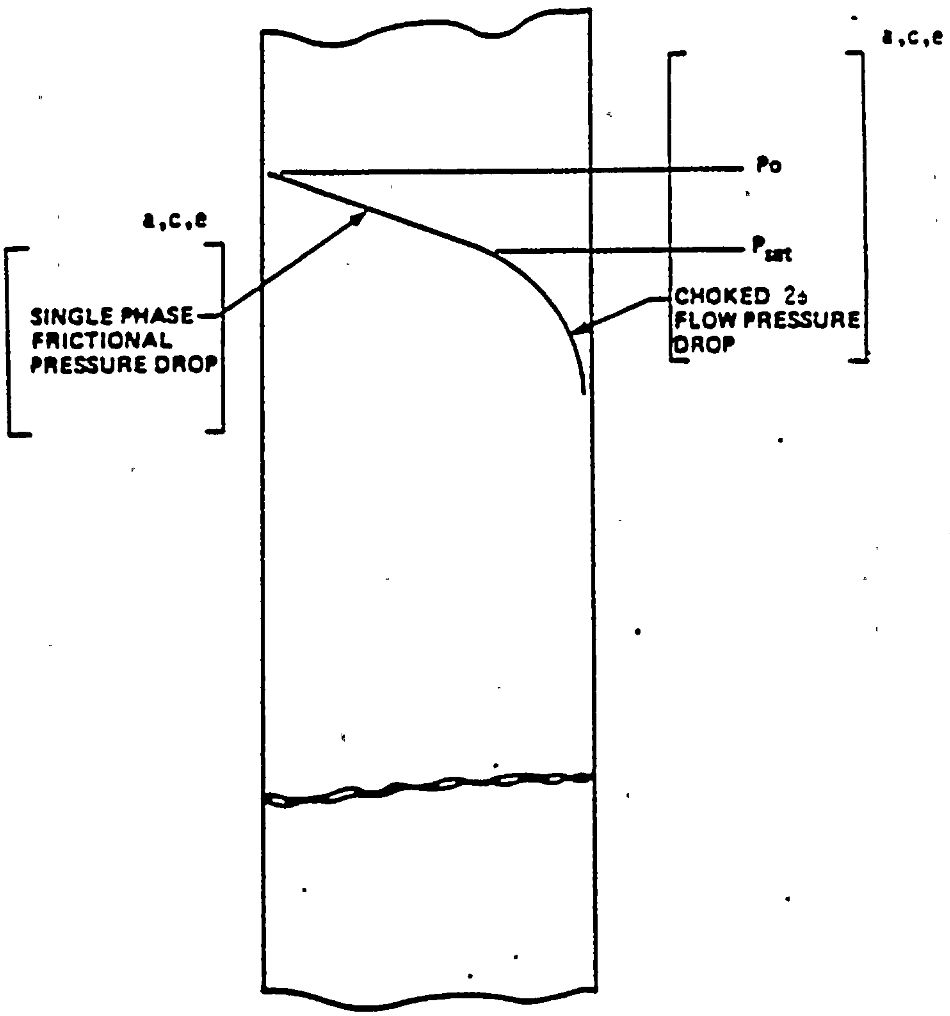

Figure 6-3. Idealized Pressure Drop Profile Through a Postulated Crack

SECTION 7.0
FRACTURE MECHANICS EVALUATION

7.1 Local Failure Mechanism

The local mechanism of failure is primarily dominated by the crack tip behavior in terms of crack-tip blunting, initiation, extension and finally crack instability. The local stability will be assumed if the crack does not initiate at all. It has been accepted that the initiation toughness measured in terms of J_{Ic} from a J-integral resistance curve is a material parameter defining the crack initiation. If, for a given load, the calculated J-integral value is shown to be less than the J_{Ic} of the material, then the crack will not initiate. If the initiation criterion is not met, one can calculate the tearing modulus as defined by the following relation:

$$T_{app} = \frac{dJ}{da} \frac{E}{\sigma_f^2}$$

where:

T_{app} = applied tearing modulus
E = modulus of elasticity
σ_f = 0.5 ($\sigma_y + \sigma_u$) (flow stress)
a = crack length
σ_y, σ_u = yield and ultimate strength of the material, respectively

Stability is said to exist when ductile tearing occurs if T_{app} is less than T_{mat}, the experimentally determined tearing modulus. Since a constant T_{mat} is assumed a further restriction is placed in J_{app}. J_{app} must be less than J_{max} where J_{max} is the maximum value of J for which the experimental T is greater than or equal to the T_{mat} used.

As discussed in Section 5.2 the local crack stability will be established by the two-step criteria:

(1) If $K_{app} < J_{Ic}$, then the crack is stable.

(2) If $J_{app} \geq J_{Ic}$, then, if $T_{app} < T_{mat}$

and $J_{app} < J_{max}$, the crack is stable.

7.2 Global Failure Mechanism

Determination of the conditions which lead to failure in stainless steel should be done with plastic fracture methodology because of the large amount of deformation accompanying fracture. One method for predicting the failure of ductile material is the plastic instability method, based on traditional plastic limit load concepts, but accounting for strain hardening and taking into account the presence of a flaw. The flawed pipe is predicted to fail when the remaining net section reaches a stress level at which a plastic hinge is formed. The stress level at which this occurs is termed as the flow stress. The flow stress is generally taken as the average of the yield and ultimate tensile strength of the material at the temperature of interest. This methodology has been shown to be applicable to ductile piping through a large number of experiments and will be used here to predict the critical flaw size in the primary coolant piping. The failure criterion has been obtained by requiring equilibrium of the section containing the flaw (figure 7-1) when loads are applied. The detailed development is provided in appendix A for a through-wall circumferential flaw in a pipe with internal pressure, axial force, and imposed bending moments. The limit moment for such a pipe is given by:

$$[M_b = 2\ \sigma_f\ R_m^2\ t\ (2\cos\beta - \sin\alpha)]^{a,c,e}$$

where:

[α = half-angle of crack in radians (refer to figure A-1, appendix A)
p = internal pressure
R_m = mean pipe radius, inches
t = pipe thickness, inches]^{a,c,e}
[σ_f = 0.5 (s_y + s_u) (flow stress)
σ_y = yield stress
σ_u = ultimate tensile strength
F = axial force
β = angular location of neutral axis (refer to figure A-1)

$$\beta = \frac{\alpha}{2} + \frac{(\pi R_i^2\, p + F)}{4\ \sigma_f\, R_m\, t}\,]^{a,c,e}$$

The analytical model described above accurately accounts for the piping internal pressure as well as imposed axial force as they affect the limit moment. Good agreement was found between the analytical predictions and the experimental results (reference 7-1).

For application of the limit load methodology, the material, including consideration of the configuration, must have a sufficient ductility and ductile tearing resistance to sustain the limit load.

7.3 Results of Crack Stability Evaluation

Stability analyses were performed at the critical locations established in section 5.1. The elastic-plastic fracture mechanics (EPFM) J-integral analyses for through-wall circumferential cracks in a cylinder were performed using the procedure in the EPRI fracture mechanics handbook (reference 7-2).

The lower-bound material properties of section 4.0 were applied (see Table 4-6). The fracture toughness properties established in section 4.3 (see Table 4-7) and the normal plus SSE loads given in Table 3-2 were used for the EPFM calculations. Evaluations were performed at the toughness critical locations identified in section 5.1. The results of the elastic-plastic fracture mechanics J-integral evaluations are given in Table 7-1. The leakage size flaws are presented on the same table.

The load critical location was identified as location 1 in section 5.1. A stability analysis based on limit load was performed for this location as described in section 7.2. Since the weld at this location is a SMAW weld, the "Z" factor correction for SMAW welds was applied (Reference 7-3) as follows:

$$Z = 1.15\ [1.0 + 0.013\ (OD-4)]$$

where OD is the outer diameter of the pipe in inches.

The Z-factor was calculated for critical location 1, using the dimensions given in table 3-1. This factor is 1.6. The applied loads were increased by the Z factor and a plot of limit load versus crack length was generated as shown in Figure 7-2. The critical flaw size is $[7.62\text{ in.}]^{a,c,e}$ and the leakage flaw sizes is $[2.9\text{ in.}]^{a,c,e}$ Lower bound base metal properties taken from ASME BPVC Section III were used for this purpose. They are $\sigma_y = 18.7$ ksi and $\sigma_u = 71.8$ ksi.

7.4 References

7-1. Kanninen, M. F., et. al., "Mechanical Fracture Predictions for Sensitized Stainless Steel Piping with Circumferential Cracks," EPRI NP-192, September 1976.

7-2. Kumar, V., German, M. D. and Shih, C. P., "An Engineering Approach for Elastic-Plastic Fracture Analysis," EPRI Report NP-1931, Project 1237-1, Electric Power Research Institute, July 1981.

7-3. ASME Code Section XI, Winter 1985 Addendum, Article IWB-3640.

TABLE 7-1

STABILITY RESULTS FOR DIABLO CANYON UNITS 1 AND 2
BASED ON ELASTIC-PLASTIC
J-INTEGRAL EVALUATIONS

		Fracture Criteria			Calculated Values	
Location	Flaw Size (in)	J_{Ic} (in-lb/in^2)	T_{mat}	J_{max} (in-lb/in^2)	J_{app} (in-lb/in^2)	T_{app}
6	16.8	567	36.6	1451	603	2.81
7	16.8	272	6.9	438	390	1.7
10	10.9	664	45.1	1755	1755	10.9

a,c,e

Leakage Flaw Size

Location	Flaw Size
6	8.4 in.
7	8.4 in.
10	5.6 in.

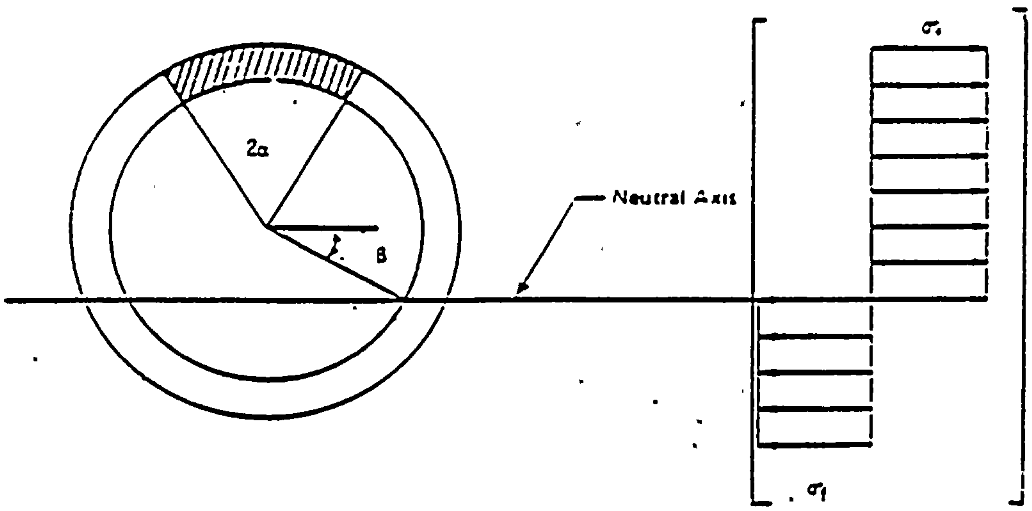

a,c,e

Figure 7-1

[Fully Plastic]^{a,c,e} Stress Distribution

a,c,e

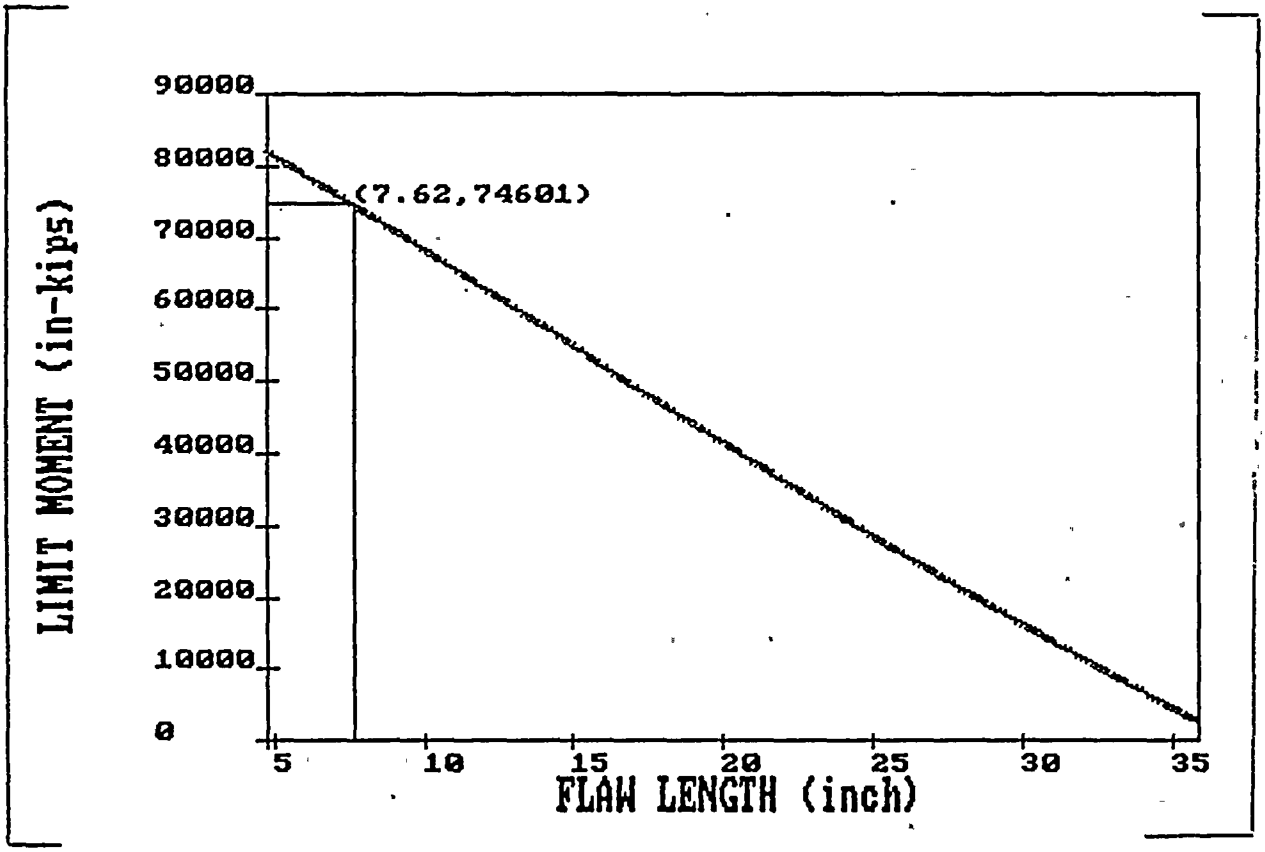

OD = 33.99 in
t = 2.395 in

σ_y = 18.7 ksi
σ_u = 71.8 ksi
(SMAW Weld)

F_a = 2161 kips
M_b = 46674 in-kips

Figure 7-2
Critical Flaw Size Prediction - Hot Leg at Location 1

SECTION 8.0
FATIGUE CRACK GROWTH ANALYSIS

To determine the sensitivity of the primary coolant system to the presence of small cracks, a fatigue crack growth analysis was carried out for the [vessel inlet nozzle safe-end]^{a,c,e} region of a typical system (see Location [14]^{a,c,e} of Figure 3-2). This region was selected because crack growth calculated here will be typical of that in the entire primary loop. Crack growths calculated at other locations can be expected to show less than 10% variation.

A [finite element stress analysis was carried out for the inlet nozzle safe end region]^{a,c,e} of a plant typical in geometry and operational characteristics to any Westinghouse PWR System. [The specific system was a plant with piping outside diameter 33 inches, and wall thickness of 2.85 inches. The corresponding dimensions for the Diablo Canyon Unit 1 are 33.06 inches in diameter and 2.675 inches wall thickness. These differences are insignificant as far as fatigue crack growth analysis is concerned.]^{a,c,e} All normal, upset, and test conditions were considered. A summary of the applied transients is provided in table 8-1. Circumferentially oriented surface flaws were postulated in the region, assuming the flaw was located in three different locations, as shown in Figure 8-1. Specifically, these were:

Cross Section A: [Inconel]^{a,c,e}
Cross Section B: [SA 508 Cl. 2 or 3 Low Alloy Steel]^{a,c,e}
Cross Section C: [Stainless Steel]^{a,c,e}

Fatigue crack growth rate laws were used [from the ASME Code Section XI for the carbon steel, shown in Figure 8-2, and developed from the literature for the other two materials. The laws were all structured for applicability to pressurized water reactor environments.]^{a,c,e} The law for stainless steel was derived from Reference 8-1, with a very conservative correction for the R ratio, which is the ratio of minimum to maximum stress during a transient. For stainless steel, the fatigue crack growth formula is:

$$\frac{da}{dn} = (5.4 \, x \, 10^{-12}) \; K_{eff}{}^{4.48} inches/cycle$$

where $K_{eff} = K_{max} \, (1-R)^{0.5}$

$R = K_{min}/K_{max}$

[The fatigue crack growth rate for Inconel 600 in a water environment was derived from a collection of data from two different sources. A relatively large body of data is available for Inconel 600 in an air environment at 600°F (Reference 8-2) and these data were used to establish the slope of the reference curve, as shown in figure 8-3. The environmental enhancement of crack growth for this material is characterized by the data available in Reference 8-3, and these points were used to set the location of the water curve at a growth rate of approximately a factor of five above the air curve. The resulting equation is:]^{a,c,e}

$$[\frac{da}{dn} = (2.23 \, x \, 10^{-13}) \; K_{eff}{}^{5.66}]^{a,c,e}$$

where: $[K_{eff} = \Delta K/(1.0-0.5R)]^{a,c,e}$

The calculated fatigue crack growth for semi-elliptic surface flaws of circumferential orientation and various depths is summarized in Table 8-2, and shows that the crack growth is very small, [regardless of which material is assumed.]^{a,c,e}

8.1 References

8-1 Bamford, W. H., "Fatigue Crack Growth of Stainless Steel Piping in a Pressurized Water Reactor Environment," Trans. ASME Journal of Pressure Vessel Technology, Vol. 101, Feb. 1979.

8-2 [James, L. A., "Fatigue Crack Propagation Behavior of Inconel 600," in Hanford Engineering Development Labs Report HEDL-TME-76-43, May 1976.]^{a,c,e}

8-3 [Hale, D. A., et. al., "Fatigue Crack Growth in Piping and RPV Steels in Simulated BWR Water Environment," Report GEAP 24098/NUREG CR-0390, Jan. 1978.]^{a,c,e}

TABLE 8-1

SUMMARY OF REACTOR VESSEL TRANSIENTS

NUMBER	TYPICAL TRANSIENT IDENTIFICATION	NUMBER OF CYCLES
	<u>Normal Conditions</u>	
1	Heatup and Cooldown at 100°F/hr (pressurizer cooldown 200°F/hr)	200
2	Load Follow Cycles (Unit loading and unloading at 5% of full power/min)	18300
3	Step load increase and decrease	2000
4	Large step load decrease, with steam dump	200
5	Steady state fluctuations	10^6
	<u>Upset Conditions</u>	
6	Loss of load, without immediate turbine or reactor trip	80
7	Loss of power (blackout with natural circulation in the Reactor Coolant System)	40
8	Loss of Flow (partial loss of flow, one pump only)	80
9	Reactor trip from full power	400
	<u>Test Conditions</u>	
10	Turbine roll test	10
11	Hydrostatic test conditions	
	Primary side	5
	Primary side leak test	50
12	Cold Hydrostatic test	10

TABLE 8-2

TYPICAL FATIGUE CRACK GROWTH AT [NOZZLE SAFE-END REGION]^{a,c,e} (40 YEARS)

	FINAL FLAW (in)		
INITIAL FLAW (IN)	[FERRITIC STEEL]^{a,c,e}	[STAINLESS]^{a,c,e}	[INCONEL]^{a,c,e}
0.292	0.31097	0.30107	0.30698
0.300	0.31949	0.30953	0.31626
0.375	0.39940	0.38948	0.40763
0.425	0.45271	0.4435	0.47421

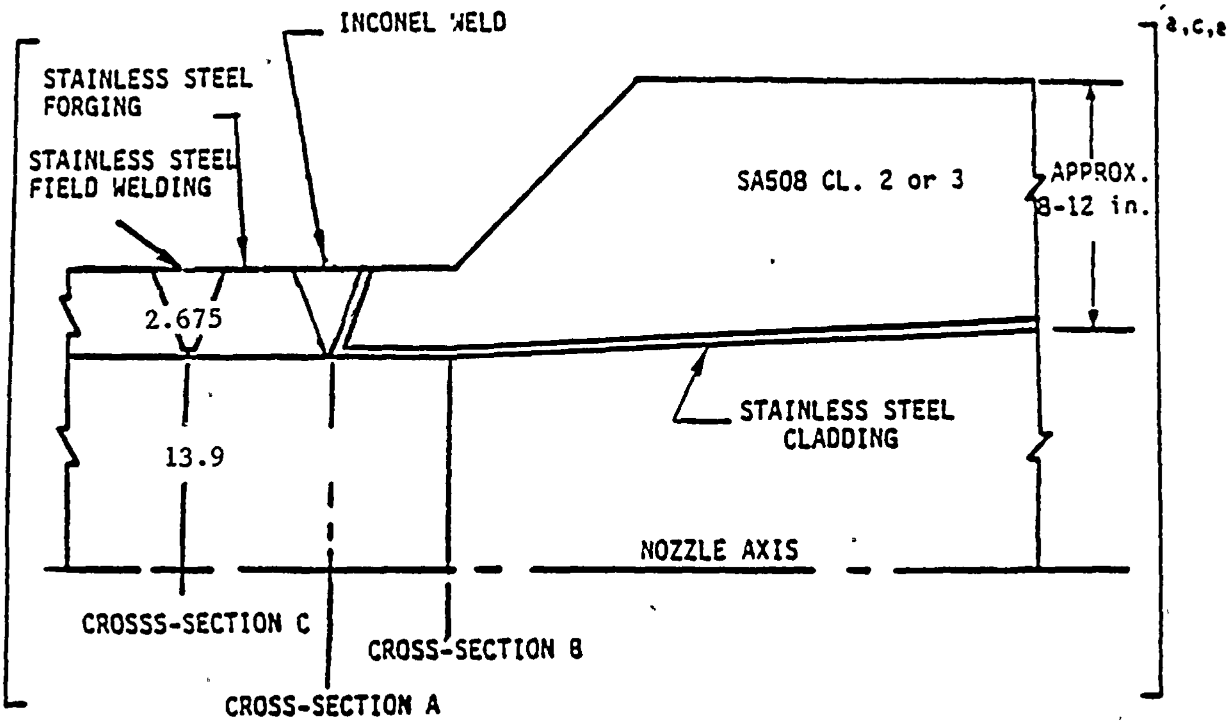

Dimensions in inches

Figure 8-1

Typical Cross-Section of [RPV Inlet Nozzle Safe-End]^{a,c,e}

a,c,e

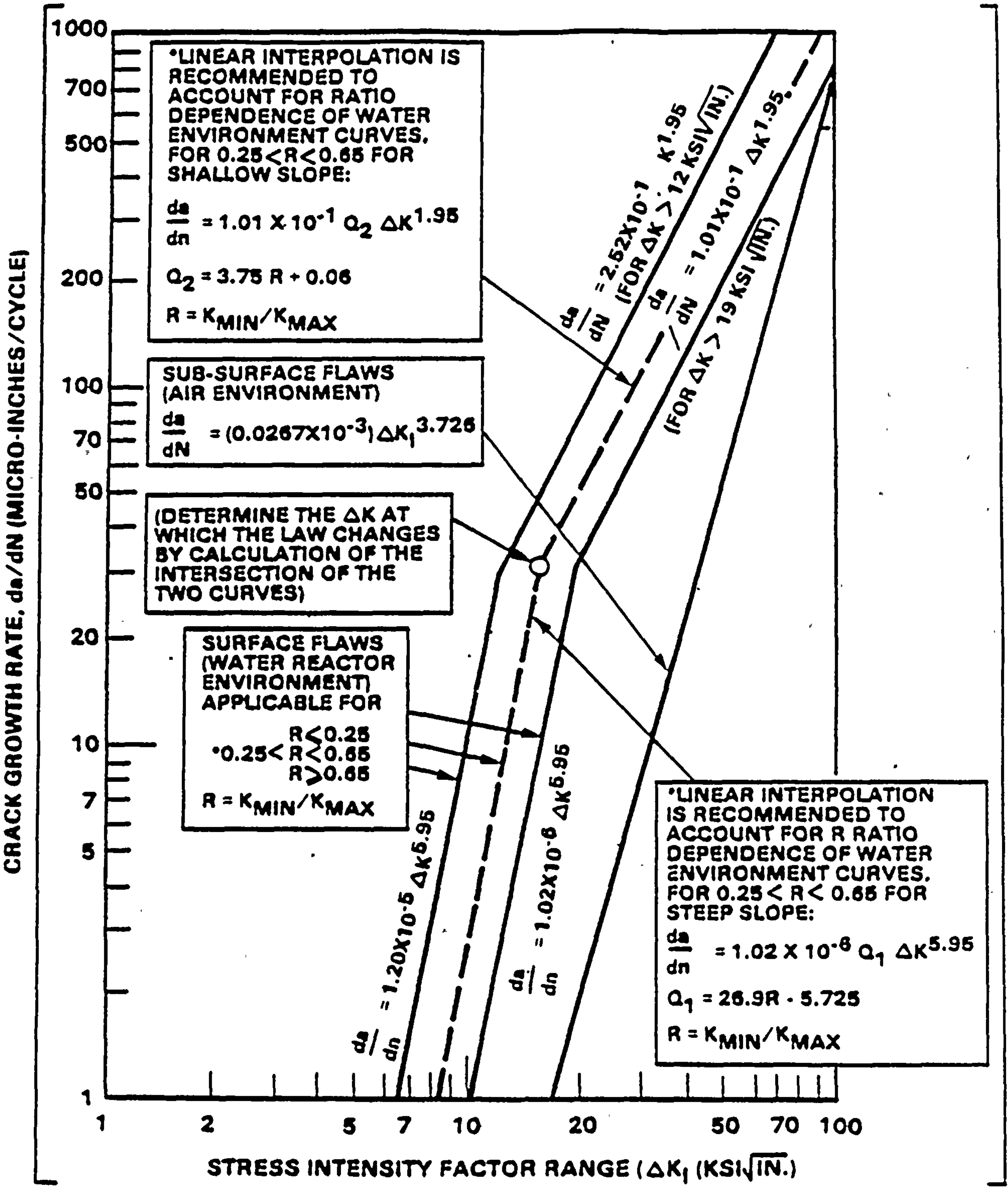

Figure 8-2. Reference Fatigue Crack Growth Curves for [Carbon and Low Alloy Ferritic Steels]^{a,c,e}

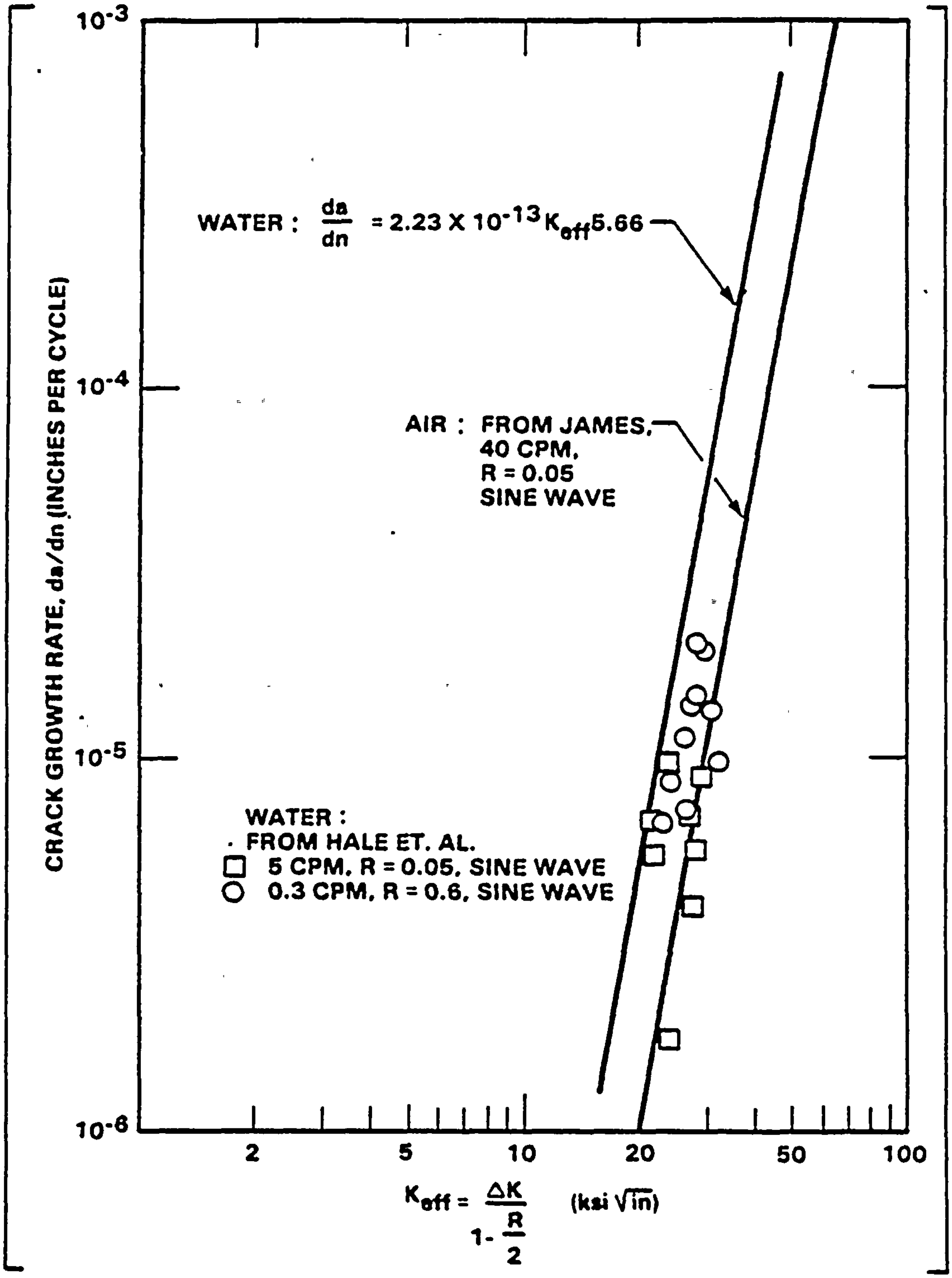

Figure 8-3. Reference Fatigue Crack Growth Law for [Inconel 600]^{a,c,e} in a Water Environment at 600°F

SECTION 9.0
ASSESSMENT OF MARGINS

The results of the leak rates of section 6.4 and the corresponding stability and fracture toughness evaluations of sections 7.2 and 7.3 are used in performing the assessment of margins. Margins are shown in Table 9-1.

In summary, at all the critical locations relative to:

1. Flaw Size - Using faulted loads obtained by the absolute sum method, a margin of about 2 exists between the critical flaw and the flaw having a leak rate of 10 gpm (the leakage flaw).

2. Leak Rate - A margin of 10 exists between the calculated leak rate from the leakage flaw and the leak detection capability of 1 gpm.

3. Loads - At the critical locations the leakage flaw was shown to be stable using the faulted loads obtained by the absolute sum method.

TABLE 9-1
SUMMARY TABLE

Location	Leakage Flaw Size	Critical Flaw Size	Margin
1	2.9 in.	7.62 in.	2.63
6	8.4 in.	16.8 in.	2.00
7	8.4 in.	16.8 in.	2.00
10	5.6 in.	10.9 in.	1.95

a,c,e

SECTION 10.0
CONCLUSIONS

This report justifies the elimination of RCS primary loop pipe breaks for the Diablo Canyon Units 1 and 2 nuclear plants as follows:

a. Stress corrosion cracking is precluded by use of fracture resistant materials in the piping system and controls on reactor coolant chemistry, temperature, pressure, and flow during normal operation.

b. Water hammer should not occur in the RCS piping because of system design, testing, and operational considerations.

c. The effects of low and high cycle fatigue on the integrity of the primary piping are negligible.

d. Adequate margin exists between the leak rate of small stable flaws and the capability of the Diablo Canyon Units 1 and 2 reactor coolant system pressure boundary Leakage Detection System.

e. Ample margin exists between the small stable flaw sizes of item d and larger stable flaws.

f. Ample margin exists in the material properties used to demonstrate end-of-service life (relative to aging) stability of the critical flaws.

For the critical locations flaws are identified that will be stable because of the ample margins in d, e, and f above.

Based on the above, it is concluded that dynamic effects of RCS primary loop pipe breaks need not be considered in the structural design basis of the Diablo Canyon Units 1 and 2 plants.

APPENDIX A

LIMIT MOMENT

[The internal stress system at the crack plane has to be in equilibrium with the applied loading, i.e., the hydrostatic pressure P, axial force F, and the bending moment M_b. The angle b which identifies the point of stress inversion follows from the equilibrium of horizontal forces (See Figure A-1). This is:

$$\left(\frac{\pi}{2} - \alpha + \beta\right) R_m t\ \sigma_f - \left(\frac{\pi}{2} - \beta\right) R_m t\ \sigma_f = \frac{\pi}{2} R_i^2\ p + F/2$$

Solving for β,

$$\beta = \frac{\alpha}{2} + \frac{\pi R_i^2\ p+F}{4R_m t\ \sigma_f}$$

The external bending moment at the instant of failure follows from the equilibrium of moments, which is most easily taken around the axis 1-1. Thus M_b can be determined from

$$M_b = 2\sigma_f R_m^2\ t\int_{\alpha}^{\frac{\pi}{2}+\beta}\cos\theta d\theta + \int_{o}^{\frac{\pi}{2}-\beta}\cos\theta d\theta)$$

or

$$M_b = 2\sigma_f\ R_m^2 t\ (\cos\beta - \sin\alpha)]^{a,c,e}$$

a,c,e

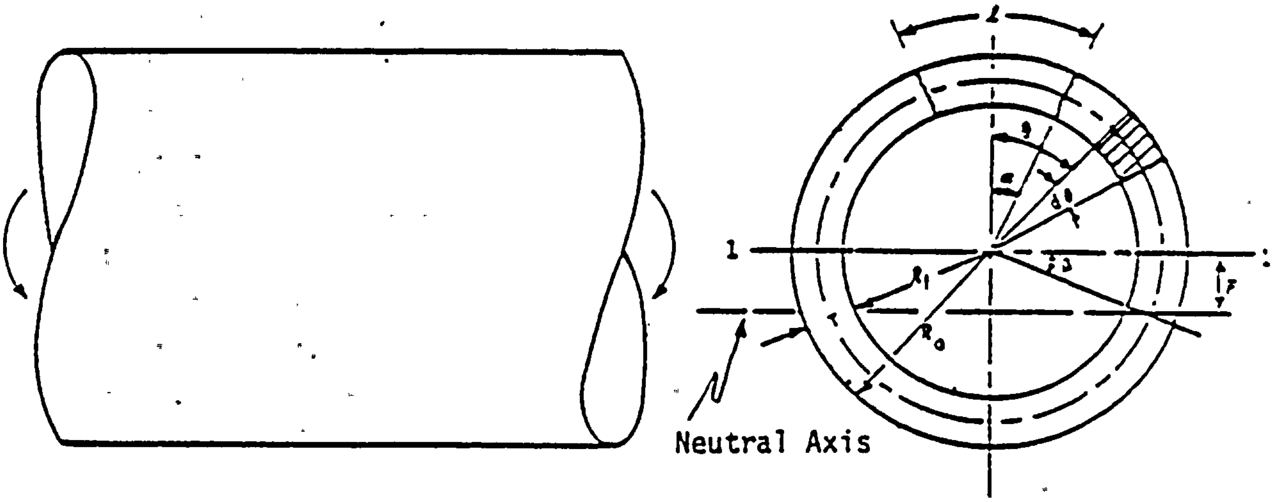

Figure A-1

Pipe with a Through-Wall Crack in Bending

APPENDIX B

ALTERNATE TOUGHNESS CRITERIA FOR THE DIABLO CANYON UNITS 1 AND 2 CAST PRIMARY LOOP COMPONENTS

B.1 Introduction

Not all of the individual cast piping components of the Diablo Canyon primary loop piping satisfy the original [Heat L]^{a,c,e} criteria (reference 4-3). In this appendix, the alternate toughness criteria for thermally aged cast stainless steel developed in Reference 4-6 will be used to categorize the various individual cast piping components thus establishing criteria based upon which the leak-before-break evaluations may be performed. Reference 4-6 has been reviewed by the NRC wherein the NRC concluded that Reference 4-6 may be utilized for establishing the fracture criteria for thermally aged cast stainless piping applicable for the leak-before-break analyses (Reference B-1).

B.2 Chemistry and KCU Toughness

Per the procedure of Reference 4-6 the correlations of Reference 4-4 which are based on the chemistry of the cast stainless steel piping was used to calculate the associated KCU values. The chemistry and end-of-service life KCU toughness values are given in Table B-1 for Unit 1 and in Table B-2 for Unit 2.

B.3 Alternate Toughness Criteria for the Diablo Canyon Primary Loop Material on a Component by Component Basis

The alternate toughness criteria for the Diablo Canyon Unit 1 and 2 cast primary loop material may be obtained by applying the methodology of Reference 4-6 to the KCU values of Tables B-1 and B-2. First, it is observed that 47 of the 53 heats fall into category 1, i.e., they are at least as tough as [Heat L]^{a,c,e}. The remaining heats fall into category 2. Typical toughness calculations using the methodology of Reference 4-6 are given below for a category 2 heat.

For example, [Heat No. 14804-1]^{a,c,e} (the 90° elbow in the crossover leg on the steam generator side of Diablo Canyon Unit 1) has the calculated end-of-service life KCU at room temperature of [1.56]^{a,c,e} daj/cm^2 which falls below that of [Heat L]^{a,c,e}. The δ-ferrite content is [20.97%]^{a,c,e}. By Reference 4-6, the [ferrite-austenite ratio, R is given by:

$$R = (16.40/20.97)(79.03/83.6)^2 = 0.699$$

Thus using table 2-8 of Reference 4-6, the fully aged KCU is 1.209 daj/cm^2, i.e. 1.73 times R].^{a,c,e} Since the end-of-service life KCU exceeds the fully aged KCU, the heat falls into category 2. Thus:

$$J_{Ic} = [750 - (4.3-1.56)(750-300(0.699))/(4.3-1.73(0.699)) = 272 \text{ in-lb/in}^2]^{a,c,e}$$

$$T_{mat} = [60 - (4.3-1.56)(60)/(4.3-1.73(0.699)) = 6.9]^{a,c,e}$$

and

$$J_{max} = [2200-(4.3-1.56)(2200-300(0.699))/(4.3-1.73(0.699)) = 438 \text{ in-lb/in}^2]^{a,c,e}$$

The fracture toughness values for each heat of material was calculated as formulated in Reference 4-6. These values are also given in Tables B-1 and B-2.

B.4 References

B-1 Letter: Dominic C., DiIanni, NRC to D. M. Musolf, Northern States Power Company, dated December 22, 1986, Docket Nos. 50-282 and 50-306.

TABLE B-1

CHEMISTRY AND FRACTURE TOUGHNESS PROPERTIES OF THE MATERIAL HEATS OF DIABLO CANYON UNIT 1

a,c,e

```
PLANT PGE1 31 IN ID X 400 ELL A351/CF8M HT NO 13174-2
CATEGORY 1       R RATIO IS     1.355                                             FRACTURE TOUGHNESS
                                                   CR(E) CR/NI DELTA    --------------------------------------------------
  %NI    %C   %MN    %N   %CR  %SI  %MO  %CB NI(E) CR(E) CR/NI FENUM    KCU  JIC40   TMAT40  JMAX40  JICFA   TMATFA  JMAXFA
  9.42   .08  1.09  .05 19.64 1.28 2.57  .00 15.91 20.17 1.267 13.08    4.57 750.     60.0   2200.    407.      .0   407.
                                                   19.14 1.203 14.37

PLANT PGE1 31 IN ID X 400 ELL A351/CF8M HT NO 13704-1
CATEGORY 2       R RATIO IS      .938                                             FRACTURE TOUGHNESS
                                                   CR(E) CR/NI DELTA    --------------------------------------------------
  %NI    %C   %MN    %N   %CR  %SI  %MO  %CB NI(E) CR(E) CR/NI FENUM    KCU  JIC40   TMAT40  JMAX40  JICFA   TMATFA  JMAXFA
  9.55   .05   .95  .05 20.00 1.28 2.43  .00 15.07 20.33 1.349 17.17    3.25 567.     36.6   1451.    281.      .0   281.
                                                   19.36 1.284 19.04

PLANT PGE1 31 IN ID X 400 ELL A351/CF8M HT NO 16654-2
CATEGORY 1       R RATIO IS     1.681                                             FRACTURE TOUGHNESS
                                                   CR(E) CR/NI DELTA    --------------------------------------------------
  %NI    %C   %MN    %N   %CR  %SI  %MO  %CB NI(E) CR(E) CR/NI FENUM    KCU  JIC40   TMAT40  JMAX40  JICFA   TMATFA  JMAXFA
  9.91   .07   .86  .05 19.11 1.27 2.51  .00 15.99 19.54 1.222 11.05    6.54 750.     60.0   2200.    504.      .0   504.
                                                   18.54 1.159 12.44

PLANT PGE1 31 IN ID X 40 D ELL A351/CF8M HT NO 16690-2
CATEGORY 1       R RATIO IS     1.793                                             FRACTURE TOUGHNESS
                                                   CR(E) CR/NI DELTA    --------------------------------------------------
  %NI    %C   %MN    %N   %CR  %SI  %MO  %CB NI(E) CR(E) CR/NI FENUM    KCU  JIC40   TMAT40  JMAX40  JICFA   TMATFA  JMAXFA
  9.69   .06  1.42  .05 18.50 1.27 2.59  .00 15.75 19.04 1.209 10.49    7.92 750.     60.0   2200.    538.      .0   538.
                                                   18.01 1.143 11.56

PLANT PGE1 31 IN X 29 IN ID X 500 RED ELL A351/CF8M HT NO 10563-2
CATEGORY 1       R RATIO IS     1.267                                             FRACTURE TOUGHNESS
                                                   CR(E) CR/NI DELTA    --------------------------------------------------
  %NI    %C   %MN    %N   %CR  %SI  %MO  %CB NI(E) CR(E) CR/NI FENUM    KCU  JIC40   TMAT40  JMAX40  JICFA   TMATFA  JMAXFA
  9.51   .07   .85  .05 19.15 1.22 2.85  .00 15.58 19.98 1.282 13.78    4.99 750.     60.0   2200.    380.      .0   380.
                                                   18.84 1.209 14.77

PLANT PGE1 31 IN X 29 IN ID X 500 RED ELL A351/CF8M HT NO 10966-1
CATEGORY 2       R RATIO IS      .915                                             FRACTURE TOUGHNESS
                                                   CR(E) CR/NI DELTA    --------------------------------------------------
  %NI    %C   %MN    %N   %CR  %SI  %MO  %CB NI(E) CR(E) CR/NI FENUM    KCU  JIC40   TMAT40  JMAX40  JICFA   TMATFA  JMAXFA
  9.40   .05   .85  .05 19.25 1.28 2.83  .00 14.87 20.14 1.354 17.46    3.98 693.     52.8   1970.    275.      .0   275.
                                                   19.01 1.278 18.74

PLANT PGE1 31 IN X 29 IN ID X 500 RED ELL A351/CF8M HT NO 11937-2
CATEGORY 1       R RATIO IS     1.126                                             FRACTURE TOUGHNESS
                                                   CR(E) CR/NI DELTA    --------------------------------------------------
  %NI    %C   %MN    %N   %CR  %SI  %MO  %CB NI(E) CR(E) CR/NI FENUM    KCU  JIC40   TMAT40  JMAX40  JICFA   TMATFA  JMAXFA
  9.53   .06   .82  .05 19.48 1.45 2.38  .00 15.29 20.00 1.308 15.04    4.51 750.     60.0   2200.    338.      .0   338.
                                                   19.05 1.246 16.72

PLANT PGE1 31 IN X 29 IN ID X 500 RED ELL A351/CF8M HT NO 12198-2
CATEGORY 1       R RATIO IS     1.801                                             FRACTURE TOUGHNESS
                                                   CR(E) CR/NI DELTA    --------------------------------------------------
  %NI    %C   %MN    %N   %CR  %SI  %MO  %CB NI(E) CR(E) CR/NI FENUM    KCU  JIC40   TMAT40  JMAX40  JICFA   TMATFA  JMAXFA
  9.79   .07  1.05  .05 19.26 1.18 2.32  .00 15.96 19.29 1.208 10.45    7.06 750.     60.0   2200.    540.      .0   540.
                                                   18.36 1.150 12.00
```

a,c,e

```
PLANT PGE1 31 IN ID X 900 ELL A351/CF8M HT NO 13421-1
CATEGORY 1        R RATIO IS     1.401                                          FRACTURE TOUGHNESS
                                                      CR(E) CR/NI DELTA   ---------------------------------------------------
  %NI     %C   %MN    %N    %CR   %SI   %MO   %CB NI(E) CR(E) CR/NI FENUM   KCU  JIC40   TMAT40  JMAX40   JICFA   TMATFA  JMAXFA
 10.02   .06  1.07   .05  19.40  1.42  2.50  .00 15.90 20.04 1.260 12.75    5.04  750.    60.0   2200.    420.      .0    420.
                                                      19.04 1.197 14.13

PLANT PGE1 31 IN ID X 900 ELL A351/CF8M HT NO 14576-1
CATEGORY 1        R RATIO IS     1.246                                          FRACTURE TOUGHNESS
                                                      CR(E) CR/NI DELTA   ---------------------------------------------------
  %NI     %C   %MN    %N    %CR   %SI   %MO   %CB NI(E) CR(E) CR/NI FENUM   KCU  JIC40   TMAT40  JMAX40   JICFA   TMATFA  JMAXFA
  9.70   .05  1.47   .05  18.66  1.47  2.88  .00 15.48 19.91 1.286 13.95    5.41  750.    60.0   2200.    374.      .0    374.
                                                      18.76 1.211 14.92

PLANT PGE1 31 IN ID X 900 ELL A351/CF8M HT NO 14804-1
CATEGORY 2        R RATIO IS      .699                                          FRACTURE TOUGHNESS
                                                      CR(E) CR/NI DELTA   ---------------------------------------------------
  %NI     %C   %MN    %N    %CR   %SI   %MO   %CB NI(E) CR(E) CR/NI FENUM   KCU  JIC40   TMAT40  JMAX40   JICFA   TMATFA  JMAXFA
  9.47   .05   .86   .05  19.94  1.43  2.89  .00 14.95 21.14 1.414 20.97    1.56  272.     6.9    438.    210.      .0    210.
                                                      19.99 1.337 22.94

PLANT PGE1 31 IN ID X 900 ELL A351/CF8M HT NO 15560-1
CATEGORY 1        R RATIO IS     1.039                                          FRACTURE TOUGHNESS
                                                      CR(E) CR/NI DELTA   ---------------------------------------------------
  %NI     %C   %MN    %N    %CR   %SI   %MO   %CB NI(E) CR(E) CR/NI FENUM   KCU  JIC40   TMAT40  JMAX40   JICFA   TMATFA  JMAXFA
  9.33   .04   .87   .05  18.73  1.41  2.42  .00 14.51 19.24 1.326 15.95    5.98  750.    60.0   2200.    312.      .0    312.
                                                      18.28 1.259 17.72

PLANT PGE1 31 IN ID X 900 ELL A351/CF8M HT NO 15823-1
CATEGORY 1        R RATIO IS     1.346                                          FRACTURE TOUGHNESS
                                                      CR(E) CR/NI DELTA   ---------------------------------------------------
  %NI     %C   %MN    %N    %CR   %SI   %MO   %CB NI(E) CR(E) CR/NI FENUM   KCU  JIC40   TMAT40  JMAX40   JICFA   TMATFA  JMAXFA
 10.00   .05   .92   .05  19.05  1.29  2.63  .00 15.51 19.68 1.269 13.15    5.69  750.    60.0   2200.    404.      .0    404.
                                                      18.63 1.201 14.25

PLANT PGE1 31 IN ID X 900 ELL A351/CF8M HT NO 15987-2
CATEGORY 2        R RATIO IS      .855                                          FRACTURE TOUGHNESS
                                                      CR(E) CR/NI DELTA   ---------------------------------------------------
  %NI     %C   %MN    %N    %CR   %SI   %MO   %CB NI(E) CR(E) CR/NI FENUM   KCU  JIC40   TMAT40  JMAX40   JICFA   TMATFA  JMAXFA
  9.68   .05   .86   .05  19.86  1.48  2.62  .00 15.16 20.76 1.369 18.31    2.54  442.    22.6    987.    257.      .0    257.
                                                      19.71 1.300 20.21

PLANT PGE1 31 IN ID X 900 ELL A351/CF8M HT NO 14535-2
CATEGORY 1        R RATIO IS     1.197                                          FRACTURE TOUGHNESS
                                                      CR(E) CR/NI DELTA   ---------------------------------------------------
  %NI     %C   %MN    %N    %CR   %SI   %MO   %CB NI(E) CR(E) CR/NI FENUM   KCU  JIC40   TMAT40  JMAX40   JICFA   TMATFA  JMAXFA
  9.90   .04   .90   .05  19.15  1.35  2.40  .00 15.10 19.55 1.294 14.37    5.55  750.    60.0   2200.    359.      .0    359.
                                                      18.59 1.231 15.99

PLANT PGE1 31 IN ID X 900 ELL A351/CF8M HT NO 16037-3
CATEGORY 1        R RATIO IS     1.730                                          FRACTURE TOUGHNESS
                                                      CR(E) CR/NI DELTA   ---------------------------------------------------
  %NI     %C   %MN    %N    %CR   %SI   %MO   %CB NI(E) CR(E) CR/NI FENUM   KCU  JIC40   TMAT40  JMAX40   JICFA   TMATFA  JMAXFA
 10.62   .06   .82   .05  19.45  1.40  2.40  .00 16.38 19.92 1.216 10.79    5.84  750.    60.0   2200.    519.      .0    519.
                                                      18.96 1.158 12.36
```

a,c

```
PLANT PGE1 31 IN ID X 900 ELL W/ SPLITTER A351/CF8M HT NO 11556-1
CATEGORY 1      R RATIO IS     1.152                                          FRACTURE TOUGHNESS
                                                 CR(E) CR/NI DELTA    -------------------------------------------------
  %NI    %C   %MN   %N   %CR  %SI  %MO  %CB NI(E) CR(E) CR/NI FENUM    KCU  JIC40   THAT40  JMAX40  JICFA   THATFA  JMAXFA
 9.92   .05   .69  .05 19.56 1.06 2.71  .00 15.31 19.95 1.303 14.80   4.52  750.    60.0   2200.    345.      .0    345.
                                                 18.87 1.232 16.03

PLANT PGE1 31 IN ID X 900 ELL W/ SPLITTER A351/CF8M HT NO 11743-1
CATEGORY 1      R RATIO IS     1.246                                          FRACTURE TOUGHNESS
                                                 CR(E) CR/NI DELTA    -------------------------------------------------
  %NI    %C   %MN   %N   %CR  %SI  %MO  %CB NI(E) CR(E) CR/NI FENUM    KCU  JIC40   THAT40  JMAX40  JICFA   THATFA  JMAXFA
 9.70   .06   .85  .05 19.59 1.28 2.41  .00 15.47 19.89 1.286 13.95   4.82  750.    60.0   2200.    374.      .0    374.
                                                 18.93 1.223 15.69

PLANT PGE1 31 IN ID X 900 ELL W/ SPLITTER A351/CF8M HT NO 11974-1
CATEGORY 1      R RATIO IS     1.444                                          FRACTURE TOUGHNESS
                                                 CR(E) CR/NI DELTA    -------------------------------------------------
  %NI    %C   %MN   %N   %CR  %SI  %MO  %CB NI(E) CR(E) CR/NI FENUM    KCU  JIC40   THAT40  JMAX40  JICFA   THATFA  JMAXFA
 9.48   .08   .87  .05 19.76 1.21 2.36  .00 15.86 19.89 1.254 12.46   5.10  750.    60.0   2200.    433.      .0    433.
                                                 18.95 1.194 14.06

PLANT PGE1 31 IN ID X 900 ELL W/SPLITTER A351/CF8M HT NO 12281-1
CATEGORY 1      R RATIO IS     1.171                                          FRACTURE TOUGHNESS
                                                 CR(E) CR/NI DELTA    -------------------------------------------------
  %NI    %C   %MN   %N   %CR  %SI  %MO  %CB NI(E) CR(E) CR/NI FENUM    KCU  JIC40   THAT40  JMAX40  JICFA   THATFA  JMAXFA
 9.62   .04   .82  .05 18.98 1.18 2.46  .00 14.78 19.20 1.299 14.62   6.11  750.    60.0   2200.    351.      .0    351.
                                                 18.22 1.233 16.05

PLANT PGE1 31 IN ID X 900 ELL W/SPLITTER A351/CF8M HT NO 13930-5
CATEGORY 2      R RATIO IS     1.347                                          FRACTURE TOUGHNESS
                                                 CR(E) CR/NI DELTA    -------------------------------------------------
  %NI    %C   %MN   %N   %CR  %SI  %MO  %CB NI(E) CR(E) CR/NI FENUM    KCU  JIC40   THAT40  JMAX40  JICFA   THATFA  JMAXFA
 9.67   .08  1.17  .05 19.85 1.25 2.73  .00 16.20 20.56 1.269 13.14   3.81  664.    45.1   1755.    404.      .0    404.
                                                 19.47 1.201 14.28

PLANT PGE1 31 IN ID X 900 ELL W/SPLITTER A351/CF8M HT NO 14251-1
CATEGORY 1      R RATIO IS     1.206                                          FRACTURE TOUGHNESS
                                                 CR(E) CR/NI DELTA    -------------------------------------------------
  %NI    %C   %MN   %N   %CR  %SI  %MO  %CB NI(E) CR(E) CR/NI FENUM    KCU  JIC40   THAT40  JMAX40  JICFA   THATFA  JMAXFA
 9.20   .04  1.04  .05 18.54 1.30 2.29  .00 14.47 18.71 1.293 14.29   7.25  750.    60.0   2200.    362.      .0    362.
                                                 17.79 1.229 15.94

PLANT PGE1 31 IN ID X 900 ELL W/ SPLITTER A351/CF8M HT NO 16690-3
CATEGORY 1      R RATIO IS     1.793                                          FRACTURE TOUGHNESS
                                                 CR(E) CR/NI DELTA    -------------------------------------------------
  %NI    %C   %MN   %N   %CR  %SI  %MO  %CB NI(E) CR(E) CR/NI FENUM    KCU  JIC40   THAT40  JMAX40  JICFA   THATFA  JMAXFA
 9.69   .06  1.42  .05 18.50 1.27 2.59  .00 15.75 19.04 1.209 10.49   7.92  750.    60.0   2200.    538.      .0    538.
                                                 18.01 1.143 11.56

PLANT PGE1 31 IN ID X 900 ELL W/ SPLITTER A351/CF8M HT NO 17388-2
CATEGORY 1      R RATIO IS     1.690                                          FRACTURE TOUGHNESS
                                                 CR(E) CR/NI DELTA    -------------------------------------------------
  %NI    %C   %MN   %N   %CR  %SI  %MO  %CB NI(E) CR(E) CR/NI FENUM    KCU  JIC40   THAT40  JMAX40  JICFA   THATFA  JMAXFA
 9.92   .07   .81  .05 19.22 1.22 2.46  .00 15.97 19.50 1.221 11.00   6.53  750.    60.0   2200.    507.      .0    507.
                                                 18.52 1.159 12.45
```

a,c,e

```
PLANT PGE1 27.5 IN ID X 22D ELL A351/CF8M HT NO 32425-1
CATEGORY 1       R RATIO IS    1.180                                       FRACTURE TOUGHNESS
                                              CR(E) CR/NI DELTA   ..................................................
  %NI    %C   %MN    %N    %CR  %SI  %MO  %CB NI(E) CR(E) CR/NI FENUM    KCU  JIC40   TMAT40  JMAX40  JICFA   TMATFA  JMAXFA
 9.62   .04   .86   .05 19.26 1.17 2.27  .00 14.80 19.20 1.298 14.53    5.95  750.    60.0   2200.    354.      .0    354.
                                              18.30 1.236 16.16

PLANT PGE1 27.5 IN ID X 22D ELL A351/CF8M HT NO 30845-1
CATEGORY 1       R RATIO IS    1.644                                       FRACTURE TOUGHNESS
                                              CR(E) CR/NI DELTA   ..................................................
  %NI    %C   %MN    %N    %CR  %SI  %MO  %CB NI(E) CR(E) CR/NI FENUM    KCU  JIC40   TMAT40  JMAX40  JICFA   TMATFA  JMAXFA
 9.86   .05   .57   .05 18.78 1.14 2.24  .00 15.19 18.64 1.226 11.24    8.06  750.    60.0   2200.    493.      .0    493.
                                              17.74 1.167 12.80

PLANT PGE1 27.5 IN ID X 22D ELL A351/CF8M HT NO 32469-2
CATEGORY 1       R RATIO IS    1.239                                       FRACTURE TOUGHNESS
                                              CR(E) CR/NI DELTA   ..................................................
  %NI    %C   %MN    %N    %CR  %SI  %MO  %CB NI(E) CR(E) CR/NI FENUM    KCU  JIC40   TMAT40  JMAX40  JICFA   TMATFA  JMAXFA
 9.62   .06   .81   .05 19.28 1.46 2.36  .00 15.37 19.78 1.287 14.00    5.20  750.    60.0   2200.    372.      .0    372.
                                              18.84 1.225 15.81

PLANT PGE1 27.5 IN ID X 22D ELL A351/CF8M HT NO 33047-4
CATEGORY 2       R RATIO IS     .929                                       FRACTURE TOUGHNESS
                                              CR(E) CR/NI DELTA   ..................................................
  %NI    %C   %MN    %N    %CR  %SI  %MO  %CB NI(E) CR(E) CR/NI FENUM    KCU  JIC40   TMAT40  JMAX40  JICFA   TMATFA  JMAXFA
 9.84   .04   .63   .05 19.66 1.29 2.52  .00 14.90 20.13 1.351 17.28    3.76  656.    48.0   1816.    279.      .0    279.
                                              19.13 1.283 18.99
```

<u>Legend</u>:

KCU - Charpy U-notch energy in daj/cm^2

JIC40 - J_{Ic} at 40 years service in in-lb/in^2

TMAT40 - T_{mat} at 40 years service

JMAX40 - J_{max} at 40 years service in in-lb/in^2

JICFA - The fully aged J_{Ic} in in-lb/in^2

TMATFA - The fully aged T_{mat} (always 0)

JMAXFA - The fully aged J_{Ic} in in-lb/in^2 (always equals JICFA)

Ni - nickel, C - carbon, Cr - chromium, Si - silicon

Mo - molybdenum, Cb - columbium, Cr(E) - chromium

equivalent, Ni(E) - nickel equivalent,

Chemistry is in percent weight

DELTA is ferrite in percent volume

(see reference 4-6 for discussion of category, fully aged toughness, etc.)

TABLE B-2

CHEMISTRY AND FRACTURE TOUGHNESS PROPERTIES OF THE MATERIAL HEATS OF DIABLO CANYON UNIT 2

a,c,e

```
PLANT PEG 31 IN X 29 IN ID X 500 RED ELL A351/CF8M HT NO 41192-2
CATEGORY 1       R RATIO IS     1.825                                                   FRACTURE TOUGHNESS
                                                         CR(E) CR/NI DELTA      --------------------------------------------------
  %NI     %C    %MN    %N    %CR   %SI   %MO   %CB NI(E) CR(E) CR/NI FENUM       KCU  JIC40   TMAT40  JMAX40  JICFA   TMATFA  JMAXFA
10.08    .06    .68   .05 19.52   .98 2.15   .00 15.77 19.01 1.205 10.34       7.35  750.     60.0   2200.    547.       .0    547.
                                                         18.15 1.151 12.04

PLANT PEG 31IN X 29 IN ID X 500 RED ELL A351/CF8M HT NO 39792
CATEGORY 1       R RATIO IS     1.334                                                   FRACTURE TOUGHNESS
                                                         CR(E) CR/NI DELTA      --------------------------------------------------
  %NI     %C    %MN    %N    %CR   %SI   %MO   %CB NI(E) CR(E) CR/NI FENUM       KCU  JIC40   TMAT40  JMAX40  JICFA   TMATFA  JMAXFA
 9.15    .05    .83   .05 18.98  1.02 2.18   .00 14.61 18.57 1.271 13.25       7.40  750.     60.0   2200.    400.       .0    400.
                                                         17.70 1.211 14.91

PLANT PEG 31 IN X 29 IN X 500 RED ELL A351/CF8M HT NO 33756-2
CATEGORY 1       R RATIO IS     1.728                                                   FRACTURE TOUGHNESS
                                                         CR(E) CR/NI DELTA      --------------------------------------------------
  %NI     %C    %MN    %N    %CR   %SI   %MO   %CB NI(E) CR(E) CR/NI FENUM       KCU  JIC40   TMAT40  JMAX40  JICFA   TMATFA  JMAXFA
 9.36    .06   1.01   .05 19.07  1.01 2.08   .00 15.21 18.51 1.216 10.80       8.23  750.     60.0   2200.    519.       .0    519.
                                                         17.68 1.162 12.56

PLANT PEG 31 IN  X 29 IN ID X 500 RED ELL A351/CF8M HT NO 37168-1
CATEGORY 1       R RATIO IS     1.680                                                   FRACTURE TOUGHNESS
                                                         CR(E) CR/NI DELTA      --------------------------------------------------
  %NI     %C    %MN    %N    %CR   %SI   %MO   %CB NI(E) CR(E) CR/NI FENUM       KCU  JIC40   TMAT40  JMAX40  JICFA   TMATFA  JMAXFA
 9.55    .06    .79   .05 19.31   .88 2.18   .00 15.29 18.69 1.222 11.05       7.67  750.     60.0   2200.    504.       .0    504.
                                                         17.82 1.165 12.70

PLANT PEG 31 IN ID X 900 ELL A351/CF8M HT NO 52665-2
CATEGORY 1       R RATIO IS     1.496                                                   FRACTURE TOUGHNESS
                                                         CR(E) CR/NI DELTA      --------------------------------------------------
  %NI     %C    %MN    %N    %CR   %SI   %MO   %CB NI(E) CR(E) CR/NI FENUM       KCU  JIC40   TMAT40  JMAX40  JICFA   TMATFA  JMAXFA
 9.13    .06    .86   .05 19.04  1.06 2.10   .00 14.91 18.58 1.246 12.12       7.68  750.     60.0   2200.    449.       .0    449.
                                                         17.74 1.190 13.96

PLANT PEG 31 IN ID X 900 ELL A351/CF8M HT NO 51712-2
CATEGORY 1       R RATIO IS     1.833                                                   FRACTURE TOUGHNESS
                                                         CR(E) CR/NI DELTA      --------------------------------------------------
  %NI     %C    %MN    %N    %CR   %SI   %MO   %CB NI(E) CR(E) CR/NI FENUM       KCU  JIC40   TMAT40  JMAX40  JICFA   TMATFA  JMAXFA
 9.69    .05    .74   .05 18.60  1.11 2.09   .00 15.11 18.20 1.205 10.30       9.22  750.     60.0   2200.    550.       .0    550.
                                                         17.37 1.149 11.95

PLANT PEG 31 IN ID X 900 ELL A351/CF8M HT NO 52282-2
CATEGORY 1       R RATIO IS     1.465                                                   FRACTURE TOUGHNESS
                                                         CR(E) CR/NI DELTA      --------------------------------------------------
  %NI     %C    %MN    %N    %CR   %SI   %MO   %CB NI(E) CR(E) CR/NI FENUM       KCU  JIC40   TMAT40  JMAX40  JICFA   TMATFA  JMAXFA
 9.31    .06    .71   .05 19.24   .75 2.43   .00 15.01 18.78 1.251 12.32       7.14  750.     60.0   2200.    440.       .0    440.
                                                         17.81 1.186 13.79

PLANT PEG 31 IN ID X 900 ELL A351/CF8M HT NO 52369-2
CATEGORY 1       R RATIO IS     1.499                                                   FRACTURE TOUGHNESS
                                                         CR(E) CR/NI DELTA      --------------------------------------------------
  %NI     %C    %MN    %N    %CR   %SI   %MO   %CB NI(E) CR(E) CR/NI FENUM       KCU  JIC40   TMAT40  JMAX40  JICFA   TMATFA  JMAXFA
 9.13    .06    .86   .05 18.82  1.10 2.21   .00 14.91 18.57 1.246 12.10       7.84  750.     60.0   2200.    450.       .0    450.
                                                         17.69 1.186 13.83
```

a,c,e

```
PLANT PEG 31 IN X 900 ELL A351/CF8M HT NO 51922-3
CATEGORY 1       R RATIO IS     1.119                                       FRACTURE TOUGHNESS
                                              CR(E) CR/NI DELTA    -------------------------------------------------
  %NI    %C   %MN   %N   %CR  %SI  %MO  %CB NI(E) CR(E) CR/NI FENUM     KCU  JIC40  TMAT40  JMAX40  JICFA  TMATFA  JMAXFA
 9.36   .06   .92  .05 19.75 1.03 2.54  .00 15.17 19.86 1.309 15.11    4.47  750.    60.0   2200.   336.      .0    336.
                                              18.85 1.242 16.50

PLANT PEG 31 IN ID X 900 ELL A351/CF8M HT NO 52665-1
CATEGORY 1       R RATIO IS     1.496                                       FRACTURE TOUGHNESS
                                              CR(E) CR/NI DELTA    -------------------------------------------------
  %NI    %C   %MN   %N   %CR  %SI  %MO  %CB NI(E) CR(E) CR/NI FENUM     KCU  JIC40  TMAT40  JMAX40  JICFA  TMATFA  JMAXFA
 9.13   .06   .86  .05 19.04 1.06 2.10  .00 14.91 18.58 1.246 12.12    7.68  750.    60.0   2200.   449.      .0    449.
                                              17.74 1.190 13.96

PLANT PEG 31 IN ID X 900 ELL A351/CF8M  HT NO. 55485-1 & 2
CATEGORY 1       R RATIO IS     1.318                                       FRACTURE TOUGHNESS
                                              CR(E) CR/NI DELTA    -------------------------------------------------
  %NI    %C   %MN   %N   %CR  %SI  %MO  %CB NI(E) CR(E) CR/NI FENUM     KCU  JIC40  TMAT40  JMAX40  JICFA  TMATFA  JMAXFA
 9.32   .06   .49  .05 19.45 1.08 2.08  .00 14.91 18.99 1.273 13.37    6.43  750.    60.0   2200.   395.      .0    395.
                                              18.16 1.218 15.32

PLANT PEG 31 IN ID X 900 ELL W/SPLITTER A351/CF8M HT NO 34900-1
CATEGORY 1       R RATIO IS     3.113                                       FRACTURE TOUGHNESS
                                              CR(E) CR/NI DELTA    -------------------------------------------------
  %NI    %C   %MN   %N   %CR  %SI  %MO  %CB NI(E) CR(E) CR/NI FENUM     KCU  JIC40  TMAT40  JMAX40  JICFA  TMATFA  JMAXFA
10.11   .06   .74  .05 18.25  .83 2.19  .00 15.83 17.57 1.110  6.58   12.91  750.    60.0   2200.   934.      .0    934.
                                              16.70 1.055  7.26

PLANT PEG 31 IN ID X 900 ELL W/SPLITTER A351/CF8M HT NO 50115-1
CATEGORY 1       R RATIO IS     1.292                                       FRACTURE TOUGHNESS
                                              CR(E) CR/NI DELTA    -------------------------------------------------
  %NI    %C   %MN   %N   %CR  %SI  %MO  %CB NI(E) CR(E) CR/NI FENUM     KCU  JIC40  TMAT40  JMAX40  JICFA  TMATFA  JMAXFA
 9.31   .05   .79  .05 19.15  .99 2.29  .00 14.75 18.85 1.278 13.57    6.77  750.    60.0   2200.   388.      .0    388.
                                              17.94 1.216 15.19

PLANT PEG 31 IN ID X 900 ELL W/SPLITTER A351/CF8M HT NO 52369-1
CATEGORY 1       R RATIO IS     1.499                                       FRACTURE TOUGHNESS
                                              CR(E) CR/NI DELTA    -------------------------------------------------
  %NI    %C   %MN   %N   %CR  %SI  %MO  %CB NI(E) CR(E) CR/NI FENUM     KCU  JIC40  TMAT40  JMAX40  JICFA  TMATFA  JMAXFA
 9.13   .06   .86  .05 18.82 1.10 2.21  .00 14.91 18.57 1.246 12.10    7.84  750.    60.0   2200.   450.      .0    450.
                                              17.69 1.186 13.83

PLANT PEG 31 IN ID X 900 ELL W/SPLITTER A351/CF8M HT NO 51712-1
CATEGORY 1       R RATIO IS     1.833                                       FRACTURE TOUGHNESS
                                              CR(E) CR/NI DELTA    -------------------------------------------------
  %NI    %C   %MN   %N   %CR  %SI  %MO  %CB NI(E) CR(E) CR/NI FENUM     KCU  JIC40  TMAT40  JMAX40  JICFA  TMATFA  JMAXFA
 9.69   .05   .74  .05 18.60 1.11 2.09  .00 15.11 18.20 1.205 10.30    9.22  750.    60.0   2200.   550.      .0    550.
                                              17.37 1.149 11.95

PLANT PEG  31 IN ID X 900 ELL W/SPLITTER A351/CF8M HT NO 52449-1
CATEGORY 1       R RATIO IS     1.331                                       FRACTURE TOUGHNESS
                                              CR(E) CR/NI DELTA    -------------------------------------------------
  %NI    %C   %MN   %N   %CR  %SI  %MO  %CB NI(E) CR(E) CR/NI FENUM     KCU  JIC40  TMAT40  JMAX40  JICFA  TMATFA  JMAXFA
 9.44   .06   .78  .05 19.35 1.21 2.23  .00 15.18 19.30 1.271 13.27    6.06  750.    60.0   2200.   399.      .0    399.
                                              18.41 1.212 15.00
```

```
PLANT PEG  PEG 31 IN ID X 900 ELL W/SPLITTER A351/CF8M HT NO 41423-1
CATEGORY 1       R RATIO IS     1.622                                              FRACTURE TOUGHNESS
                                                   CR(E) CR/NI DELTA     --------------------------------------------------
  %NI    %C   %MN   %N   %CR  %SI  %MO  %CB NI(E) CR(E) CR/NI FENUM      KCU  JIC40   TMAT40  JMAX40   JICFA   TMATFA  JMAXFA
 9.28   .07   .81  .05 19.19 1.14 2.10  .00 15.33 18.85 1.229 11.37     7.43  750.    60.0   2200.    487.      .0    487.
                                                18.01 1.174 13.08

PLANT PEG  31 IN ID X 900 ELL W/SPLITTER A351/CF8M HT NO. 50362
CATEGORY 1       R RATIO IS     1.434                                              FRACTURE TOUGHNESS
                                                   CR(E) CR/NI DELTA     --------------------------------------------------
  %NI    %C   %MN   %N   %CR  %SI  %MO  %CB NI(E) CR(E) CR/NI FENUM      KCU  JIC40   TMAT40  JMAX40   JICFA   TMATFA  JMAXFA
 9.15   .05   .71  .05 18.84  .92 2.17  .00 14.55 18.27 1.255 12.52     8.15  750.    60.0   2200.    430.      .0    430.
                                                17.40 1.195 14.09

PLANT PEG  31 IN ID X 900 ELL W/ SPLITTER A351/CF8M HT NO. 49686
CATEGORY 1       R RATIO IS     1.566                                              FRACTURE TOUGHNESS
                                                   CR(E) CR/NI DELTA     --------------------------------------------------
  %NI    %C   %MN   %N   %CR  %SI  %MO  %CB NI(E) CR(E) CR/NI FENUM      KCU  JIC40   TMAT40  JMAX40   JICFA   TMATFA  JMAXFA
 9.25   .08   .67  .05 19.35 1.17 2.21  .00 15.53 19.21 1.236 11.69     6.66  750.    60.0   2200.    470.      .0    470.
                                                18.33 1.180 13.39

PLANT PEG  27.5IN ID X 22D ELL A351/CF8M HT NO. 39716-1 & 4
CATEGORY 1       R RATIO IS     1.127                                              FRACTURE TOUGHNESS
                                                   CR(E) CR/NI DELTA     --------------------------------------------------
  %NI    %C   %MN   %N   %CR  %SI  %MO  %CB NI(E) CR(E) CR/NI FENUM      KCU  JIC40   TMAT40  JMAX40   JICFA   TMATFA  JMAXFA
 9.14   .05  1.00  .05 19.63  .90 2.30  .00 14.69 19.21 1.308 15.03     5.56  750.    60.0   2200.    338.      .0    338.
                                                18.29 1.245 16.68

PLANT PEG  27.5 IN ID X 22D ELL A351/CF8M HT NO. 40874-3 & 4
CATEGORY 1       R RATIO IS     1.880                                              FRACTURE TOUGHNESS
                                                   CR(E) CR/NI DELTA     --------------------------------------------------
  %NI    %C   %MN   %N   %CR  %SI  %MO  %CB NI(E) CR(E) CR/NI FENUM      KCU  JIC40   TMAT40  JMAX40   JICFA   TMATFA  JMAXFA
 9.11   .07   .90  .05 18.47 1.03 2.30  .00 15.21 18.25 1.200 10.09     9.32  750.    60.0   2200.    564.      .0    564.
                                                17.33 1.139 11.30

PLANT PEG  31 IN ID X 400 ELL A351/CF8M HT NO. 38408
CATEGORY 1       R RATIO IS     1.829                                              FRACTURE TOUGHNESS
                                                   CR(E) CR/NI DELTA     --------------------------------------------------
  %NI    %C   %MN   %N   %CR  %SI  %MO  %CB NI(E) CR(E) CR/NI FENUM      KCU  JIC40   TMAT40  JMAX40   JICFA   TMATFA  JMAXFA
 9.36   .08  1.18  .05 19.14 1.38 2.10  .00 15.90 19.16 1.205 10.32     7.42  750.    60.0   2200.    549.      .0    549.
                                                18.32 1.152 12.11

PLANT PEG  31 IN ID X 400 ELL A351/CF8M HT NO. 39231
CATEGORY 1       R RATIO IS     1.257                                              FRACTURE TOUGHNESS
                                                   CR(E) CR/NI DELTA     --------------------------------------------------
  %NI    %C   %MN   %N   %CR  %SI  %MO  %CB NI(E) CR(E) CR/NI FENUM      KCU  JIC40   TMAT40  JMAX40   JICFA   TMATFA  JMAXFA
 9.12   .07   .76  .05 19.49 1.03 2.43  .00 15.15 19.45 1.284 13.85     5.56  750.    60.0   2200.    377.      .0    377.
                                                18.48 1.219 15.45

PLANT PEG  31 IN ID X 400 ELL A351/CF8M HT NO. 39445
CATEGORY 1       R RATIO IS     1.670                                              FRACTURE TOUGHNESS
                                                   CR(E) CR/NI DELTA     --------------------------------------------------
  %NI    %C   %MN   %N   %CR  %SI  %MO  %CB NI(E) CR(E) CR/NI FENUM      KCU  JIC40   TMAT40  JMAX40   JICFA   TMATFA  JMAXFA
 9.26   .06   .91  .05 18.84 1.14 2.05  .00 15.06 18.43 1.223 11.11     8.40  750.    60.0   2200.    501.      .0    501.
                                                17.61 1.169 12.86
```

a,c,e

WESTINGHOUSE PROPRIETARY CLASS 2

```
PLANT PEG  31 IN ID X 400 ELL A351/CF8M HT NO. 34900
CATEGORY 1      R RATIO IS    3.113                                                    FRACTURE TOUGHNESS
                                                   CR(E) CR/NI DELTA     -----------------------------------------------------
  %NI    %C   %MN   %N   %CR  %SI  %MO  %CB NI(E) CR(E) CR/NI FENUM      KCU  JIC40   TMAT40  JMAX40  JICFA   TMATFA  JMAXFA
10.11   .06   .74  .05 18.25  .83 2.19  .00 15.83 17.57 1.110  6.58    12.91  750.     60.0   2200.    934.      .0    934.
                                                 16.70 1.055  7.26
```

Legend:

KCU - Charpy U-notch energy in daj/cm^2

JIC40 - J_{Ic} at 40 years service in in-lb/in^2

TMAT40 - T_{mat} at 40 years service

JMAX40 - J_{max} at 40 years service in in-lb/in^2

JICFA - The fully aged J_{Ic} in in-lb/in^2

TMATFA - The fully aged T_{mat} (always 0)

JMAXFA - The fully aged J_{Ic} in in-lb/in^2 (always equals JICFA)

Ni - nickel, C - carbon, Cr - chromium, Si - silicon

Mo - molybdenum, Cb - columbium, Cr(E) - chromium

equivalent, Ni(E) - nickel equivalent,

Chemistry is in percent weight

DELTA is ferrite in percent volume

(see reference 4-6 for discussion of category, fully aged toughness, etc.)